# MOLECULAR RECOGNITION OF BACTERIA AND CANCER CELLS USING ssDNA APTAMERS

By

DIANE TUREK

A DISSERTATION PRESENTED TO THE GRADUATE SCHOOL
OF THE UNIVERSITY OF FLORIDA IN PARTIAL FULFILLMENT
OF THE REQUIREMENTS FOR THE DEGREE OF
DOCTOR OF PHILOSOPHY

UNIVERSITY OF FLORIDA

2013

To Matthieu and to my Family

ACKNOWLEDGMENTS

I give a special thanks to my advisor Dr. Weihong Tan who gave me his support and encouragement throughout my time in his research group at the University of Florida. I would also like to thank Dr. Kenneth Wagener who always found the right words to encourage me and guided me to make the right choices for my career. I would like to thank Dr. Kenneth Sloan, who passed me his critical eye and passion for scientific inquiry. I also would like to recognize Dr. Judith Johnson, Mohammed Rashid, Dr. Marco Salemi, and David Nolan whose assistance was irreplaceable in the bacteria project; and I would like to thank Dr. Chen Liu, Le Trinh and Dr. Williams Puszyk who helped me considerably on the liver project.

In addition, I appreciate the patience and support from Dr. James Leonard and Dr. Dimitri Van Simaeys whom took the time to mentor me respectively in Dr Wagener's and Dr. Tan's research group: their help and friendship have been invaluable during my graduate school experience. I am deeply grateful for the many discussions and friendships cultivated with all group members and lab mates, especially Dr. Kwame Sefah, Sena Cansiz, Dr. Elizabeth Jimenez, Dr. Dalia Lopez Colon, Dr. Meghan O'Donoghue, Dr. Xiangling Xiong, Dr. Guizhi Zhu, Carole Champanhac, Liqin Zhang, Danny Chang, I-Ting Teng, Stephanie Weisberg, Benjamin Arline, Emir Yasun, Ismail Ocsoy and my dear Dr. Pamela Havre. Dr. Kathryn Williams and Lori Clark have been exceptionally helpful as well.

I wish to recognize my committee members Dr. Nicole Horenstein, Dr. Gail Fanucci Dr. David Ostrov and Dr Benjamin Smith who have been critical of my work and helped me become a better scientist.

Finally and above all, I would not be in the position I am today without my family's support. My parents, Leopold and Rosita Turek, and my sister Claire will always be my biggest inspiration and their love carries me to go forward. My deepest thank goes to Matthieu, who amazed me by staying so strong and loving throughout these years apart; I could not have done it without him (love you Matthieu!). My amazing friends: Chloé, Antoine, Marie, Carole, Gaelle, Joel, Brian, Frances, Melissa, Stacey, David, Whitney, Mike, Hridis, Kostas, Erica, Veronica, Chris and Xenothon, aka Xenomon, always found the right words to push me forward. For all this support, I am eternally grateful.

TABLE OF CONTENTS

page

LIST OF TABLES

LIST OF FIGURES

LIST OF ABBREVIATIONS

| | |
|---|---|
| A | Adenine |
| AMA | Ammonium hydroxide: methylamine (50:50) |
| ATCC | American type culture collection |
| Au-NP | Gold-nanoparticle |
| Au-NR | Gold-nanorod |
| BB | Binding buffer |
| BSA | Bovine serum albumin |
| C | Cytosine |
| CA | Cancer antigen |
| CDS | Coding sequence |
| CGRC | Cancer and Genetics Research Center |
| CPG | Controlled pore glass |
| CTAB | Cetyltrimetylammonium bromide |
| DI | Deionized |
| DMEM | Dulbecco's Modified Eagle Media |
| DNA | Deoxyribonucleic acid |
| DNAse | Deoxyribonuclease |
| dNTP | Deoxyribonucleotide triphosphate |
| dsDNA | Double-stranded DNA |
| *E. faecalis* | *Enterococcus faecalis* |
| ELAA | Enzyme linked aptamer assay |
| ELISA | Enzyme linked immunosorbent assay |
| ELONA | Enzyme linked oligonucleotide assay |
| FACS | Fluorescence activated cell sorting |

| | |
|---|---|
| FBS | Fetal bovine serum |
| FDA | Food and Drug Administration |
| FITC | Fluorescein isothiocyanate |
| G | Guanine |
| GPC3 | Glypican 3 |
| GS | Glutamine synthetase |
| hGPC3 | Human glypican 3 |
| HPLC | High performance liquid chromatography |
| HSP | Heat stock protein |
| ICBR | Interdisciplinary Center for Biotechnology Research |
| IDT | Integrated DNA Technologies |
| MAFFT | Mulyiple alignment program fror amino acid or nucleotide sequences |
| MES | 2- (N-morpholino) ethanesulfonic acid buffer |
| MID | Multiplex identifier sequence |
| *MRSA* | *Methicillin-resistant Staphylococcus aureus* |
| *MSSA* | *Methicillin-sensitive Staphylococcus aureus* |
| OCCA | Ovarian clear cell adenocarcinoma |
| NCBI | National Center for Biotechnology Information |
| NIR | Near infrared |
| NP | Nanoparticle |
| NR | Nanorod |
| nt | Nucleotide |
| PBS | Phosphate buffered saline |
| PBP | Penicillin binding protein |

| | |
|---|---|
| PCR | Polymerase chain reaction |
| *SA* | *Staphylococcus aureus* |
| SDS-PAGE | Sodium dodecyl sulfate polyacrilamide gel electrophoresis |
| SELEX | Systematic evolution of ligands by exponential enrichment |
| SI | Supplemental information |
| ssDNA | Single-stranded DNA |
| T | Thymine |
| TBE | Tris-borate-EDTA buffer |
| TCEP | Tris (2-carboxyethyl) phosphine |
| TEAA | Triethylamine Acetate |
| TVU | Transvaginal ultrasound |
| UF | University of Florida |
| UV | Ultraviolet |
| WB | Washing buffer |

Abstract of Dissertation Presented to the Graduate School
of the University of Florida in Partial Fulfillment of the
Requirements for the Degree of Doctor of Philosophy

# MOLECULAR RECOGNITION OF BACTERIA AND CANCER CELLS USING ssDNA APTAMERS

By

Diane Turek

December 2013

Chair: Weihong Tan
Major: Chemistry

Methicillin-resistant *Staphylococcus aureus* (*MRSA*) is any strain of *Staphylococcus aureus* that has developed resistance to beta-lactam antibiotics, including the penicillins and the cephalosporins. Once confined to hospital settings, *MRSA* can now be contracted in community settings as well. Although many new antibiotics against *MRSA* are in phase II and III clinical trials, a tool that would enable the recognition of *MRSA* through its membrane structure could lead to new therapeutic approaches to eradicate the *MRSA* superbug, either without the use of antibiotics or with a strain-specific antibiotic. Therefore, since the aptamer molecule has shown outstanding target-specific binding, this study presents the generation of four *MRSA* strain-specific aptamers that can be easily modified as molecular probes for bioanalysis or antibiotics-free therapy. The Cell-SELEX technology was used to develop target-specific aptamers. Binding studies of those aptamers were performed by flow cytometry on a panel of clinical strains and preliminary investigation of their use after chemical modifications using AuNP was also carried out until no more binding of the aptamers was observed over time.

Cancer is commonly referred to as the disease of our century. While budgets of billions dollars are granted toward cancer research, very little improvement is observed statistically. Liver cancer, which usually occurs on liver suffering of cirrhosis, shows a very low survival rate. The hepatocellular carcinoma is the most common liver cancer and the protein GPC3 is over-expressed on cancer patients. For that reason, GPC3 is a good candidate for early cancer detection or diagnosis. We used an hGPC3-overexpressed mouse cancer cell line (IMEA) to study aptamer generation specific to GPC3. In this study, no aptamers were found to be specific to the protein; this raises questions about the stability and the quality of such cell lines. Finally, another cancer cell line, the ovarian cancer cells TOV21G, for which aptamers had been developed in the past from our research group, was used to study the cytotoxicity of the gold-nanorods through thermoactivation. Results of this study showed that the aptamer TOV6-gold-nanorod complex was able to internalize in the ovarian cancer cell and showed cytotoxicity after thermoactivation through an NIR laser beam.

# CHAPTER 1
# GENERAL INTRODUCTION AND BACKGROUND

In this chapter, three main research topic backgrounds will be presented: 1) the *Methicillin-resistant Staphylococcus aureus* bacteria; 2) cancer, in general and more specifically liver and ovarian cancers; and 3) molecular recognition, with an emphasis on the SELEX technique used in our laboratory.

## *Methicillin-Resistant Staphylococcus Aureus*

### History and Identification

*Staphylococcus*, which originally comes from the greek noun “Kokkos” meaning “berry”, is a bacteria that grows in grape-like cluster of cells [Figure 1-1] and was first discovered by Pasteur and Koch in 1877-78 from furuncle pus and osteomyelitis[1]. A few years later, in 1881-82, Ogston put together a detailed study of *Staphylococcus*[2] and Rosenbach was able to isolate those bacteria and produce pure cultures[3]. *Staphylococcus aureus* was named this way because of its gold color, from the Latin “aurum” for gold. Still in 1884, Gram succeeded in detecting bacteria using a coloration method from gentian violet: *Staphylococcus* was then classified under the Gram-positive bacteria[4]. In contrast with Gram-negative bacteria that may have a peptidoglycan layer between two cell membranes, the outer cell layer of Gram-positive bacteria is constituted of a thick layer of peptidoglycan that is able to retain the crystal violet stain.

### Epidemiology and Resistance

*S. aureus* is a commensal bacteria, harmlessly carried in the nose or on the skin of about 33% of the population[5]. Three profiles of nasal carrier are distinguished: approximately 20% of healthy individuals are permanent carriers, 60% are intermittent

carriers, and 20% are non-carriers[6]. Those profiles can change overtime and the mechanism induced in nasal carriage is still not well understood. Permanent carriers have a high bacterial density and by such, a high risk of infection[7]. Studies have shown than most permanent carriers are colonized by the same *S. aureus* strain whereas intermittent carriers are colonized at different time by different strains[8]. No genetical characteristics have yet been identified to explain the development of intermittent or permanent strains.

Infectious diseases are one of the leading causes of death, particularly *Staphylococcus aureus* infections, with mortality rates exceeding 80%. From 1944-1954, it was common to combat strains of *S. aureus* using penicillin. Resistance against it began to develop. In 1959, methicillin was introduced, allowing survival rates to rise to a level similar to those seen when penicillin was first introduced[9]. However, not long after its introduction, the first methicillin-resistant strain was documented[10]. While the incidence of *Methicillin-resistant Staphylococcus aureus (MRSA)* has formerly been confined to hospital settings, it has recently been observed in the community at large. Cases of community-associated MRSA infections were first reported in the late 1980s and early 1990s. Not long after the first introduction of methicillin as a treatment for bacterial infections, resistant strains against this antibiotic were described[10]. Similar resistance against other antibiotics has been reported[11]. This resistance can be transmitted among different bacteria (inter- or intra-species), indicating that proper use of antibiotics is vital to preventing the emergence of resistance. This has been hard to accomplish as antibiotics are, and have been, misused or overused[11]. As a result, several so-called ‘superbugs’ have been emerging, including *MRSA* [Figure 1-2]. By its

own heterogeneity, *MRSA* can make eradication difficult, as some bacteria show multidrug resistance. The latest estimations of the occurrence of this pathogen are staggering, rising to epidemic proportions in hospitals where, by an estimate provided by the European Antimicrobial Resistance Surveillance System, 40-60% of all infections were caused by *S. aureus* in the US and the UK[12,13].

*MRSA*'s resistance towards the ß-lactam family originates from primary, or intrinsic, and secondary ß-lactam drug resistance. Primary ß-lactam drug resistance is caused by ß-lactamases, an enzyme that breaks down the ß-lactam ring, making the molecule ineffective. Secondary drug resistance arises from the altered expression of membrane-bound penicillin binding proteins (PBPs) as well as the alteration of cell wall permeability to ß-lactams. PBPs, which are coded by the mecA gene, are involved in the synthesis of the cell wall or, more precisely, the synthesis of peptidoglycan. In non-resistant *S. aureus*, ß-lactams irreversibly inactivate these enzymes such that cell wall formation is hampered, leading to lower viability of the bacteria by susceptibility to osmotic pressure. *MRSA*, however, has developed PBPs with a lower affinity towards ß-lactams, e.g., PBP2a. This lower affinity towards ß-lactams renders the antibiotics less effective[12,14,15] [Figure 1-3].

*Staphylococcus aureus* developed resistance toward glycopeptides, the most common being vancomycin, by a thickening of the bacterial membrane. Indeed, glycopeptides target the D-ala-D-ala residue of the peptidoglycan, when facing a thicker membrane, the glycopeptides get trapped in superficial membrane layer and cannot reach the cytoplasmic membrane where the peptidoglycans are synthesized[16]. The

genetic reason of that resistance is not well understood but it does not involve the gene mecA[17].

**Pathology, Risk Factors and Treatment**

*MRSA* is difficult to treat because of its resistance towards ß-lactams, i.e., methicillin and penicillin, a class of antibiotics that inhibit the construction of the cell wall of gram-positive bacteria, such as *Staphylococcus aureus*[9,15,18,19]. Examples of mode of transmissions are by contact with nasal carriers, from draining lesions, by ingestion of food containing staphylococcal enterotoxin, and from mother to neonate during delivery. Most risk factors come from catheter, intravenous toxicomania and dermal wounds[20-22].

Suppurative infections are characterized by several phases: bacterial proliferation, invasion, tissue destruction, local or systemic inflammation. Virulence factors involved are surface proteins that start the tissue colonization and factors that inhibit phagocytosis[21]. *Staphylococcus aureus* binds to cells and extracellular matrix collagen thanks to surface-associated proteins called “adhesins”: protein A (Spa), collagen-binding protein (Cna), fibrinogen-binding protein (ClfA), fibronectin-binding protein (FnBP), and elastin-binding protein (EbpS)[23,24]. Resistance to phagocytosis occurs by formation of a biofilm and intracellular penetration of *S. aureus*[25,26].

*MRSA* bacteria synthesize their virulence factors in two phases. At the beginning of the bacteria growth, genes coding for adhesins are activated. Later on, genes coding for toxins get activated. This sequential activation is regulated by a virulence regulation system named agr (accessory gene regulator)[27,28]. The agr system triggers a stage mechanism, the quorum sensing: it codes for a peptide that is secreted in the extracellular space and its accumulation acts as a signal on the cellular density that triggers the agr system[29].

Treatments of Staphylococcal infections can be done locally by draining a boil for instance, but also include antibiotic therapy and symptomatic treatment of visceral failure[30]. The antiobiotic therapy against *Methicillin-sensitive Staphyloccocus aureus (MSSA)* lies on the use of β-lactam based antibiotics usually coupled with an aminoside. In the case of allergies, fluoroquinolones, synergistines, and lincosamides are the alternative treatments chosen. Failure of the treatment is usually due to the virulence of the strain, deeper secondary infectious point, or insufficient posology[31].

**Cancer**

According to the American Cancer Society, the estimated number of new cancer cases in the US for 2013 is 1,660,290 and 580,350 deaths are expected from those diagnosed cancers[32]. As it can be observed in Figure 1-4, and recalling the constant increase of US population, neither the number of new cancer cases nor cancer deaths seem to reduce over time, despite billions of dollars invested in cancer research.

Understanding the differences between a cancer cell and a healthy cell is essential and begins with the understanding of cell growth. A healthy adult cell has an asymetrical growth[33,34]. Under normal conditions, one mother cell going under mitosis generates two daughter cells: the first one is a generative cell similar to its mother cell which will be able to go under mitosis as well, and the second one is a labor cell with a specific function in the body and a limited time of life.

Statistically, cells might develop in the wrong way in our body, showing mutations that are the consequence of external factors or internal mistakes. Our immune system detects those malignant cells and forces them to die. Nevertheless, it is known since 1961 that each stem cell is limited to 70 divisions (mitosis) : 50 divisions are used to get to adult maturation of the organism and 20 more are able to replace cells for the rest of

our life[35]. Once this reserve is used, the cell line disappears. Contrary to what one could think, cancer cells are frequently apprearing while cancerization remains exceptional. Cancerization is a hyperplasia that happens to compensate the reduction of normal cells that become unable to fulfill their function. In other words, if a cell line cannot fulfill their function, the immune system does not kill the mutant cells in order to compensate the loss in cells and the need to fulfill a particular function[36].

Growth of cancer cells is different from the healthy cells : one mother cancer cell divides into two similar cells that are both able to go through mitosis with no time limit. Unlike healthy cells that maintain their cellular mass, cancer growth follows an exponential curve[37,38]. One explanation for the difference in growth between healthy cells and cancer cells is explained by Dr. Beljanski. He showed that the fundamental difference between the DNA of healthy cells and malignant cells lies in their secondary structure : the double helix of cancer cells shows permanent relaxation of the two strands whereas healthy DNA shows only temporary or local strand relaxation to allow replication or gene expression[39] [Figure 1-5].

Dr. Hanahan and Dr. Weinberg claimed that cancer has six distinctive abilities : growth signal self-sufficiency, insensitivity to growth signal inhibitors, capacity to avoid apoptosis, capacity to replicate indefinitely, angiogenesis induction and the capacity to form metastasis[40]. Then in 2011, they added two more properties of cancer cells : the deregulation of the energetic cellular metabolism and the ability to avoid destruction by the immune system[40]. Our body contains two categories of genes that allow cancer to grow : oncogenes and tumor suppressor genes. When someone has cancer, they have a higher level of oncogenes switched on with a higher level of tumor suppressor genes

switched off. A few decades ago, Dr. Burzinsky showed that specific peptides, called antineoplastons, present in healthy individuals are responsible to turn the tumor suppressor genes on and the oncogenes off, preventing the cells from becoming cancerous[41]. While urine analyses of healthy individuals shows the presence of those peptides, similar analyses of cancer patients does not.

**Liver Cancer**

Cases of liver cancers have increased considerably in the past 20 years. According to the American Cancer Society, 30,640 diagnosed cases of liver primary cancer (22,720 male cases and 7920 female cases) are estimated in 2013 for the US [Figure 1-6]. 21,670 death cases are expected for that disease (14,890 males and 6,780 females). It is the 5$^{th}$ most common cause of cancer death for men and the 9$^{th}$ for women[32].

Liver can show the formation of different types of neoplasms: hepatocellular carcinoma (HCC), hepatoblastoma, haemangiosarcoma and cholangiocarcinoma. HCC is the most common and correspond to 83% of all liver cancers. Etiology and cellular alteration leading to HCC are relatively understood by the scientific community but molecular mechanisms of the hepatocarcinogenesis are not, which explains the difficulties encountered to find a treatment.

Most frequently, malignant liver tumors are secondary tumors (all cancer with the exception of neurocancer are able to metastasize in the liver). The most common primary malignant tumor is the hepatocellular carcinoma, which will be of our interest in one of our studies. HCC appears in most cases on liver suffering of cirrhosis and viral cirrhosis, whether it is alcohol related or not. Cirrhosis due to chronic liver disease like

the hemochromatosis or the alpha-antotrypsin deficience is likely to develop a HCC. In Asia and Africa, where the B virus contamination happens generally during the pregnancy, HCC appears on young adults. In Europe and the US, HCC essentially appears on B or C virus cirrhosis or alcoholic cirrhosis after the age of 50, predominantly on men. Common etiological factors responsible for hepatocarcinogenesis are summarized in Table 1-1.

Since the hepatocarcinoma is generally detected late, the understanding of molecular events initiating the transformation of healthy liver cells into cancer cells is poor. The American Association for the Study of Liver Disease (AASLD) recommends an echography every 6 months to monitor the evolution of the liver state[42].

**Glypican 3 and Hepatocellular Carcinoma**

Recently, studies have shown that the protein Glypican 3 (GPC3) is over-expressed in HCC while they are not present in healthy cells[43] [Figure 1-7].

That observation confers great potential to GPC3 for liver cancer diagnosis, by immunohistochemistry, at an early stage of the disease. Glypicans are part of the heparan sulfate proteoglycan family susceptible to bind to the outter plasmic membrane by a glycosyl-phosphatidyl inositol (GPI) anchor. Glypicans regulates the cell response to proteins BMP (Bone Morphogenic Proteins) and to IGF-2 (Insulin-like Growth Factor-2). Both proteins are involved in cellular division and differentiation[44]. There are different types of glypicans but all of them have 20 to 50% homology in their sequence. They are able to stabilize the interaction between a ligand and its receptor by electrostatic interactions through their HS chains. They can trap extracellular ligands and control their diffusion. They play a role on growth factors signalization and transport; more particularly, they play a negative regulatory role in hepatocyte proliferation[45]. It is

important to note that glypicans 3 are found to be over-expressed in well-differentiated hepatocellular carcinoma[46]. Hepatic adenoma have different morphological behaviour that play a role in determining the risk of malignancy. Hepatic tumors are classified in different groups and the absence of makers such as glypican 3 or HSP 70 allows the distinction between these tumors and HCC[47]. Alpha-fetoprotein is a well-established serum marker for HCC. However, it has low sensitivity (25% to 30%) where GPC3 immunoreactivity has reported a sensitivity of 77% and specificity of 96% in the diagnosis of small HCC[48]. Best results are found with the combination of several markers of malignancy (GPC3, HSP70 and GS) where the specificity is found to be 100%.

**Ovarian Cancer**

According to the American Cancer Society, ovarian cancer is the ninth most common cancer among women. 22,240 women are expected to be diagnosed for new cancer cases in 2013 in the US and 14,230 will die from ovarian cancer [Figure 1-8][32].

Ovarian cancer is a cancerous growth arising from the ovary. They can originate from three different type of cell: surface epithelium that are cells covering the lining of the ovaries; germ cells that are destined to form eggs; and stromal cell that release hormones. Epithedial ovarian cancers are the most common type of malignancy, accounting for more than 80% of the ovarian cancers[49]. The stage of the ovarian cancer can be determined during surgery and are described in Table 1-2[50].

Symptoms that could indicate ovarian disease include bloating, pelvic or abdominal pain, difficulty eating and frequent urination, which can go unnoticed until the cancer has made serious progress. At early stages, the long-term survival rate is approximately 90% [51,52]. Transvaginal ultrasound (TVU) and serum biomarker testing are used for

early detection[53]: the cancer antigen 125 (CA-125) is a transmembrane glycoprotein that is highly expressed in epithelial ovarian cancers. Since this protein appears elevated in other gynecological conditions, the CA-125 is mostly used to monitor the ovarian cancer progression[54,55] or coupled with the TVU.

## Molecular Recognition

### Aptamers

For a very long time, nucleic acids were ascribed only one function: carrying genetic information that encodes proteins. With more exploration and understanding of molecular mechanisms of genetics, the search of other functions appeared possible. Aptamers, from the Latin “aptus”, meaning fitting, are short single-stranded oligonucleotides that shows specific binding to a target. They are able to form stable three-dimensional structures in aqueous solution. The binding between the aptamer and the target is based on molecular recognition: each aptamer has a unique tertiary binding structure and will interact with the target through Van der Waals forces, electrostatic forces and hydrogen bonds [Figure 1-9][56-58].

For cost purposes, aptamers are ideally made the smallest possible, either by a short length of primers and random sequence or by further optimization after the cell SELEX process. They are generally under 100 nucleotides. Targets can range from small molecules, tissues, proteins to a whole organism and the binding affinity is in the micro or picomolar scale. The affinity is quantified through the dissociation constant $K_d$. A small value of this parameter represents a high affinity of the aptamer.

### Aptamers vs Antibodies

Aptamers and antibodies have similar high specificity and affinity for their targets. A few important characteristics make the aptamers a particular interesting tool for *in-*

*vivo* applications. Firstly, aptamers can be synthesized chemically, for a relatively low price, in a reproducible way allowing chemical modifications (addition, deletion or substitution)[59-61]. Secondly and contrary to antibodies, *in-vivo* use of aptamers do not target xenoreactions from the immune system[62-64]. Thirdly, aptamers are smaller than antibodies and for that reason are able to easily penetrate into tissues.

The main disadvantage of aptamers development through cell-SELEX is that it is done on an entire cell, which does not give information on the target identification. Nevertheless, the outcome of a selection is, in most cases, the generation of different aptamers able to bind the same target. The ability to get several aptamers for the same target reduces the occurrence of false positive or false negative during detections.

Aptamers are used for analytical purposes in ELISA-type assays, ELONA or ELAA, where studies have shown they are able to replace or give similar results as antibodies[65-68]. The possibility of generating aptamers when antibodies are not necessarily available is an excellent tool which has been shown with the aptamer SELH2A, able to recognize the antigen H2A for which no antibody is commercially available[69]. The other method for which aptamers are used is flow cytometry. In this method that is used for clinical diagnosis, particles can be distinguished based on their color, structure and size. The use of aptamers can replace the most commonly used antibodies. Indeed, it is easy to detect fluorescent aptamers once linked to their target and the affinity of the aptamer to its target remains the same whether there is addition of a fluorophore. Aptamers are of a great advantage in immune system cells analysis. Indeed, those cells have receptors of antibodies Fc region on their surface, which can

generate interferences. The use of aptamers prevents that problem. A brief comparison between aptamers and antibodies is presented in Table 1-3[70-72].

**Cell-SELEX Method**

The identification of oligonucleotide aptamers is performed using the SELEX – systematic evolution of ligands by exponential enrichment – method. This strategy is an *in-vitro* aptamer selection that was developed in 1990 by Gold and Szostak[73,74]. It begins with the elaboration of a random library framed by two primers, one on the 5'-end region and one on the 3'-end region. $10^{13}$ to $10^{15}$ different random motifs are then used to begin a selection. The pool of random sequences is incubated with both the target and a counter target: for instance, if the target is a specific cell line, then the counter target will be another cell line which we do not want the sequences to bind to. All sequences binding to the counter target are eliminated after each round and the sequences binding to the target are amplified by polymerase chain reaction. The new pool obtained is then used for the next round [Figure 1-10]. Each round of SELEX allows the random pool to enrich with binding sequences and removes the non-binding sequences[75]. Typically, up to 20 to 25 rounds are performed for an entire selection. The evolution of the selection is monitored by flow cytometry, where the binding of the pool can be assessed.

Some conditions make the selection process more successful. On one hand, the target needs to be present in a sufficient amount and in a highest purity possible in order to minimize enrichment of non-specific oligonicleotide and by such, increase the selectivity of the aptamers. On the other hand, some characteristics of the target itself facilitate the selection process: plan groups (aromatic groups for instance), positive

charged groups and hydrogen donor functional groups or hydrogen-bond acceptors[76-78]. Selections appear to be more challenging on hydrophobic or anionic targets.

**Applications of Aptamers**

Owing high selective binding properties, aptamers have the asset to be an excellent tool in nanotechnology. In the laboratory, aptamers have shown good results in different techniques. For protein purification, aptamers-based Histidine-specific columns present better results than the original metal ion affinity chromatography where the isolation of Histidine-conjugated molecules is made possible because of the interaction of Histidine and nickel or cobalt ions from the column[79]. For the same purpose, aptamers have been used coupled with polymeric beads or magnetic nanoparticles[80]. Two other standard techniques where aptamers are successfully used are western blot and flow cytometry. In western blot research, the use of aptamers has been shown to be equally effective and even more sensitive than antibodies[81]. In flow cytometry, reversible labeling techniques have been develop allowing the label to be removed after sorting through flow cytometry[82]. Such technique could not be possible with antibodies without affecting the cell membrane proteins.

In the medical field, the use of aptamers is promising. Besides quantitative evaluation, aptamers can serve as probes to image tumor cells. The ability of aptamers to undergo conformational change upon binding makes it a good candidate as a fluorescent molecular beacon[83]. Electrochemical sensors using aptamers have shown good results as well. They typically consist of an electrode coated with an aptamer, which undergoes conformational change upon binding and affect the current flow through the system. Those measurable changes of electric current can be monitored for analytical purposensen[84]. Optical properties also play a role in cell specific detection

using nanoparticle vehicles. For instance switch of color from pink to blue have been observed after aggregation of NP on cell surface[85]. Radiolabeling is an analytical option to use with aptamer; late studies show the use of $^{99m}Tc$[86] and $^{64}Cu$[87].

Aptamer therapeutic applications are extensively investigated. While most therapeutic methods used aptamers as inhibitors[88], drug delivery vehicles using aptamer specificity show encouraging results[89]. The use of micelles or liposomes as a means of transportation and the ability to get multifunctional nanoparticle conjugates are very promising for such application that focus on cell specificity[90-93].

The current literature covering nanoparticle research seems to observe no cytotoxicity from gold-nanoparticles. Those toxicity conclusions are generally drawn after viability studies and do not enter into the details of mechanisms involved in the cell[94]. Other studies on nanorods show that the origin of cytotoxicity when handling nanorods is due to free CTAB used in making the NR. High purification of such vehicles and nanorod surface modifications can improve those results[95].

## Overview of the Dissertation

The research presented in this dissertation tackles different topics. One of the projects involves working with the biosafety level 2 bacteria *Methicillin-resistant Staphylococcus aureus* on which a selection was run in order to generate aptamers specifically binding to *MRSA*. Those aptamers were further tested on clinical samples obtained on site at Shands hospital, University of Florida.

Besides the bacteria selection, the Cell-SELEX method was used with the aim of generating aptamers on a genetically modified mouse cell line carrying the human protein and hepatocancer marker Glypican 3. The rationale for this selection was to counter two problems: the first one being that Cell-SELEX is not a method that gives the

opportunity to know the target of the aptamer on the surface of the cell. By using a cell modified by the only overexpression of the protein Glypican 3 and by using the wild cell as a counter cell, we were increasing our chances to develop an aptamer recognizing the glypican 3 protein. The second being that protein selection have been done using proteins on magnetic beads but the main problem encountered in this technique is that the protein, when expressed on the surface of the cell does not necessirely fold in the exact same configuration and binding can be lost[80].

Finally, the last project lies on using gold-nanorods bound to aptamers known to bind to ovarian cancer cells. Once exposed to the beam of a NIR laser, nanorods are thermoactivated and their cytotoxicity was assessed.

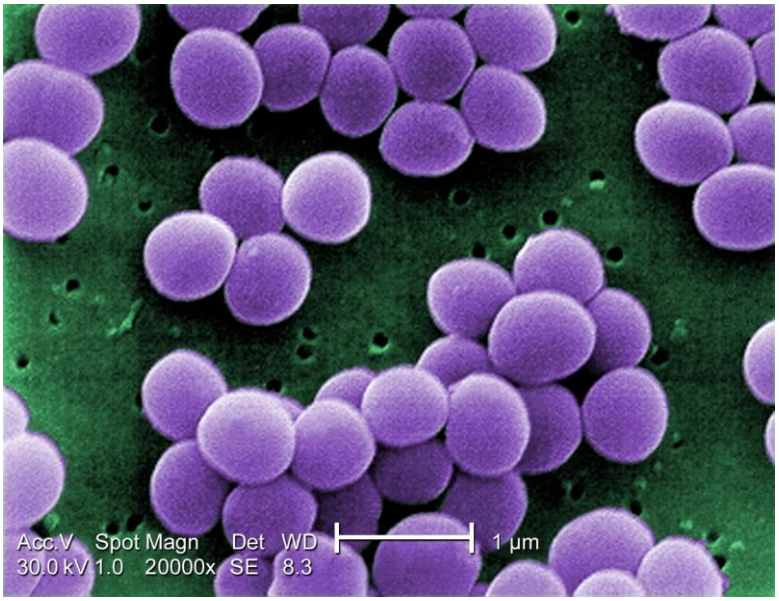


Figure 1-1. Scanning electron micrograph of *Staphylococcus aureus*.

This image is in the public domain and thus free of any copyright restrictions. Courtesy of Centers for Disease Control and Prevention's Public Health Image Library (PHIL).

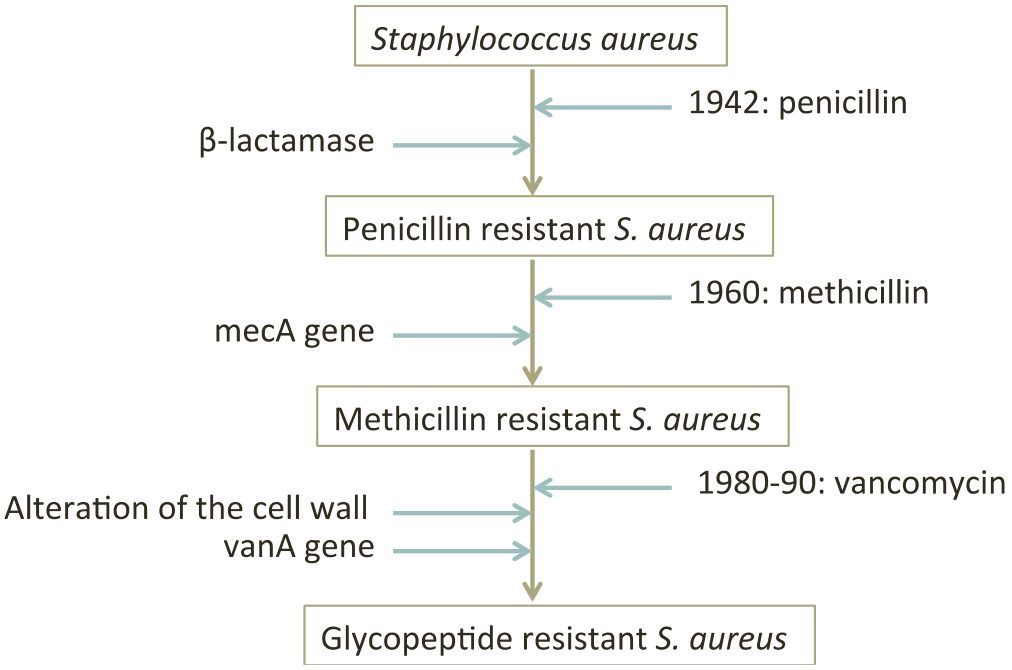


Figure 1-2. Summary of the main resistance developed by the *Staphylococcus aureus* after antibiotic use.

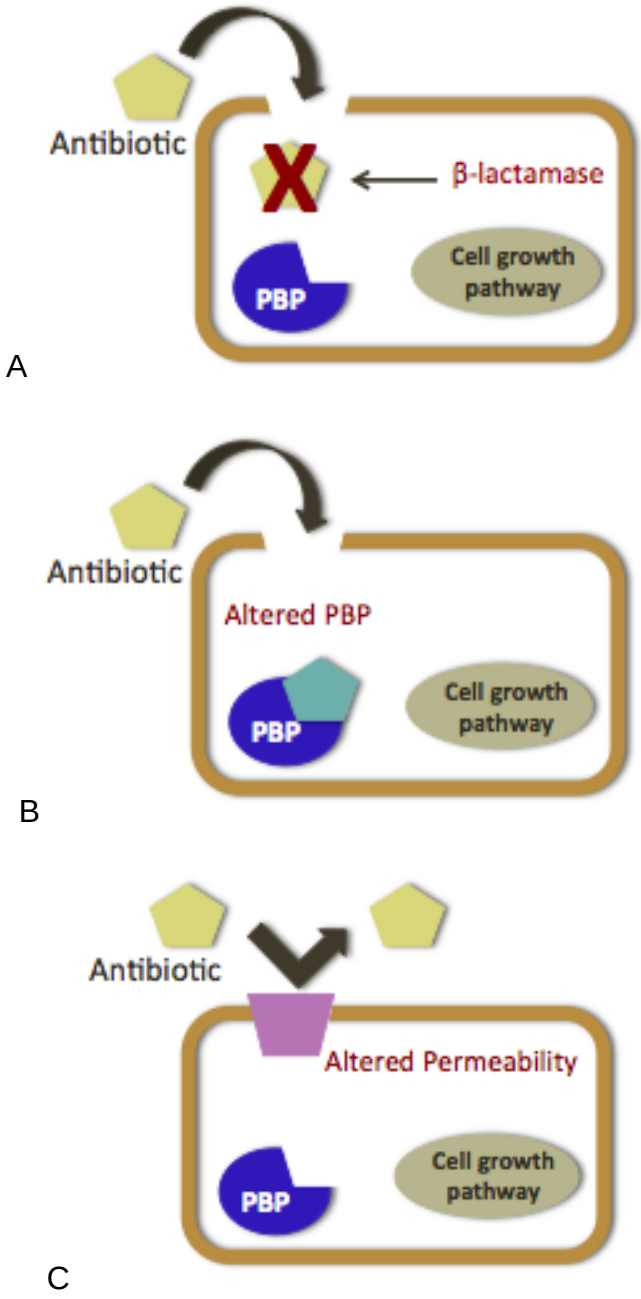


Figure 1-3. *MRSA* Resistance mechanism: A) through ß-lactamase; B) through an alteration of the PBP and C) through an alteration of the cell membrane.

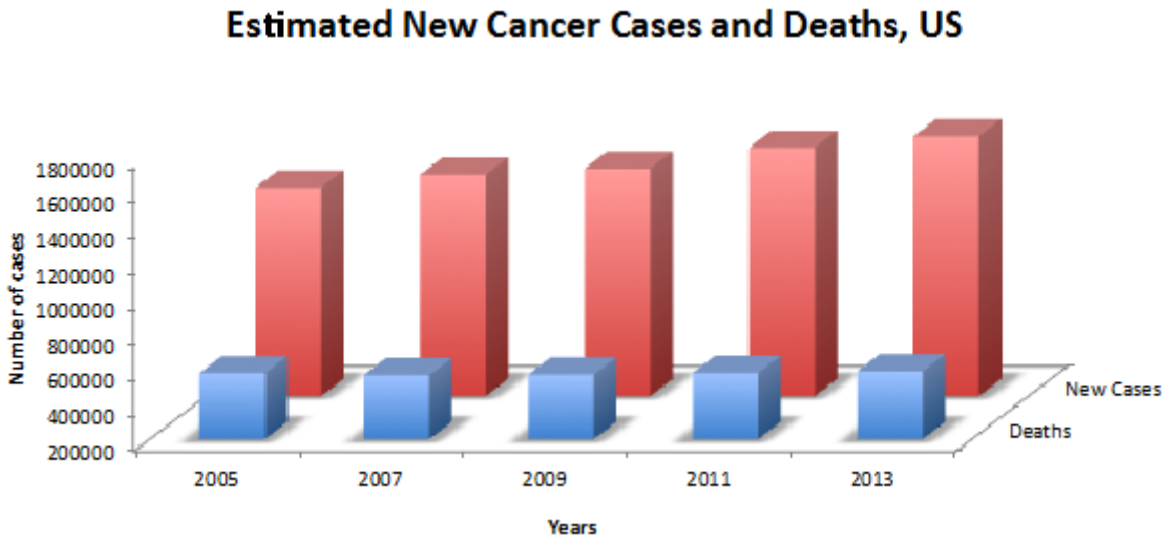


Figure 1-4. Estimated new cancer cases and deaths in the US from 2005 to 2013. The figure summarizes data from the American Cancer Society website.

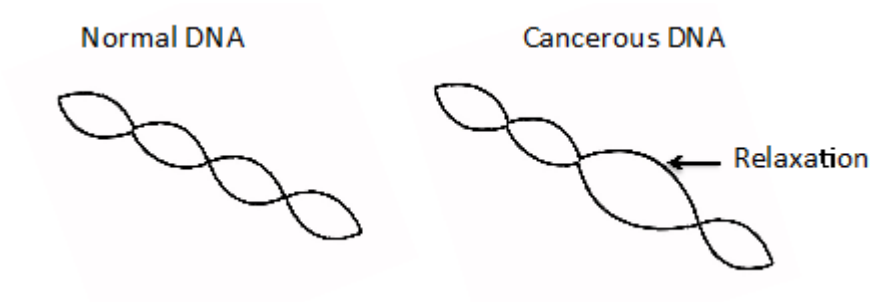


Figure 1-5. Schematic representation of DNA strands. A) Normal DNA and B) Cancerous DNA.

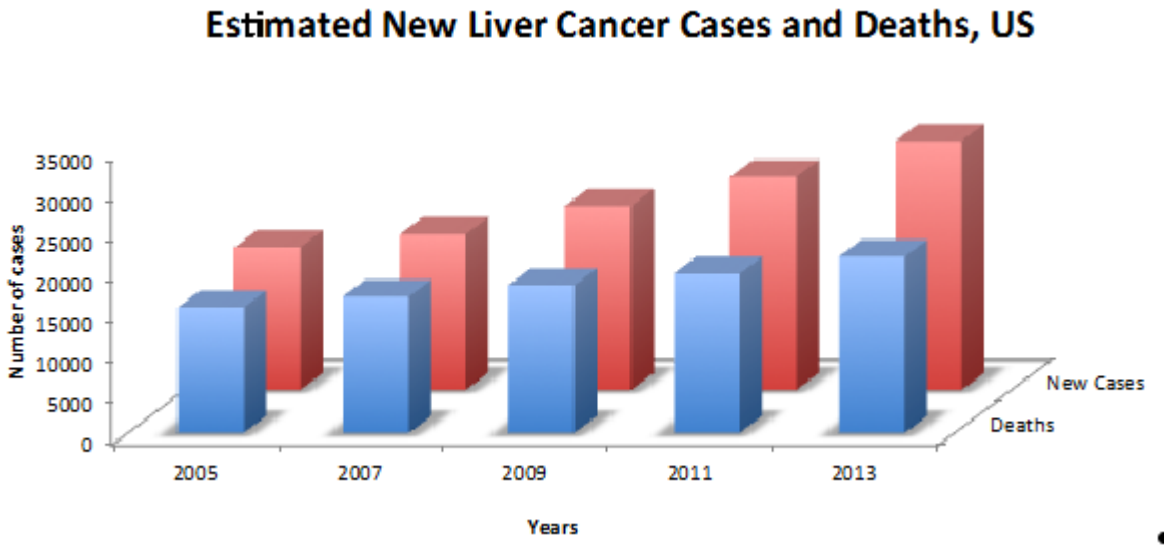


Figure 1-6. Estimated new liver cancer cases and deaths in the US from 2005 to 2013. The figure summarizes data from the American Cancer Society website.

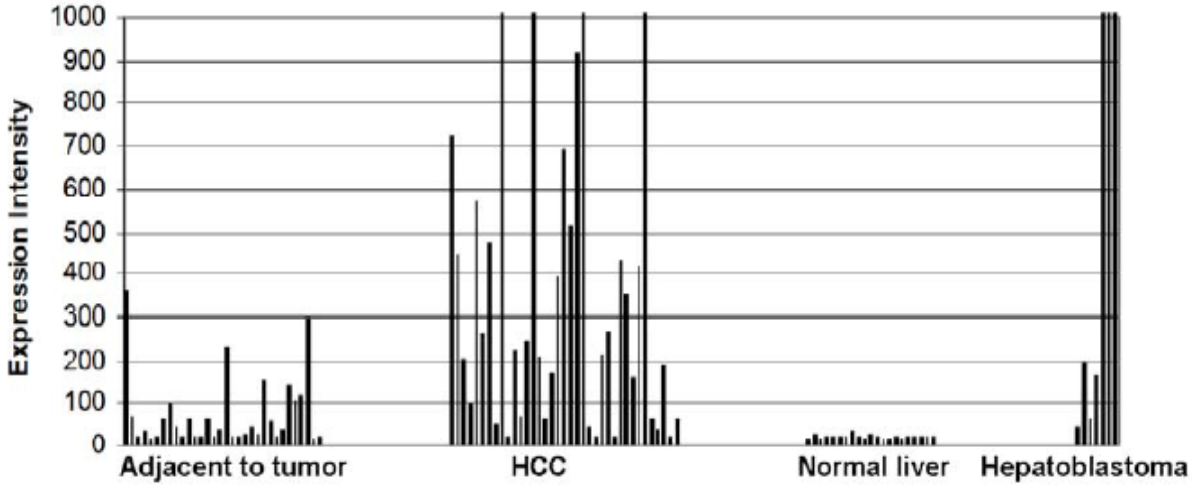


Figure 1-7. Comparative pattern of expression of Glypican 3 gene in adjacent to tumor, HCC, normal liver and hepatoblastoma cells.

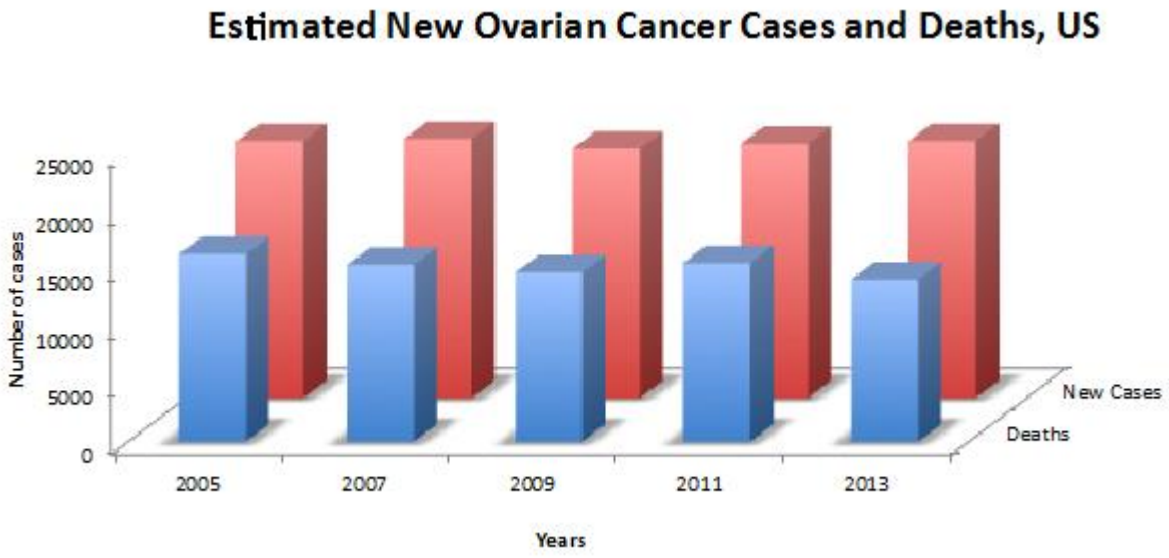


Figure 1-8. Estimated new ovarian cancer cases and deaths in the US from 2005 to 2013. The figure summarize data from the American Cancer Society website.

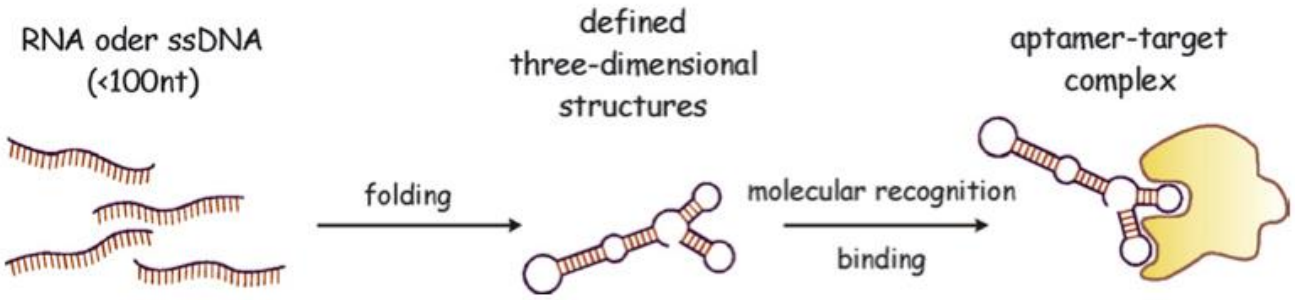


Figure 1-9. Schematic representation of molecular recognition by an aptamer.

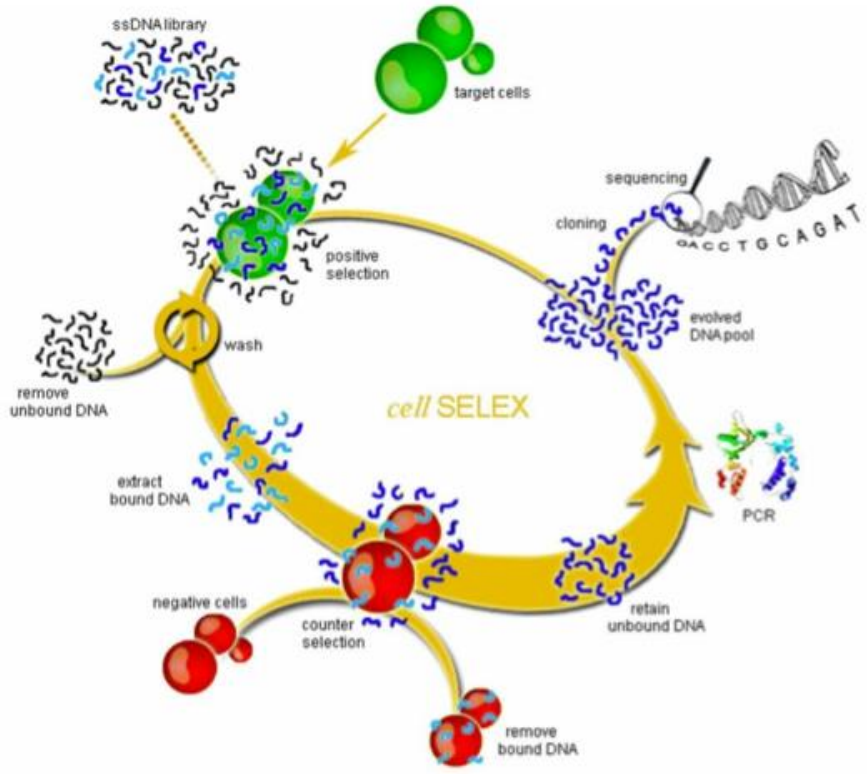


Figure 1-10. Schematic summary of the cell-based aptamer selection technique, cell-SELEX[64].

Table 1-1. Major etiological factors responsible for hepatocarcinogenesis.

| Risk Factors | Outcome |
|---|---|
| Hepatitis B (HBV) | Hepatitis and cirrhosis |
| Hepatitis C (HCV) | Hepatitis and cirrhosis |
| α-toxins | Genotoxicity and cytotoxicity |
| Alcohol consumption | Alcoholic cirrhosis |

Table 1-2. Description of the various stages of ovarian cancer.

| Stage of ovarian cancer | Description |
|---|---|
| Stage I | Growth of the cancer is limited to the ovary or ovaries. |
| Stage IA | Growth is limited to one ovary and the tumor is confined to the inside of the ovary. There is no cancer on the outer surface of the ovary. There are no ascites present containing malignant cells. The capsule is intact. |
| Stage IB | Growth is limited to both ovaries without any tumor on their outer surfaces. There are no ascites present containing malignant cells. The capsule is intact. |
| Stage IC | The tumor is classified as either Stage IA or IB and one or more of the following are present: (1) tumor is present on the outer surface of one or both ovaries; (2) the capsule has ruptured; and (3) there are ascites containing malignant cells or with positive peritoneal washings. |
| Stage II | Growth of the cancer involves one or both ovaries with pelvic extension. |
| Stage IIA | The cancer has extended to and/or involves the uterus or the fallopian tubes, or both. |
| Stage IIB | The cancer has extended to other pelvic organs. |
| Stage IIC | The tumor is classified as either Stage IIA or IIB and one or more of the following are present: (1) tumor is present on the outer surface of one or both ovaries; (2) the capsule has ruptured; and (3) there are ascites containing malignant cells or with positive peritoneal washings. |
| Stage III | Growth of the cancer involves one or both ovaries, and one or both of the following are present: (1) the cancer has spread beyond the pelvis to the lining of the abdomen; and (2) the cancer has spread to lymph nodes. The tumor is limited to the true pelvis but with histologically proven malignant extension to the small bowel or omentum. |

Table 1-2. Continued.

| Stage of ovarian cancer | Description |
|---|---|
| Stage IIIA | During the staging operation, the practitioner can see cancer involving one or both of the ovaries, but no cancer is grossly visible in the abdomen and it has not spread to lymph nodes. However, when biopsies are checked under a microscope, very small deposits of cancer are found in the abdominal peritoneal surfaces. |
| Stage IIIB | The tumor is in one or both ovaries, and deposits of cancer are present in the abdomen that are large enough for the surgeon to see but not exceeding 2 cm in diameter. The cancer has not spread to the lymph nodes. |
| Stage IIIC | The tumor is in one or both ovaries, and one or both of the following is present: (1) the cancer has spread to lymph nodes; and/or (2) the deposits of cancer exceed 2 cm in diameter and are found in the abdomen. |
| Stage IV | This is the most advanced stage of ovarian cancer. Growth of the cancer involves one or both ovaries and distant metastases (spread of the cancer to organs located outside of the peritoneal cavity) have occurred. Finding ovarian cancer cells in pleural fluid (from the cavity which surrounds the lungs) is also evidence of stage IV disease. |



Table 1-3. Comparison between aptamers and antibodies.

| Parameter | Antibodies | Aptamers |
|---|---|---|
| Production | - In-vivo<br>- Long, expensive<br>- Difficult purification<br>- Immunogen targets<br>- Affinity changes from one batch to another | - In-vitro<br>- Quick, low cost<br>- High standard purification<br>- All type of targets<br>- Reproducibilty from one batch to another |
| Stability | Sensitive to temperature (irreversibility of the denaturation) | Stable: transport at room temperature |
| Chemical modifications | Decrease or lost of affinity after modifications | No change of affinity (control on the position of modification) |

# CHAPTER 2
# SELECTION ON *METHICILLIN-RESISTANT STAPHYLOCOCCUS AUREUS* AND GENERATION OF APTAMERS

## Introduction

As mentioned in the introduction, *Staphylococcus aureus* bacterial infection is a worldwide health concern. Not only are cases found in hospital environments but also infected cases have been reported in the community[9,12,15,18]. Those infections are treated using beta-lactam drugs. Nevertheless, with the increasing appearance of resistant strains, the most common being the *methicillin-resistant Staphylococcus aureus* (*MRSA*), treatment can be challenging, and post-treatment outbreaks are reported in the global literature. Over the course of the past two decades, mammalian cells have been the focus of most aptamer studies using the SELEX technique[54,64,96]. Since Staphylococcal infections have shown a dramatic global increase over the last few decades[97] and since the *Staphylococcus aureus* bacterium is a superbug, which has developed resistance to all drugs generated so far[9,12,15,18], we proposed that an aptamer selection of *MRSA* would provide a useful tool to further investigate *MRSA*-targeted applications. Indeed, an aptamer, which is a single-strand DNA, would offer molecular recognition and could easily be chemically modified if necessary.

The bacterial cell-based selection of aptamers described in this chapter was performed using the well-established SELEX technique, which is usually used on mammalian cells, throughout several rounds of incubation[75]. A good quality bacterial culture is essential to the success of this technique, as well as the level of gene expression of the bacteria, since the recognition occurs on the membrane of the cell.

This chapter describes the methods used to carry out the selection, generate aptamers, and characterize their binding properties.

## Materials and Methods

### Instrumentation, Reagents and Buffers

Bacterial culture in broth was performed using the Forma Orbital Shaker – Hepa filter from Thermo Electron Corporation. Centrifugations were run either in an Eppendorf Centrifuge 5810R, 15 amp version, or in an Eppendorf Centrifuge 5417R. DNA concentrations and OD600 were determined using a Biorad Smart Spec Plus spectrometer, and electrophoresis gels were read on the GE Image Quant 400. Then, electrophoresis gels were cast and analyzed on a Biorad minisub cell GT.

All PCR mixtures contained 50 mM KCl, 10 mM Tris HCl (pH 8.3), 1.5 mM $MgCl_2$, dNTPs (each at 2.5 mM), 0.5 µM each primer, Hot start Taq DNA polymerase (5 units/µL) (TaKaRa) and DNase-free water. Amplification was carried out on a BIO-RAD thermocycler at 95°C for 30 sec, 60.7°C for 30 sec, and 72°C for 30 sec, followed by the final extension for 3 min at 72°C. Pool enrichment was monitored by flow cytometry analysis using a FACScan cytometer (BD Immunocytometry Systems).

Dulbecco's Phosphate Buffered Saline (PBS) was used to prepare the binding buffer (4.5 g/L glucose, 5 mL $MgCl_2$, 1.0 g/L bovine serum albumin and 100 mg/L tRNA) and the 90:10 $H_2O$: PBS washing buffer. Gel electrophoresis was prepared and run using TBE buffer: 1X Tris/Borate/EDTA (TBE) buffer (Fisher Scientific Inc.).

### Bacteria Strains and Growth

*Methicillin-resistant Staphylococcus aureus* (*MRSA*), standard strain 43300, lot number 58228213, was purchased from ATCC, and a clinical strain of *Enterococcus faecalis (E. faecalis)* was obtained from the Emerging Pathogens Institute at the University of Florida.

*MRSA* was cultured at 37°C in ATCC medium 18 - Trypticase soy agar with addition of 4mg/L of sterile methicillin in order to maintain the resistant structural property of the bacteria. *E. faecalis* was cultured at 37°C in ATCC medium 260 – Trypticase soy agar with defibrinated sheep blood and in the corresponding broth with no blood.

The *MRSA* bacterial strain 43300, also designated F-182, is a clinical isolate from Kansas[98]. The *E. faecalis* strain donated by the Emerging Pathogens Institute is a clinical isolate from Shands Hospital, University of Florida. The culture of *MRSA* required biosafety-level II certification.

Stock solutions of each cell line were prepared for the selection study and aptamer characterization: a total of four solutions were made. The best results were obtained by the following procedure. Cell lines were incubated overnight at 37°C on their respective agar plates. The folllowing day, a single colony from each plate was replated and incubated overnight at 37°C; then 3-4 bacterial colonies were transferred from the agar plate to 15 mL Corning centrifuge tubes filled with 6-7 mL of the corresponding broth and incubated overnight at 37°C. From this stock, 3 drops of bacterial solution were transferred to another 15mL Corning centrifuge tube containing 4 mL of corresponding broth and incubated for 3-4 hours. These two batches of incubated cells (*MRSA* and *E. faecalis*) were separately washed twice with PBS and fixed in 70:30 methanol: DNase-free water. As a precaution to minimize clumping, DNase-free water was added first, and cells were resuspended, followed by the corresponding volume of methanol. After 2 h of fixation at 4°C, cells were stored in 10% PBS: DNase-free water. Finally, OD600 was measured for each batch, and a mixture was prepared to obtain the lowest OD600

measured out of the two batches. In other words, an equimolar mixture of the two time of growth (overnight and 3-4 h) was obtained.

Four stock solutions of each bacterium were used for the entire selection. For *MRSA*, stock solution 1: OD600 = 2.08, 15 mL; stock solution 2: OD600 = 1.03, 22 mL; stock solution 3: OD600 = 1.73, 18.7 mL; stock solution 4: OD600 = 1.58, 59.5 mL. For *Enterococcus faecalis*, stock solution 1: OD600 = 1.18, 12.5 mL; stock solution 2: OD600 = 0.762, 17.5 mL; stock solution 3: OD600 = 2.49, 14 mL; stock solution 4: OD600 = 2.27, 66 mL.

**Growth Curve Determination**

The growth curves of both *MRSA* and *E. facecalis* were determined over a period of 12 h. A single plate colony of each bacterium was cultured using the corresponding broth. Then a measurement of the absorbance was performed every hour for 12 hours. And finally the log (absorbance) versus the time was plotted to obtain the growth curve.

**SELEX Library and Primers**

The library consisted of a 40-base randomized region flanked by primer regions, each consisting of 18 nucleotides (5'- ATC CAG AGT GAC GCA GCA $(N)_{40}$ TGG ACA CGG TGG CTT AGT -3'). The forward primers were labeled with 5'-FITC, and the reverse primers were labeled with 5'-biotin:

- Forward primer (sense): 5'-FAM-ATC CAG AGT GAC GCA GCA-3'
- Reverse primer (anti-sense): 5'-Biotin- ACT AAG CCA CCG TGT CCA-3'

FITC labeling enabled fluorescence monitoring during selection by flow cytometry, while biotin was used for separation of the sense strand from the antisense strand after PCR amplification through streptavidin-biotin interaction and subsequent alkaline denaturation. All oligonucleotides were synthesized by standard phosphoramidite

chemistry using an ABI 3400 DNA synthesizer (Applied Biosystems) and purified by reverse phase HPLC (Varian Prostar).

### Chemical Synthesis of the Random Library and Other DNA Sequences with the ABI 3400 DNA Synthesizer

In nature, DNA is synthesized by incorporation of nucleotides by the DNA polymerase in the 5'-3' direction. Chemically, synthetic nucleic acids are synthesized by solid phase using phosphoramidite chemistry in a DNA synthesizer [Figure 2-1].

Phosphoramidite chemistry allows the DNA synthesis to occur without the presence of any enzyme, which, in nature, uses the energy stored in the triphosphate bonds to catalyze the formation of a new phosphodiester bond between the bases.

The synthesis occurs in the 3'-5' direction. A controlled pore glass (CPG) serves as a solid support; it is a non-swellable glass bead with narrow pore size distribution and high surface area. The CPG contains the first 3' base or modification (dye for instance) of the sequence. Subsequent bases are introduced as phosphoramidites, on which all active groups are blocked by protecting groups. The oxygen on the 3'-position is protected by a dimethoxytrityl group (DMT); the 5'-phosphate group is protected with a di-isopropylamine and a 2-cyanoethyl group; and the base itself is protected by a benzoyl group.

Each base addition occurs according to the following steps: first, the DMT protecting group on the 5'-end is removed by reaction with the dichloroacetic acid, giving a 5'-hydroxyl group; second, the base to be added is activated with a tetrazole molecule for the coupling reaction; third, the coupling occurs and forms the phosphite linkage; and finally, there is oxidation of the phosphite linkage into a more stable phosphate linkage.

Any unreacted 5’-hydroxyl group is capped by reaction with an acetic anhydride molecule. The capping prevents the sequence to continue coupling with other bases that could form a sequence with a deletion.

**DNA Deprotection**

At the end of the DNA synthesis, the newly synthesized DNA strand is still attached to the CPG bead on its 5’-end and protected at different levels: a 2-cyanoethyl group protects the free oxygen in the phosphate groups, a benzoyl group protects the bases, and a DMT group protects the 3’-end. Since the DMT groups are needed for the HPLC, all other protecting group needed to be removed. Each column of DNA was dried with air and the beads were transfered to a test tube for deprotection. They were incubated for 30 min at 65°C with 2-3 mL of AMA. Once the solution was cooled, the supernatant was transfered to a centrifuge tube, leaving behind the CPG beads. Based on the supernatant volume, 1/10 volume of 3 M NaCl and 2.5 volume of cold ethanol were added. The solution was vortexed and frozen for 30 min for the DNA to precipitate.

**HPLC Preparation and Purification**

The high performance liquid chromatography was used to purify the DNA from the truncated DNA sequences present at the end of the synthesis. The DNA precipitate obtained after DNA deprotection was centrifuged for 30 min at 4,000 rpm. The supernatant was discarded and the DNA was resuspended in 0.10 M TEAA. The solution was centrifuged at 14,000 rpm for an additionnal 1 min to remove any CPG beads left from the precipitation step. This step is critical since any remaining beads could osbtruct the HPLC column.

The purification was accomplished using a ProStar HPLC station (Varian CA) equiped with a $C_{18}$ reversed-phase column (Econosil, 5 µM, 250 x 4.6 mm) from Alltech

(Deerfield, IL). On a reversed-phase column, polar compounds elute faster than non-polar compounds. The separation was possible because full-length DNA sequences contained a DMT group on the 3'-end, while truncated sequences had an acetate group, which is smaller and more polar than the DMT group. For that reason, the full-length DNA sequences interacted with the stationary phase for a longer time. The elution was achieved using a gradient elution with acetonitrile and 0.10 M triethylamine acetate in water. The chromatography began at 100% TEAA, which is an ionic solution. It is important to note that DNA is ionic and therefore, it does not interact well with the stationary phase by itself. The DNA sequences are made neutral and less polar by pairing the anionic phosphate linkages with triethylammonium cations. As the HPLC progressed, the percentage of acetonitrile is gradually increased until full elution of the sample.

After purification, the sample was dried by centrifugal evaporation. Then a final incubation with 80% acetic acid for 30 min was performed to remove the DMT protecting group and speed vacuumed. Finally, the DNA was resuspended in water and the absorbance of this stock solution was measured at 260-280 nm. The concentration of DNA was calculated using the Beer-Lambert law $A=\varepsilon lc$, where A is the absorbance of the DNA sample, $\varepsilon$ is the molar absorptivity of each DNA oligonucleotide, l is the light path of the cuvette and c is the sample concentration.

**Optimization of PCR Conditions for the SELEX Procedure**

Polymerase chain reaction (PCR) is a technique used to increase the DNA concentration exponentially. It is divided in three stages: denaturation, annealing and elongation. In order to determine the annealing temperature, the optimization was performed using 8 samples: 6 containing the random library and 2 negative controls

[Table 2-1]. The temperature range for the random library was: 51.5°C, 52.2°C, 53.4°C, 55.2°C, 57.6°C, 59.5°C, 60.7°C and 61.5°C. The control tubes were set at the lowest and highest temperatures.

**Gel Electrophoresis**

PCR products can also be analyzed using agarose gel electrophoresis. During the selection process, this technique is used to analyze the PCR products from the cycle optimization and to determine the most efficient number of rounds. The PCR samples were loaded on a 3% agarose gel and the DNA was visualized using 0.5 mg/mL ethinium bromide, which fluoresces upon exposure to UV light. The 7x7 $cm^2$ 3% agarose gel was prepared by mixing 1.2 g agarose and 40 mL of TBE buffer and melting by heat (microwave for 1 min). Then 0.2 µL of ethinium bromide was added and the mixture was poured in a gel cast using an 8-well comb and allowed to cool before loading. Each mixture was loaded using 8 µL of the PCR product or control, and 2 µL of loading buffer (bromophenol blue and glycerol). A 25 bp ladder was used to estimate the size of the DNA. The gel was run at constant voltage of 100 V for 23 min to move the negatively charged DNA toward the positive electrode. The resulting gel was analyzed under UV light.

***In-Vitro* Cell-SELEX Procedure**

In this selection, *MRSA* standard strain 43300 was used as the target cell line and *E. faecalis* was used for the counter selection. For the first round, all subsequent $10^7$ cells were incubated with 22 nmol of naïve ssDNA library dissolved in BB. All other rounds were incubated with 25 pmol of the library obtained from the previous round. Before incubation, the DNA library was denatured at 95°C for 5 min and quickly cooled on ice for 10 min, allowing each sequence to form the most stable secondary structure.

Each round was performed with the counter selection first with an incubation of 1 hour in an orbital shaker at 4°C. The counter selection is used strategically in the SELEX technique to remove non-specific binding. In this particular example, sequences binding to *MRSA* cells are put aside and amplified whereas sequences binding to *E. faecalis* (the counter cell line) are removed from the pool. The supernatant containing the unbound DNA sequence was then incubated with the positive cell line for 30 min in the same conditions. The pellet obtained was then washed two or three times, depending on the round with the stringency of the washes increased to 3 washes with 1 mL of WB for 3 min. After centrifugation, the pellet was resuspended in DNase-free water, denatured at 95°C for 15 min and centrifuged at 14,000 rpm for 2 min.

The supernatant containing the ssDNA was recovered and amplified by PCR using FITC- and biotin-labeled primers to increase the number of copies of individual sequences. Two preparative PCRs were performed at the end of each round using the latest enriched pool as the template. The first was used to optimize the number of rounds using 6 PCR tubes and 1 for negative control; and the second PCR amplified the pool using the optimum number of rounds on 1 mL of PCR solution (10 tubes). The optimum round was determined by analysis of the gel electrophoresis [Figure 2-2].

As showed in Figure 2-2, amplifications were carried out with an initial denaturation for 3 min at 95°C, followed by the PCR round including 30 sec at 95°C, 30 sec at 60.7°C, and 30 sec at 72°C, and ended by final extension for 3 min at 72°C. PCR tubes were selectively removed from rounds 14 to 24 for further analysis by gel electrophoresis. The optimum cycle was representated by the brightest single band of the agarose gel, which is 24 cycles in this example.

The sense ssDNA strands obtained after the preparative PCR were separated from the biotinylated antisense ssDNA by streptavidin-coated Sepharose beads (GE Healthcare Bioscience). The ssDNA was eluted from the beads by melting in 0.2 M NaOH. The resulting solution was desalted using a NAP5 column, dried and resuspended in BB to a concentration of 250 nM. The purification steps are detailed below.

The selection process was repeated until the level of enrichment, monitored by flow cytometry, reached a plateau. Once the plateau was reached, pools of interest were submitted for sequencing using both the 454 and Ion Torrent techniques.

**DNA Purification**

As mentioned in the section above, dsDNA is obtained after the PCR amplification and the ssDNA FITC-labeled needs to be separated from the Biotin-labeled ssDNA in order to be used in the SELEX protocol. This purification was performed by affinity chromatography. The column, mounted at the tip of a syringe, was filled with 140 µL Streptavidin beads (Streptavidin Sepharose, GE Healthcare) and washed with 2500 µL PBS. The amplified sample was then passed through the column 3 times to make sure the pool stayed on the beads by Biotin-Streptavidin interaction and primers were removed by washing with 2500 µL PBS. Then, 500 µL 200 nM NaOH was added to dissolve the DNA and collect the FITC single strand. Finally the filtrate was passed through a desalting column. The column was washed with 15 mL DI water and, after the filtrate was passed through, 1000 µL DNase free water was added and the filtrate was collected. After the DNA concentration of the pool was measured spectrophotometrically at 260-280 nm and the appropriate volume of binding buffer for storage at 250 nM or 500 nM was added.

### Monitoring of the Binding Through Flow Cytometry

Binding assays were used for three purposes: (1), to monitor the progression of the selection; (2), to assess the potential aptamer candidates; and (3), to determine their apparent dissociation constants.

Binding assays to monitor the selection and to assess the potential aptamers followed a protocol based on the target cells, here *MRSA* ($10^7$ cells), which were incubated at 4°C for 30 min with 100 µL binding buffer and with 250 nM of either enriched library-FITC-labeled or 5'-FITC-labeled aptamers to monitor the selection or to assess potential aptamers, respectively. In the case of the apparent dissociation constant determination, the incubation at 4°C was performed using a panel of concentrations of the aptamer. The fluorescence intensity was determined by FACScan cytometry (BD Immunocytometry Systems) by counting 60,000 events for binding assays and 30,000 for Kd determination. Details about the flow cytometry mechanism of action are given in chapter 3. The intensity for cells only with random library (Library 0) was used as the background signal. The specific binding was obtained by subtracting the mean background intensity from the mean fluorescence intensity of the cells plus aptamers.

The equilibrium dissociation constant (Kd) was obtained by fitting a plot of the specific binding intensity (Y) versus the aptamer concentration (X) to the equation Y = Bmax.X/(Kd+X), using SigmaPlot (Jandel, San Rafael, CA).

## Results and Discussion

### Bacteria Growth Study

As stated in the chapter introduction, a good quality bacterial culture and appreciable gene expression level are essential for the success of a cell-selection.

While the resistant genes of *MRSA* bacteria are maintained by including the Methicillin antibiotic in its culture agar or broth, it is important to note that *MRSA* bacteria synthesize their virulence factors in two phases. At the beginning of bacterial growth, also known as the exponential or logarithmic phase, genes coding for adhesins are activated. Later, genes coding for toxins are activated. This sequential activation is regulated by a virulence regulation system named agr (accessory gene regulator)[27,28]. To make sure cultural batches would contained both types of virulence factors, growth curves of both *MRSA* and *E. faecalis* were determined [Figure 2-3].

Based on the *MRSA* growth curve [Figure 2-3A], the beginning of the exponential phase was determined to be around 3 h and the end of growth was about 8h. In order to make sure that all virulence genes were expressed, the stock solution mixture of growth was chosen to be an equimolar mixture of the 3-4 h and overnight (12 h) growths. *E. faecalis*, a common gut bacterium, was considered to be a good fit as a counter selection because of its Gram-positive structure, similar to *MRSA*. To ensure that bacteria were alive before fixation with methanol, neither bacterium was cultured longer than 12 h.

**Optimization of PCR Conditions**

During the PCR process, there is a risk of getting primers at the wrong position. The higher annealing temperature increases the likelihood that the primers will bind to their expected priming positions. For that reason, the annealing temperature of the primers used throughout the selection process was optimized to be the highest for efficient amplification with minimal non-specific binding in the desired temperature range.

The PCR was run between 51.5°C and 61.5°C, and the PCR products were compared by gel electrophoresis. Since the likelyhood of the primers to bind with their expected priming region increases at high temperature, the optimal annealing temperature was determined to be 60.7°C.

**Cell-SELEX Selection**

In order to select aptamers binding to *MRSA*, a random library of ssDNA was subjected to sequential binding with the objective of selecting those sequences from the pool having high binding affinity to surface markers on the target *MRSA* bacterium. Counter-selection using the Gram-positive commensal bacterium *Enterococcus faecalis* was performed on each round. This step was necessary to eliminate sequences binding to common surface markers, and at the same time, to enrich specific markers on the target bacterium. Both negative and positive cell lines were fixed with methanol before being used in the selection process. Four stock solutions of each fixed bacterium were prepared, as explained in the “Materials and Methods” Section. The first stock solution was used for rounds 1 to 11; the second for rounds 12 to 14; the third for rounds 15 to 17; the fourth was used for binding assays. The eluted pool of each round was amplified by PCR and monitored by flow cytometry. Since the pools were enriched throughout different rounds with sequence binding *MRSA*, an increase in fluorescent signal was observed. The flow cytometry analysis of enrichment of the libraries and the binding assays with individual aptamers were performed on batch four. At the end of the 14th round of selection, a significant increase of specific pool enrichment was observed [Figure 2-4]. After 15 rounds, a plateau was reached, and the selection was continued until round 17 to maximize homology within binding sequence families. The summary of progression of the selection is presented in Tables 2-2 and 2-4.

As observed in Figure 2-4, the last libraries of the selection showed specific binding to the targeted cell line *MRSA*. Since those results were obtained using fixed solutions of both *MRSA* and *E. faecalis*, we further investigated whether the enriched pools generated from fixed cells could also bind to live *MRSA* cells (The selection was performed on fixed cells rather than live cells for safety reasons, since *MRSA* is a biosafety level II hazard). In order to verify whether methanol had an adverse effect on the binding of the enriched pools, we compared the binding of fixed cells with that of live cells [Figure 2-5].

As can be observed in Figure 2-5, the binding was maintained when using live cells, demonstrating little permanent adverse effect on the structure of the membrane proteins of the bacteria.

After successful enrichment, selection pools 15 and 17 were chosen and prepared for sequencing. Pool 15 represents the point at which enrichment started a plateau observable by flow cytometry, and pool 17 is the end of the plateau. Sequencing was performed with the Ion Torrent™ sequencing platform using a different MID per pool. MIDs, or multiplex identifiers adaptors, are added as a tail to the primerof the sequences by PCR amplification. This technique allowed the identification of the pool analyzed once the detail of the sequences was generated. In our case 2 pools were analyzed (pool 15 and 17) and 600,000 sequences were identified.

In analyzing the data, the 40 nt random regions were aligned using the MAFTT alignment program. The alignment generated several different homologous families, and representative sequences were identified using the MAFTT and mfold oligo analyzer software programs. Putative DNA aptamers were then synthesized, labeled

with FAM, purified by HPLC and quantified. Binding assays were performed for each sequence on *MRSA* cells and *Enterococcus faecalis* cells to determine the relevant aptamer sequences.

Initially, we chose all candidates showing observable binding to the target *MRSA*, in comparison with the unselected library as a control. Positive sequences were further screened with *Enterococcus faecalis* to select those aptamers showing specific binding to *MRSA*. All flow cytometry data were obtained with unlabeled cells and random library (Library 0) as the negative control. As shown in Figure 2-6, four of those sequences showed specific binding to *MRSA*.

Details about the sequences of the aptamers generated against *MRSA* are listed in Table 2-4 with their corresponding percentage in the overall pool sequenced. It is interesting to note that, even though the initial random library contained a 76mers, the aptamers generated varied slightly in length, most probably due to some modifications during the amplification process such as loss or substitution of nucleotides.

During the sequencing analysis, one tends to select for the more abundant sequences. Based on the results shown in Table 2-4, it is interesting to note that even though it is the most obvious strategy, the aptamer structure itself is just as meaningful based on its binding properties. This is demonstrated with DTMRSA4, which represents only 0.32 % of the total sequences, yet shows similar binding affinity as DTMRSA2, which is the most abundant aptamer sequence.

The dissociation constant, usually denoted Kd, is used as an indicator of the affinity of a biomolecular interaction (smaller Kd indicates higher affinity). In our case, we are interested in knowing the affinity between the aptamer and its targeted

bacterium, i.e. how tightly an aptamer binds to its aptamer target. The dissociation constants were obtained by measuring the aptamer-target binding at 4°C, with increasing concentrations of the aptamer, to produce a saturation binding curve as shown in Figure 2-7. After the curve was obtained, the SigmaPlot software was used to obtain the value of the apparent dissociation constant Kd.

Based on the Kd values obtained [Table 2-5], we believe that these affinities are sufficient for *MRSA* detection assays. Indeed, apparent dissociation constants have been studied for aptamers chosen by cell-SELEX on other bacteria[99,100], and values typically ranged between 30 and 250 nM, similar to those observed here.

## Conclusion

*Methicillin-resistant Staphylococcus aureus* is a bacterium that is resistant to many antibiotics. In the community, most *MRSA* infections are found to be skin infections. In medical facilities, *MRSA* infections cause bloodstream life-threatening infections, surgical site infections and pneumonia. Finding new means to fight against those infections is an emergency. This study demonstrated the possibility of using the SELEX technique on fixed bacteria cells to develop aptamers binding to *MRSA* with the same binding results on live bacterial cells. Four aptamers were generated after 17 rounds of selection to recognize the bacterial membrane with Kd constants varying between 90 and 200 nM. Since the smaller the Kd, the tighter the binding, DTMRSA4 is the aptamer showing the best binding properties with a Kd of 95 nM. The aptamer's ability to selectively bind to whole cells presents a potential clinical use of the selected aptamers as nanocarriers for the identification of antibiotic-resistant cell lines in patients. The successful development of an assay that can differentiate the resistance of

*Staphylococcus aureus* colonies could facilitate the search for a more effective treatment and management of the disease. Finally, research development based on aptamers would offer a cheaper alternative to the use of antibodies and would offer larger possibilities of chemical modifications within the aptamers.


Figure 2-1. ABI 3400 DNA Synthesizer.

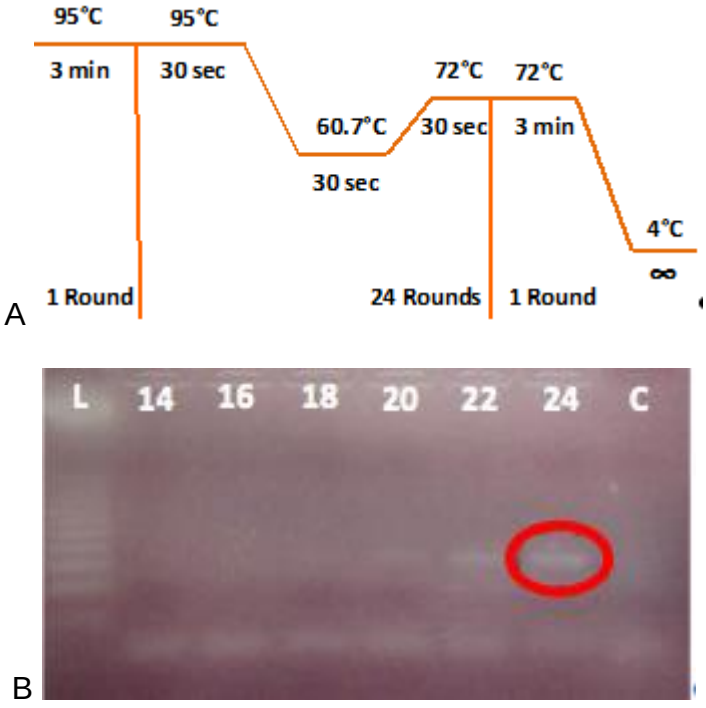


Figure 2-2. Example of PCR optimization and gel analysis after Round 5 of selection. A) Optimized PCR cycles conditions, here 24 PCR rounds are used, B) Gel electrophoresis analysis: L: 25 bp ladder; 14-24: rounds analyzed; and C: negative control.

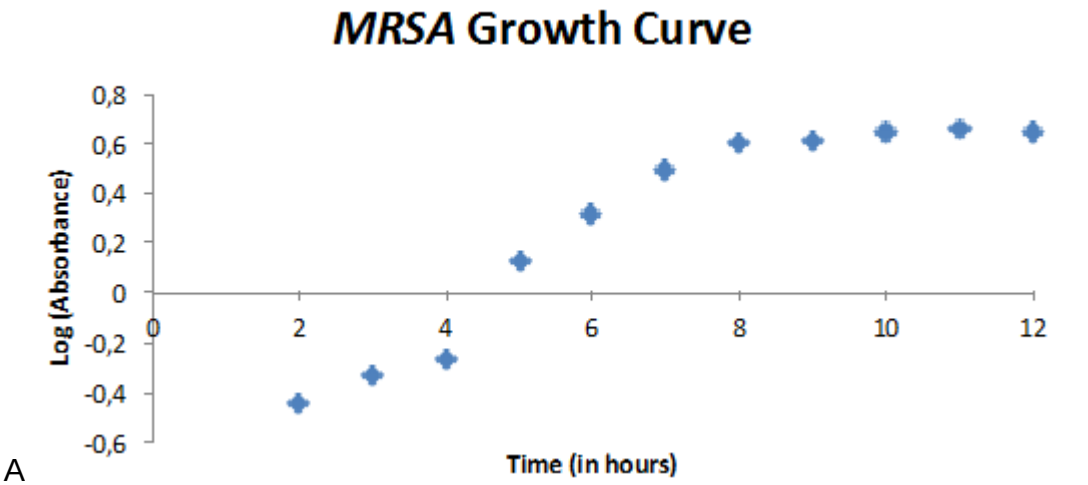


A

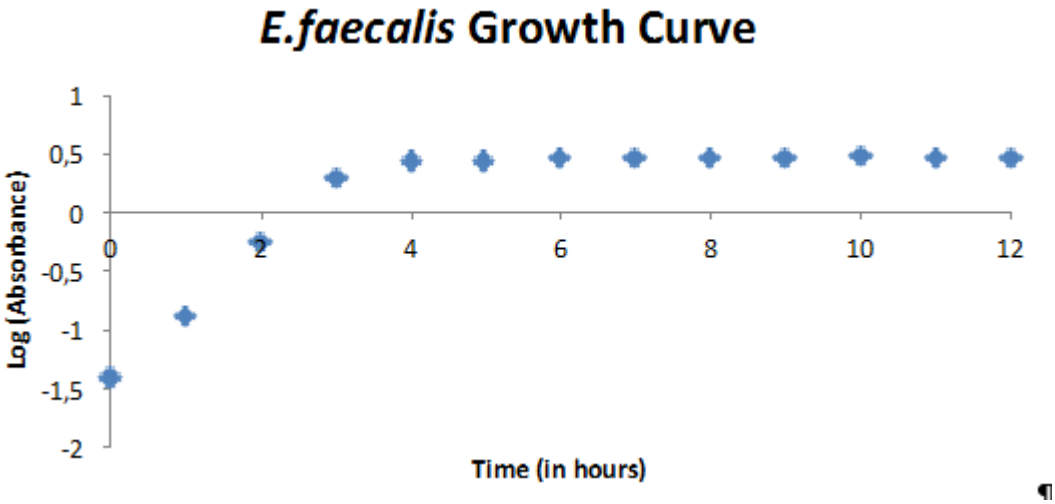


B ¶

Figure 2-3. Growth curves of the bacteria used in the selection. A) *MRSA* 43300 strain. B) *E. faecalis* clinical strain.

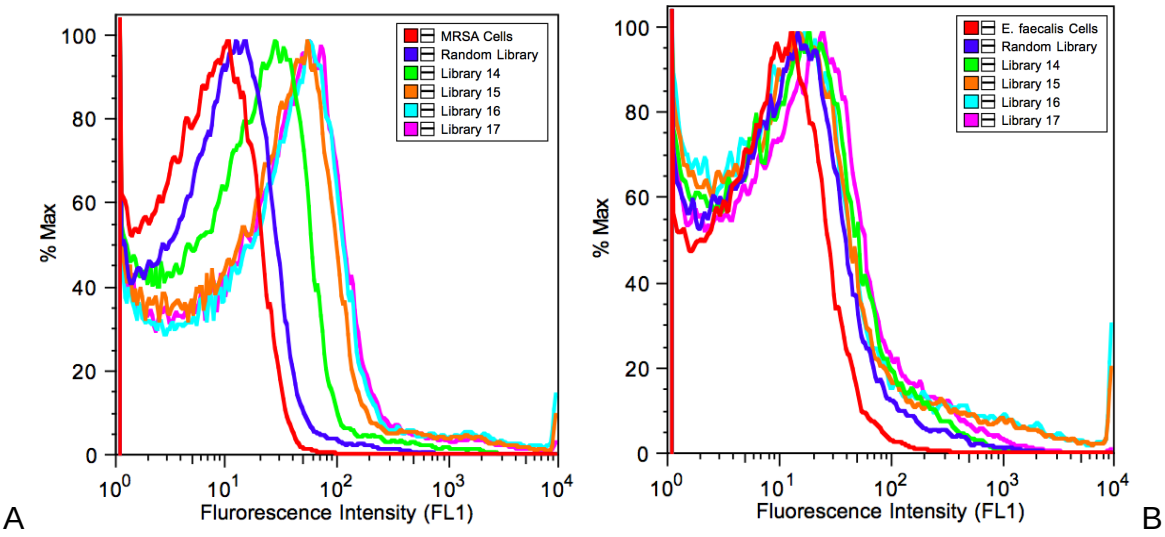


A B

Figure 2-4. Flow cytometry analysis near the end of the selection. A) Targeted cell line *MRSA*, B) Counter cell line *Enterococcus faecalis*.

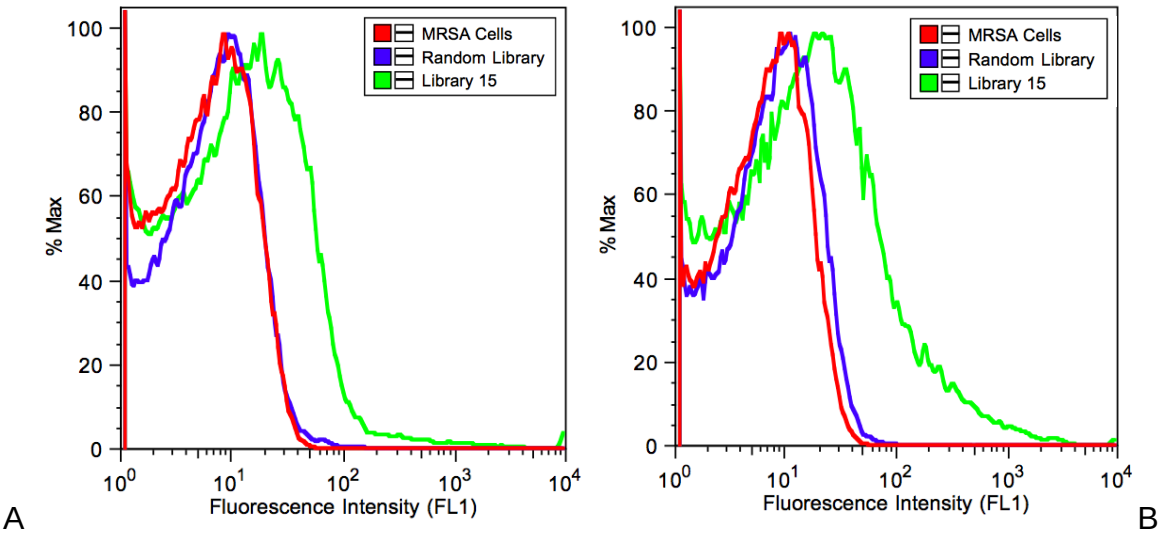


A B

Figure 2-5. Comparison of the binding results of Library 15. A) On fixed *MRSA* cells, B) On live *MRSA* cells.

Accepted to the World Journal of Translational Medicine, written by Turek D., Van Simaeys D., Johnson J., Ocsoy I., Tan W., for future publication.

DTMRSA1

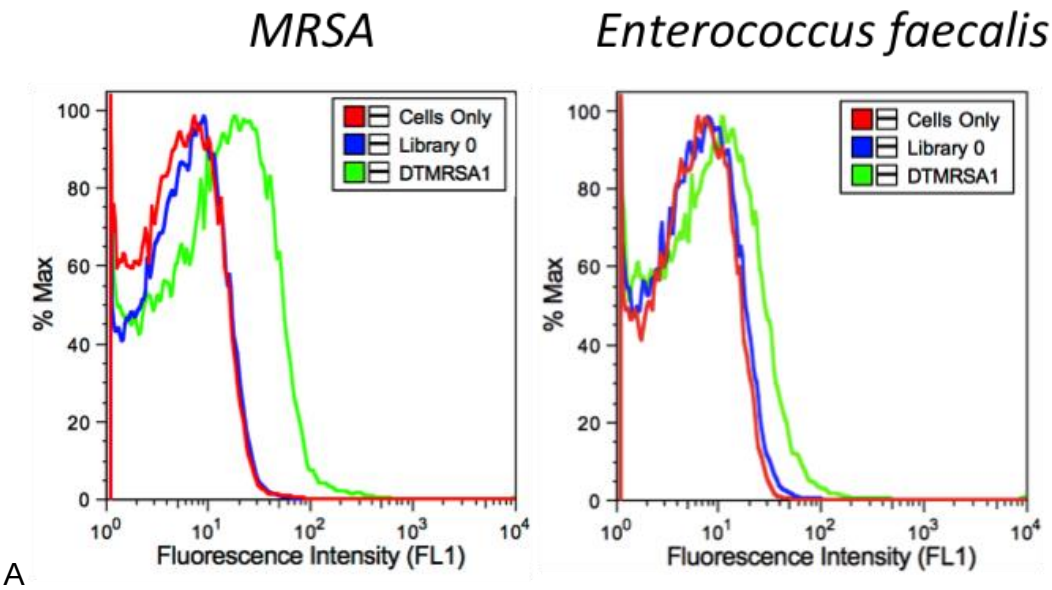


A

DTMRSA2

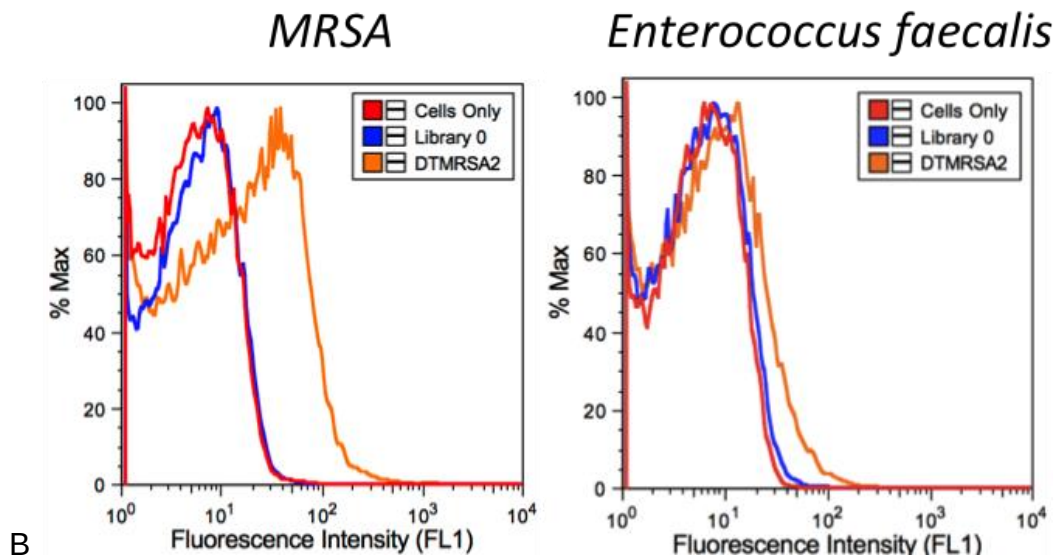


B

C

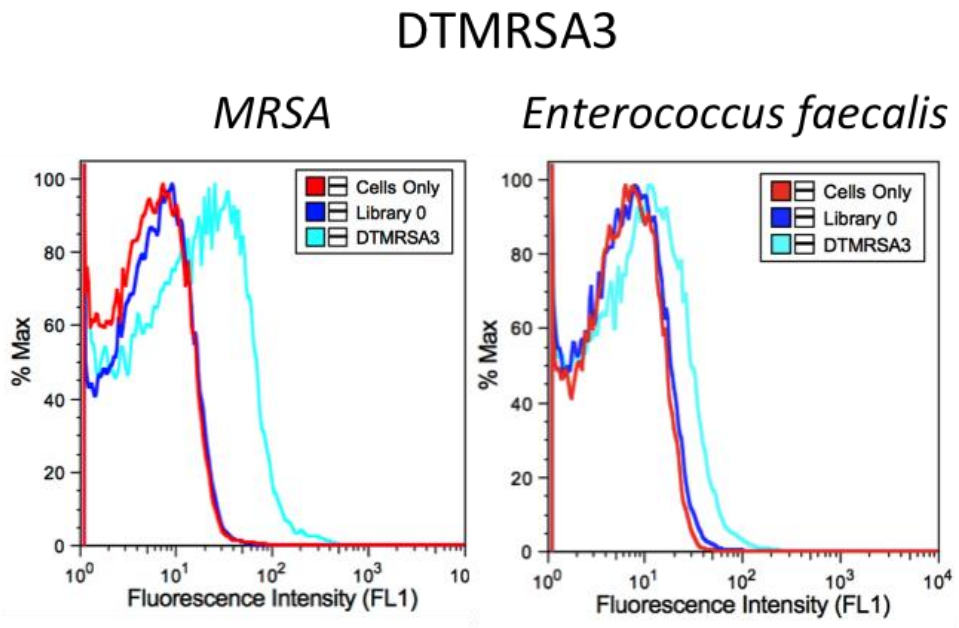


D

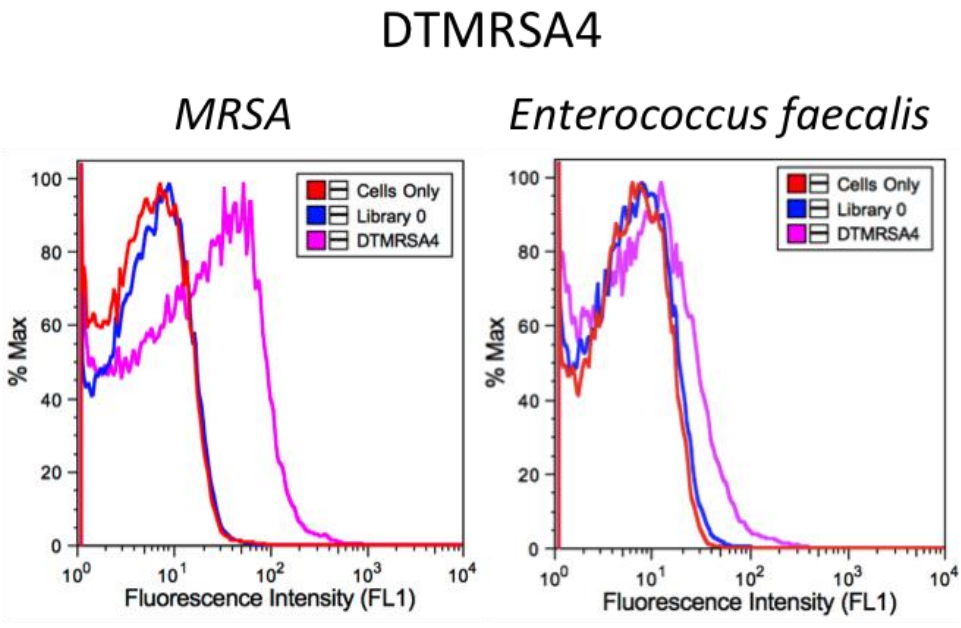


Figure 2-6. Flow cytometry histograms of relevant aptamer candidates for *MRSA*. A) Aptamer DTMRSA1, B) Aptamer DTMRSA2, C) Aptamer DTMRSA3 and D) Aptamer DTMRSA4.

Accepted to the World Journal of Translational Medicine, written by Turek D., Van Simaeys D., Johnson J., Ocsoy I., Tan W., for future publication.

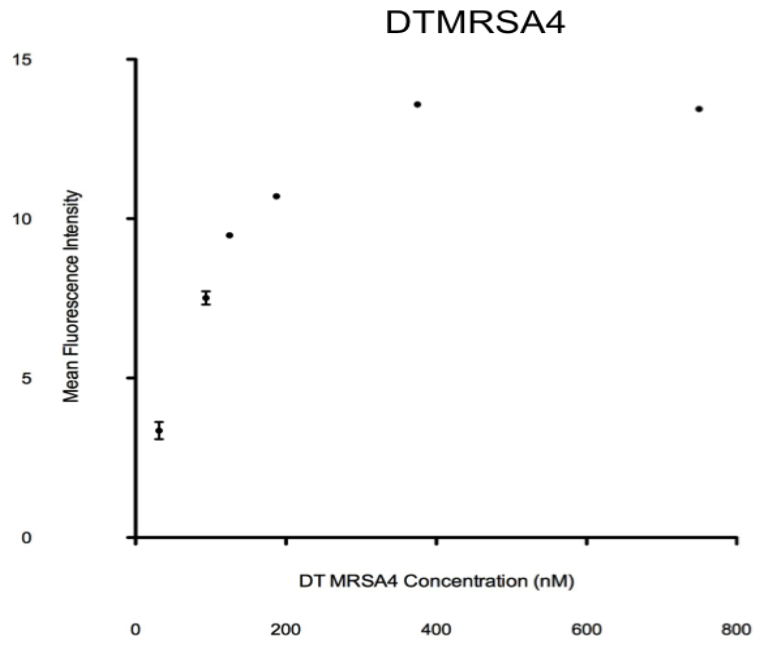


Figure 2-7. SigmaPlot binding curve of the aptamer DTMRSA4 used for the Kd value determination.

Accepted to the World Journal of Translational Medicine, written by Turek D., Van Simaeys D., Johnson J., Ocsoy I., Tan W., for future publication.

Table 2-1. Preparation of the PCR tubes for the optimization of PCR conditions.

| Random Library PCR Tubes | Control PCR Tubes |
|---|---|
| 33.35 µL DNase-free water | 33.35 µL DNase-free water |
| 5 µL 10X PCR Buffer | 5 µL 10X PCR Buffer |
| 4 µL dNTP (2.5 mM) | 4 µL dNTP (2.5 mM) |
| 2.5 µL Primers (10 µM) | 2.5 µL Primers (10 µM) |
| 0.15 µL *Taq* polymerase | 0.15 µL *Taq* polymerase |
| 5 µL Random Library | 5 µL DNase-free water |

Table 2-2. Number of bacteria cells used for each round of selection and incubation times.

| Cell line | Number of cells | Incubation time |
|---|---|---|
| *MRSA* 43300 | $10^8$ | 30 min |
| *Enterococcus faecalis* | $0.5 \times 10^8$ | 1 hour |

Table 2-3. Summary of progression of *MRSA* selection.

| Rounds | Negative selection round | Number of washes, time, volume of WB | PCR amplification cycles | Volume of eluted DNA at 250 nM |
|---|---|---|---|---|
| 1 | No | 2, 2 min, 2000 µL | 22 | 656.4 µL |
| 2 | Yes | 2, 30 s, 300 µL | 28 | 192.8 µL |
| 3 | Yes | 3, 30 s, 300 µL | 20 | 316.4 µL |
| 4 | Yes | 3, 2 min, 1000 µL | 20 | 124.8 µL |
| 5 | Yes | 3, 2 min, 1000 µL | 24 | 266.4 µL |
| 6 | Yes | 3, 3 min, 1000 µL | 22 | 562.0 µL |
| 7 | Yes | 3, 3 min, 1000 µL | 22 | 285.2 µL |
| 8 | Yes | 3, 3 min, 1000 µL | 12 | 296.4 µL |
| 9 | Yes | 3, 3 min, 1000 µL | 22 | 161.2 µL |
| 10 | Yes | 3, 3 min, 1000 µL | 20 | 474.8 µL |
| 11 | No | 3, 3 min, 1000 µL | 12 | 327.6 µL |
| 12 | Yes | 3, 3 min, 1000 µL | 18 | 487.2 µL |
| 13 | Yes | 3, 3 min, 1000 µL | 16 | 308.4 µL |
| 14 | Yes | 3, 3 min, 1000 µL | 18 | 513.6 µL |
| 15 | Yes | 3, 3 min, 1000 µL | 16 | 444.8 µL |
| 16 | Yes | 3, 3 min, 1000 µL | 16 | 535.2 µL |
| 17 | Yes | 3, 3 min, 1000 µL | 16 | 634.0 µL |

Table 2-4. Quantitative representation of the different homologous families and *MRSA* aptamer sequences.

Accepted to the World Journal of Translational Medicine, written by Turek D., Van Simaeys D., Johnson J., Ocsoy I., Tan W., for future publication.

| Name of the aptamer | Percent of total sequences | Sequence |
|---|---|---|
| DTMRSA1 | 2.57 % | ATCCAGACGTGACGCAGC$(N)_{38}$TGGACACGGTGGCTTAGTA<br>$(N)_{38}$=ATGCGGTTGGTTGCGGTTGGGCATGATGTATTTCTGTG |
| DTMRSA2 | 33.74 % | ATCCAGAGTGACGCAGCA $(N)_{36}$ TGGACACGGTGGCTTA<br>$(N)_{36}$=CGACACGTTAGGTTGGTTAGGTTGGTTAGTTTCTTG |
| DTMRSA3 | 10.05 % | ATCCAGAGTGACGCAGCA $(N)_{40}$ TGGACACGGTGGCTTAGTA<br>$(N)_{40}$=GTAGATGGTTTGGTTGGTGTGGTTTCCTACTGATGTTGGG |
| DTMRSA4 | 0.32 % | ATCCAGAGTGACGCAGCA $(N)_{39}$ TGTGGACACGGTGGCTTA<br>$(N)_{39}$=TTATGGGGTGTGGTGGGGGGTTAATGCGTTGGTTATCCG |

Table 2-5. Apparent dissociation constants (Kd) of the four aptamers recognizing *MRSA* bacteria.

Accepted to the World Journal of Translational Medicine, written by Turek D., Van Simaeys D., Johnson J., Ocsoy I., Tan W., for future publication.

| Name of the aptamer | Kd (nM) |
|---|---|
| DTMRSA1 | $1.6 \pm 0.5 \times 10^2$ |
| DTMRSA2 | $2.0 \pm 0.6 \times 10^2$ |
| DTMRSA3 | $1.3 \pm 0.5 \times 10^2$ |
| DTMRSA4 | $9.5 \pm 2 \times 10^1$ |

# CHAPTER 3
# CLINICAL SAMPLE RECOGNITION BY *MRSA* APTAMERS AND VISUALIZATION OF THE BACTERIA-APTAMER BINDING

## Introduction

*Staphylococcus aureus* has always been a stumbling block for anti-microbial chemotherapy and has survived all the therapeutic reagents that have been developed in the past 50 years. How this bacterium is able to develop the expression of a number of resistance and/or virulence determinants has been a major concern. The latest estimates of the occurrence *MRSA* are staggering, rising to epidemic proportions in hospitals where, by an estimate provided by the European Antimicrobial Resistance Surveillance System, 40-60 % of all infections were caused by *S. aureus* in the U.S. and UK[14,101]. The erosion of the effectivenes of β-lactam antibiotics since their first use is particularly worrisome, and the ability of the *MRSA* membrane to structurally change through time in order to survive is a characteristic that increases its lethality and decreases its controllability[9,97]. Consequently, the binding ability of the four aptamers generated against *MRSA 43300* was compared in the context of different clinical *MRSA* strains, as well as clinical *Staphylococcus aureus* and *Enterococcus faecalis* strains. Those aptamers were also coupled with gold-nanoparticles (Au-NP) probes and used for visualization by transmission electron microscopy (TEM). The ability of *MRSA* bacteria to change over time in order to survive and counter all medications developed to eradicate it is highlighted in the discussion of this chapter.

## Materials and Methods

### Instrumentation, Reagents and Buffers

Bacterial culture in broth was performed using the Forma Orbital Shaker – Hepa filter from Thermo Electron Corporation. Centrifugations were run in either the

Eppendorf Centrifuge 5810R 15 amp version or the Eppendorf Centrifuge 5417R. DNA concentrations and OD600 were determined using a Biorad Smart Spec Plus spectrometer. Aptamer binding was monitored by flow cytometry analysis using a FACScan cytometer (BD Immunocytometry Systems).

Dulbecco's Phosphate Buffered Saline (PBS) was used to prepare a 90:10 $H_2O$: PBS washing buffer and the binding buffer (4.5 g/L glucose, 5 mL $MgCl_2$, 1.0 g/L bovine serum albumin and 100 mg/L tRNA).

**Bacteria Strains and Growth**

For all binding tests, bacteria were used in their live state. Clinical *MRSA* bacteria were kindly provided by Dr Salemi's research group from the Emerging Pathogens Institute (EPI) at UF. The bacteria will be called *MRSA 2, MRSA 4, MRSA 6 and MRSA 7* in this document. Clinical *Staphylococcus aureus* and *Enterococcus faecalis* were kindly provided by Dr Judith Johnson from the Emerging Pathogens Institute (EPI) at UF. They will be called *S. aureus 164*, *S. aureus 165, S. aureus 166 and E. faecalis 43, E. faecalis 44, E. faecalis 45.* All clinical samples came from patients from Shands Hospital at UF. An equimolar mixture of overnight culture and 2-3h culture of those bacteria strains were prepared to make sure all virulence genes were expressed during the binding.

**Binding Studies using Flow Cytometry**

All binding assays of this study were monitored by flow cytometry on the FACScan flow cytometer (Becton Dickinson Immunocytometry Systems) [Figure 3-1]. In this technique, analyses are performed by passing thousands of cells per second through a laser beam and capturing the light that emerges from each cell as it passes. Particles between 0.5 and 40 μm can be detected using three different fluorescence channels or

wavelengths: 525 nm (FL1), 575 nm (FL2) and 620 nm (FL3). Specific data, such as cell size, complexity and health, can be detected and analyzed by the accompanying software.

Cells are hydrodynamically focused by using a sheath solution that compresses the stream of cells to roughly one cell in diameter [Figure 3-2 A]. Since the aptamers synthesized carry a fluorophore (FITC or Biotin futher bound to PE-cy® 5.5), the greater the number of cells bound to aptamers after incubation, the higher the detector output.

All clinical cell lines were incubated with 250 nM aptamers at 4°C for 30 min and washed twice with 10 % PBS solution before flow analysis. The more shifted to the right the fluorescence histogramm, the more aptamers are binding to the cell.

The software FlowJo© was used to process flow cytometry data and translated into histogramms.

**Aptamer-Gold Nanoparticle Coupling Reaction**

Aptamers DTMRSA1, DTMRSA2, DTMRSA3 and DTMRSA4 were synthesized with a 5'-thiol modification in our laboratory using the ABI 3400 Synthesizer. Ismail Ocsoy, from our nanoparticle subdivision research group, provided the gold-nanoparticles (Au-NP) for this experiment.

Each *MRSA* aptamers (70 µM, final concentration) was diluted and incubated with 1 mL of Au-NP (7.2 nM) for 12 hours. Then 50 µL of 10 mM PBS buffer (pH 7.5) was added to the AuNP-aptamer solution and incubated for another 12 hours. The conjugate AuNP-aptamer was purified by rinsing with PBS and centrifuging at 9600 g for 10 min. This process was repeated twice. The final product was dispersed in DI water and stored at 4°C prior being used for binding assays in the TEM visualization study.

### TEM Visualization of *MRSA* Aptamers via Gold-Nanoparticles

*MRSA* bacteria were dispersed in 1 mL of PBS (pH 7.5) after methanol fixation and concentrations of the bacteria in their stock solution were determined by measuring the absorbance at 600 nm (1 OD600= $10^8$ cells/mL). *MRSA* cells ($10^7$) from the stock solution were mixed with 100 µL of Aptamer-AuNP conjugates (7.2 nM/mL) and incubated for one hour with gentle shaking (130 rpm) at room temperature. At the end of the incubation, unbound nanoparticles were removed with water (300 µL) by repeated centrifugation (3,000 rpm, 8 min, 3 times). After analysis by TEM, 2 µL aliquots of the nanoparticle-conjugated bacteria were allowed to settle on the grid for 20 s and were then blotted using a filter paper (Whatman #4), undisturbing the system. The grids were stained with 1 % uranyl acetate for 30 s to provide contrast for the cell membrane.

TEM assays were performed after incubations of cells only, AuNPs only, sgc8-AuNPs only (sgc8 is a random aptamer) and DTMRSA-AuNP conjugates. Note that the centrifugation speed applied to obtain these results was low (3,000 rpm), compared to the usual speed applied when using AuNPs (10,000 rpm). This made it easier to observe the NPs upon target binding since they were collected with the cell pellet, whereas nonbinding NPs observed in the control tended to remain in the discarded supernatant.

## Results and Discussion

### Aptamer Binding Assays using Clinical Bacteria Strains

After the selection was performed on *MRSA* bacteria cells, it seemed relevant and interesting to check the binding of the four aptamers generated on clinical strains. *Staphylococcus aureus* infection being a very common nosocomial disease[101], we were able to obtain those clinical samples *in-sito* with Shands Hospital, Gainesville. It was

decided, based on the clinical samples obtained, to verify the recognition of the aptamers on four strains of *MRSA*, three strains of *S. aureus* and three strains of *E. faecalis* bacteria [Figure 3-3 A, B and C].

*Methicillin-resistant Staphylococcus aureus* (*MRSA*), *Staphylococcus aureus* (*SA* or *S. aureus*) and *Enterococcus aureus* (*E. faecalis*) are all gram-positive bacteria. Based on their morphological similarities, common binding can be expected by the commonality of proteins among the strains, whereas other proteins are more specific to each type of bacterium. A summary of the binding study is presented in the following table [Table 3-1].

The selected aptamers bound to all clinical *MRSA* strains tested, suggesting that the proteins targeted by those aptamers are common for the different *MRSA* strains. DTMRSA1 and DTMRSA3 show the best specificity and therefore appear to be the best candidates for *MRSA* treatment investigation, DTMRSA1 being the better one of the two, while DTMRSA2 and DTMRSA4 bind to all three types of bacteria.

**Transmission Electron Microscopy (TEM) Analysis**

The four aptamers DTMRSA1 to DTMRSA4 collectively represent a powerful tool to study the membrane structure of *MRSA*, as well as to develop potential treatment modalities to combat this pathogen. As an empirical example of such use, we performed a study to visualize the binding sites of *MRSA* aptamers on the bacterial external membrane. To accomplish this, *MRSA* aptamers were conjugated to gold nanoparticles (AuNPs) for visualization of target binding via transmission electron microscopy (TEM) [Figure 3-4]. The conjugation of the aptamers, 5'-thiol modified, to the gold-nanoparticles was possible because thiols efficiently bind to gold surfaces[102].

Although flow cytometry is one of the best tools to measure the abundance of a membrane protein on cells[103], the introduction of a nanoparticle-aptamer conjugate detectable by TEM instead of a dye could be a valuable adjunct to complement the information obtained from the expression of aptamer targets on the bacteria. This technique allows the visualization of both the binding site of aptamers upon target binding and the structure of the cell wall[104-106]. No binding between *MRSA* and bare gold or a random aptamer (Sgc8) conjugated to gold nanoparticles was observed. However DTMRSA2-AuNP conjugates were attached to the surface of *MRSA*, as detected by TEM. With this successful visualization of the aptamers on *MRSA* cells, we showed that the adduction of nanoparticles on the aptamers did not change their binding properties. Since nanoparticles have unique properties of their own[107,108], we believe this approach can be further extended, depending on the choice of nanoparticles, to study the morphology of the bacteria, as well as detect and/or eradicate them.

### *MRSA* Aptamer Binding after Time and Troubleshooting Tests

Approximately one year after the *MRSA* selection began (a few months after the aptamers were generated), the use of those aptamers in biological applications was to be studied. In that particular case, the intent of the study was to examine their sensitivity under a mixed population of bacteria. For that purpose, aptamers were synthesized with a 3'-biotin modification. Nevertheless, when those aptamers were tested with live *MRSA* cells using the PE-cy® 5.5 dye, no binding was observed.

Following that observation, the following troubleshooting experiments and tests were performed:

1. Binding assays with the 3'-biotin labeled aptamers were repeated. Results were the same: no binding was observed.

2. The 3'-biotin labeled aptamers were resynthesized and the aptamer binding was tested by flow cytometry on live *MRSA* cells. No binding was observed under those conditions.

3. The aptamer stock solution used during the selection was then checked. The flow histogram obtained from this study showed no binding either.

4. The same binding assays were performed on new cells from ATCC (same strain: 43300) and binding was not observed.

After obtaining these results, work by other researchers came to our attention. From those results, previous observations raised our attention. In 2009, the group of Dr Ninsheng Shao at the Beijing Institute of Basic Medical Sciences, Beijing (China) generated aptamers against *Staphylococcus aureus* [Figure 3-5][99].

While working on the *MRSA* selection and to determine if Cao *et al.* had, indeed, previously developed viable aptamer candidates for the recognition of *MRSA* cells, we tested their binding with our commercial strain. As shown in the flow data, those aptamers showed no binding with the resistant strain [Figure 3-6]. These results were interesting and somehow surprising, because one could assume that some proteins must be common to both the non-resistant and the resistant *Staphylococcus aureus*, and the chance of selecting aptamers binding to those common proteins is high.

These observations made three years after publication of Cao's *Staphylococcus aureus* aptamer study, alone with the results obtained in our *MRSA* selection, raised a serious question. Could it be possible that the *MRSA* bacterium changes over time to the point that the bacterium loses the proteins recognized by these aptamers?

While we will try to answer that question a bit further, more troubleshooting binding assays were performed on *MRSA* and *Staphylococcus aureus* clinical strains: *MRSA* 2, *MRSA* 6, *SA* 164 and *SA* 165. For those tests, new 250 nM stock solutions of Cao's

aptamers were prepared; DTMRSA1 aptamer from our own selection was synthesized by the Integrated DNA Technologies (IDT) company, the largest supplier of customed nucleic acids, as well as $APT^{SEB1}$ aptamer, which was developed by DeGrasse[109] against the *Staphylococcus aureus* Enterotoxin B [Figure 3-7]:

5'GGTATTGAGGGTCGCATCCACTGGTCGTTGTTGTCTGTTGTCTGTTATGTTG TTTCGTGATGGCTCTAACTCTCCTCT3'

De Grasses' selection against the Enterotoxin B was performed using the protein directly on a magnetic bead support in order to control the target of the selection. Unfortunately, no binding assay of the aptamer $APT^{SEB1}$ was performed on whole *MRSA* cells, which means that binding to *MRSA* was not proven.

These results show that there is no clear binding with any of these aptamers. The aptamers developed by Cao's in 2009 against *S. aureus* show no binding on clinical *S. aureus* or *MRSA*. Our aptamers selected against *MRSA* show no binding after time, and $APT^{SEB1}$ develop against the Enterotoxin B protein does not show binding on the whole cell either *S. aureus* or *MRSA*.

The main issue with these results is that the intended positive control, $APT^{SEB1}$, which was recently selected, does not bind to *MRSA* cells. Since the binding of this aptamer to whole cells was not verified by DeGrasse, there is no previous proof of success of such binding. In fact, one can assume that the folding of a protein bound to a magnetic bead may be different than the tertiary structure of the same protein on the outer membrane of a cell. That difference in folding could modify the interaction and recognition of the aptamer to the protein targeted.

After performing these experiments, we returned to our original question.

**Is it Possible that *Staphylococcus aureus* Bacterium Changes over Time to the Point that the Bacterium Loses the Proteins Recognized by the Aptamers?**

The best way to answer that question would be to perform a comparison of the genome analysis of the commercial *MRSA* cells from ATCC used to carry out the selection to the genome analysis of the same strain after lost of the binding properties. A fully automated sequencing instrument became commercially available in 1987 (Applied BioSystem, ABI 370). The *MRSA* strain 43300 was clinically isolated in 1986, and at that time, ATCC did not perform a genome analysis. Only the translation elongation factor Tu (tuf) gene and partial CDS are available on the NCBI database (GenBank: AF298796).

The scientific literature however contains considerable information on the history of the disease. As any other bacterium, *S. aureus* simple constitutive gene expression is strongly dependent upon the growth of the culture[110]. For that reason, in this research, the bacteria were always tested as a mixture of different growths.

The emergence of resistant *S. aureus* strains occured in the early 1950s with the notorious penicillin-resistant *S. aureus*, known as phage type 80/81[111]. In 1961, just one year after the launch of methicillin, *S. aureus* was not eradicated and instead more resistant clones appeared worldwide[112]. In addition to the appearance of strains resistant to all agents that had been developed to eradicate this bacterium, the hospital-acquired (HA) *MRSA* evolved into the community-acquired (CA) *MRSA* few decades later.

While the origins of major *MRSA* clones are still poorly understood, studies showed that *MRSAs* were descended from a single ancestral S. aureus strain that acquired the gene *mecA*[113]. Other *MRSA* strains are divergent, implying that *mecA* had

been transferred between *S. aureus* lineages[114,115]. New strains of *MRSA* are reported in the news and in the literature on a regular basis around the world showing the ability of this superbug to be an extraordinarily adaptable pathogen[116].

In our particular case, if the aptamers bound to a protein common to the different *MRSA* cells tested, a structural modification of the target could explain the loss of recognition by the aptamers from this study, as well as those selected by Cao *et al.* and by DeGrasse.

## Conclusion

The clinical study of aptamer recognition showed that the selected aptamers bound to all clinical *MRSA* strains tested, suggesting that the proteins targeted by those aptamers are common for the different *MRSA* strains. DTMRSA1 and DTMRSA3 showed the best specificity, with DTMRSA1 being the better of the two, while DTMRSA2 and DTMRSA4 bound to all three types of bacteria: *MRSA*, *Staphylococcus aureus* and *Enterococcus faecalis.* Further investigation on the aptamers showed that conjugation to gold-nanoparticles did not affect the binding, which was visualized by transmission electron microscopy.

After time, the aptamers generated showed no binding with the bacteria. The observed results and the evolution history of the *Staphylococcus Aureus* superbug suggest that the aptamers may have been specific to a common target and that the tested bacteria morphology changed over time. How these highly adaptable bacteria can orchestrate the expression of a variable number of resistance and virulence determinants is a major concern and still a mystery. The *Staphylococcus aureus* bacterium represent a paradigm in its ability to accomodate antibiotic-resistance

determinants and to produce an incredible panel of virulence determinants, making these pathogens among the most infectious diseases in humans.

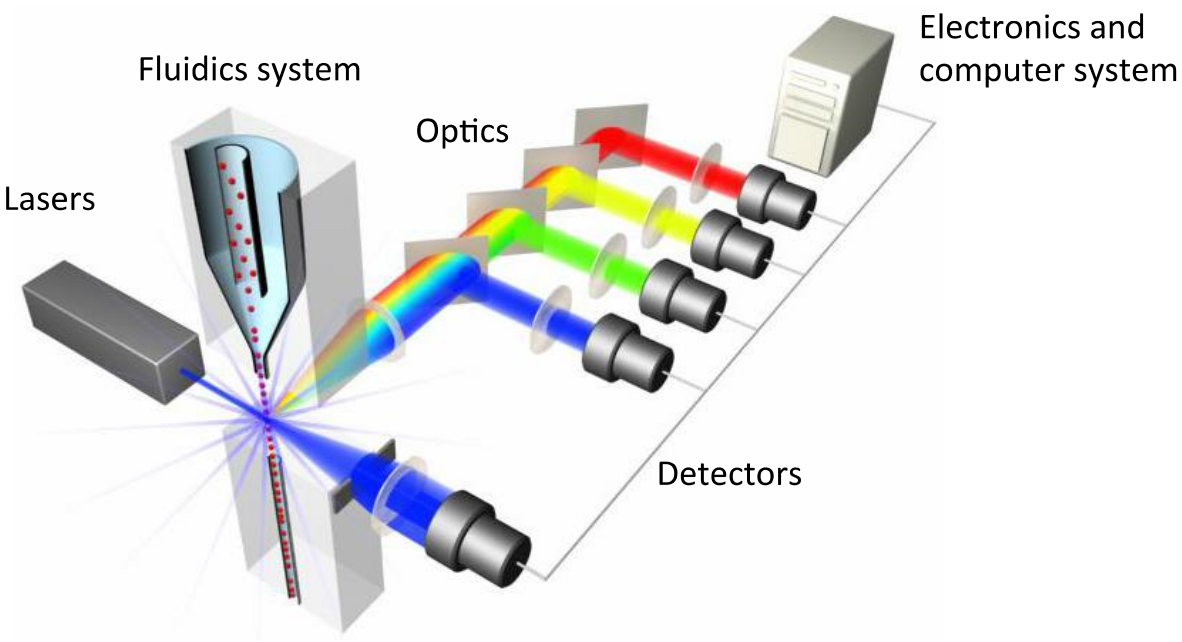


Figure 3-1. Schematic of the flow cytometry instrumentation.

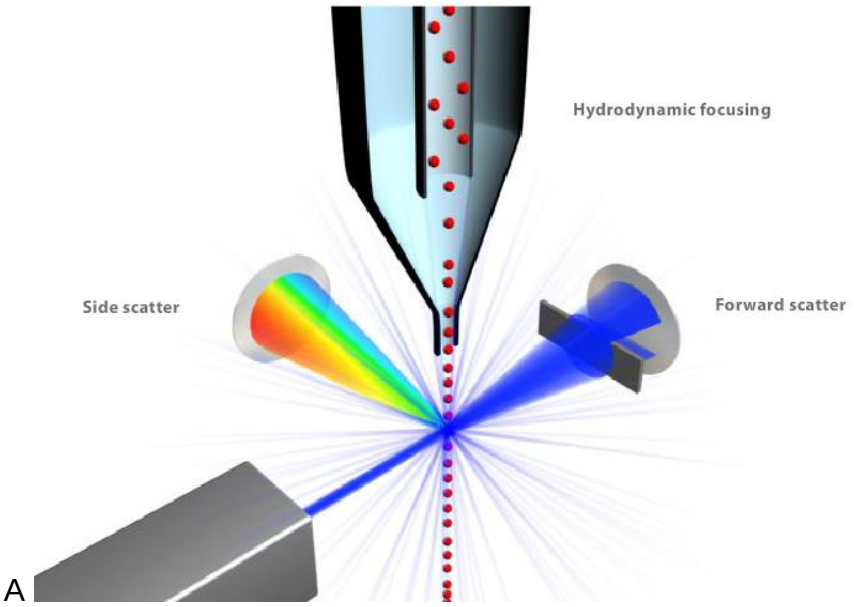


A

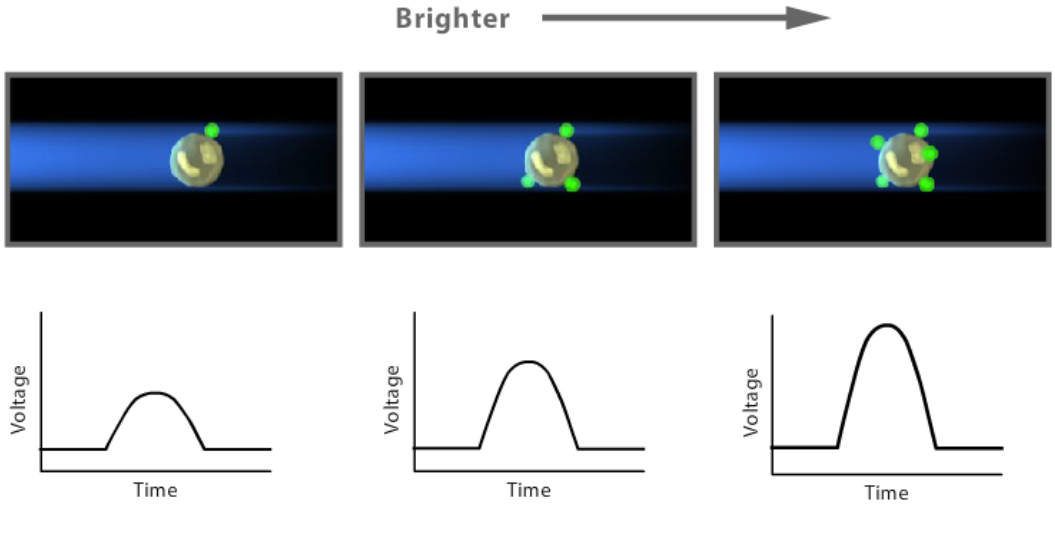


B

Figure 3-2. Flow cytometry mechanism. A) Light scatter of the laser beam, B) Conversion of the fluorescence intensity into voltage.

A

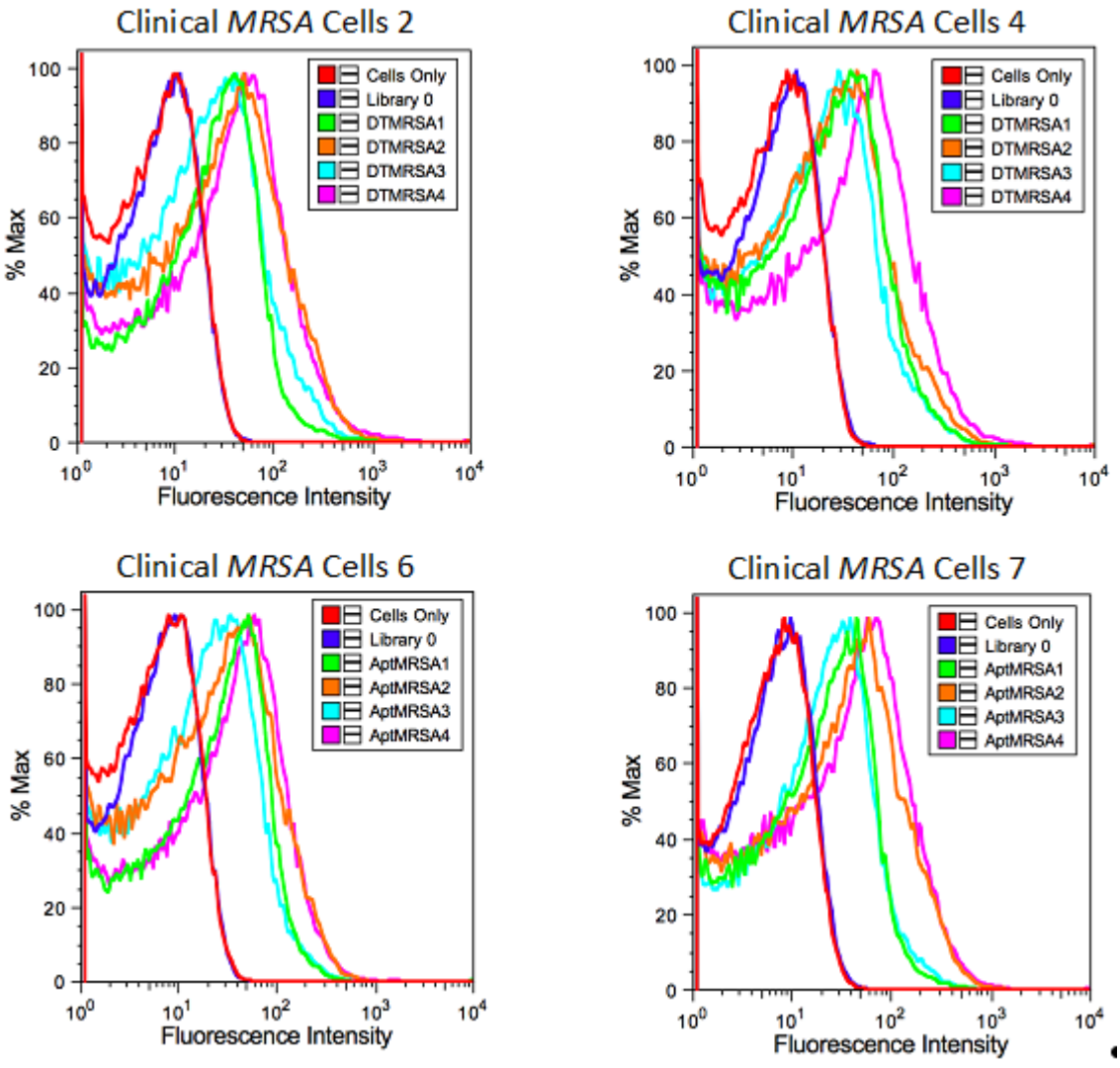
Clinical MRSA Cells 2
Cells Only
Library 0
DTMRSA1
DTMRSA2
DTMRSA3
DTMRSA4
% Max
Fluorescence Intensity
Clinical MRSA Cells 4
Cells Only
Library 0
DTMRSA1
DTMRSA2
DTMRSA3
DTMRSA4
% Max
Fluorescence Intensity
Clinical MRSA Cells 6
Cells Only
Library 0
AptMRSA1
AptMRSA2
AptMRSA3
AptMRSA4
% Max
Fluorescence Intensity
Clinical MRSA Cells 7
Cells Only
Library 0
AptMRSA1
AptMRSA2
AptMRSA3
AptMRSA4
% Max
Fluorescence Intensity

B

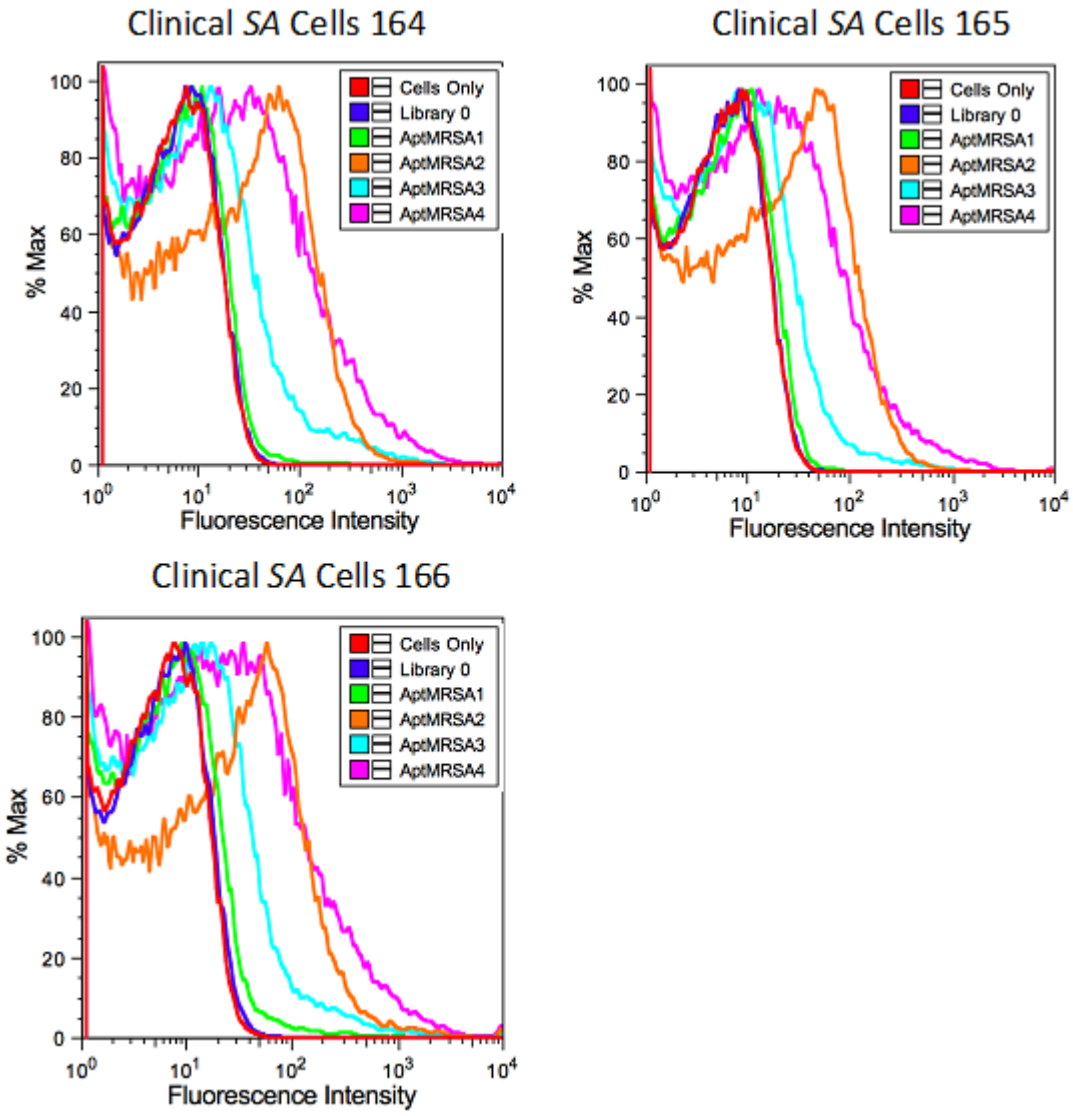
Clinical SA Cells 164
Clinical SA Cells 165
Clinical SA Cells 166
Cells Only
Library 0
AptMRSA1
AptMRSA2
AptMRSA3
AptMRSA4
% Max
Fluorescence Intensity

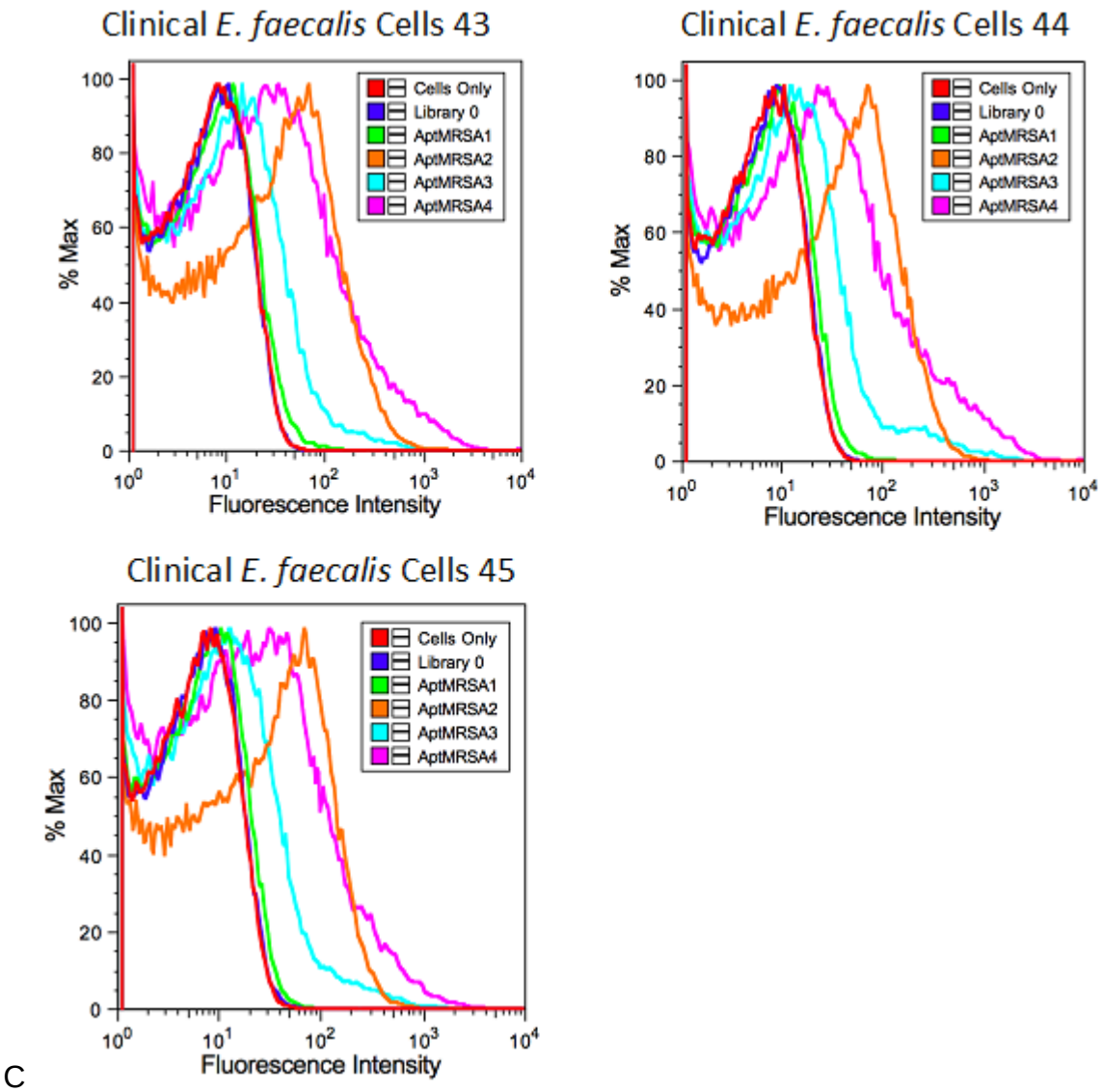


Figure 3-3. Aptamer recognition monitored by flow cytometry. A) *MRSA* cells, B) *S. aureus* cells, C) *E. faecalis* cells.

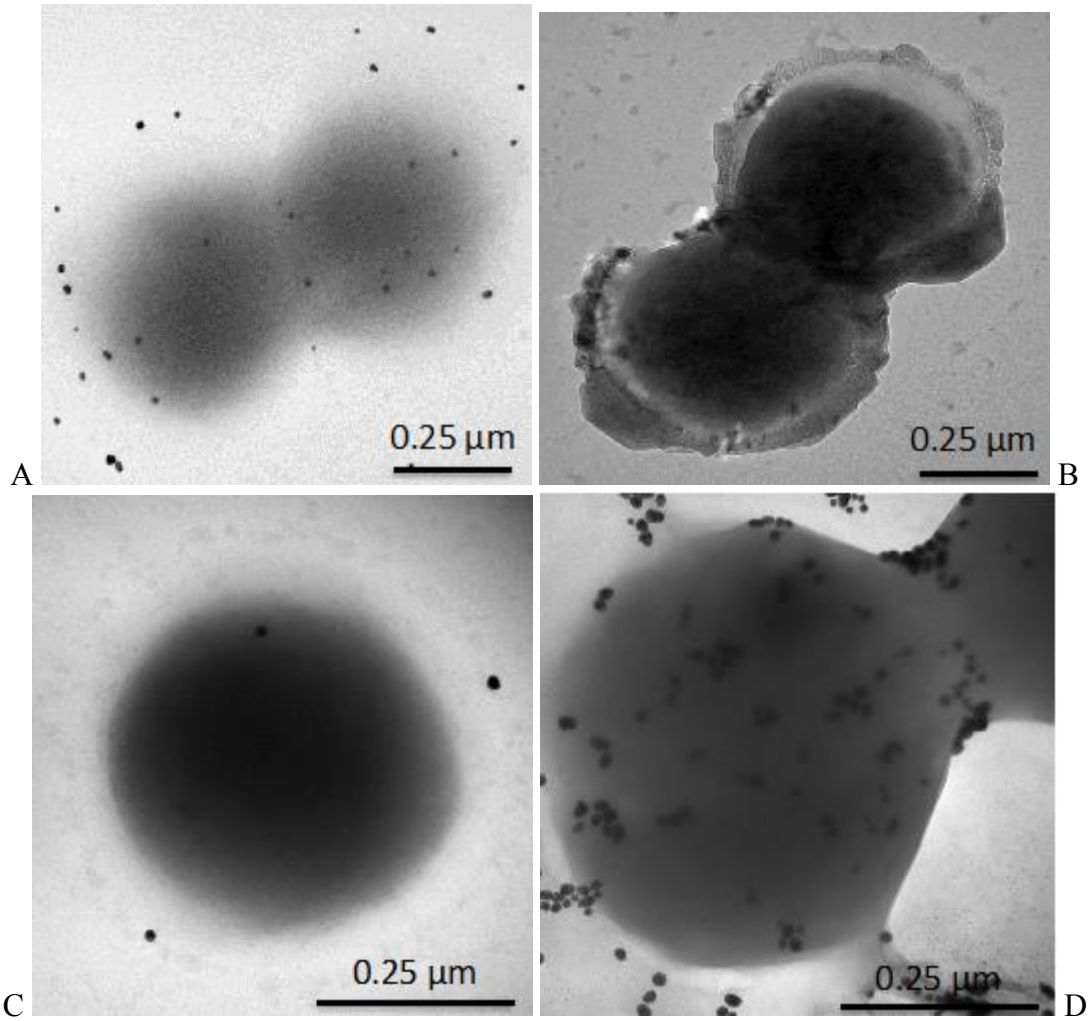


Figure 3-4. TEM visualization of *MRSA* bacteria with AuNPs. A) *MRSA* bacteria only, B) *MRSA* bacteria with bare AuNPs, C) *MRSA* bacteria with random aptamer coupled with AuNPs, and D) *MRSA* bacteria with DTMRSA2 coupled with AuNPs.

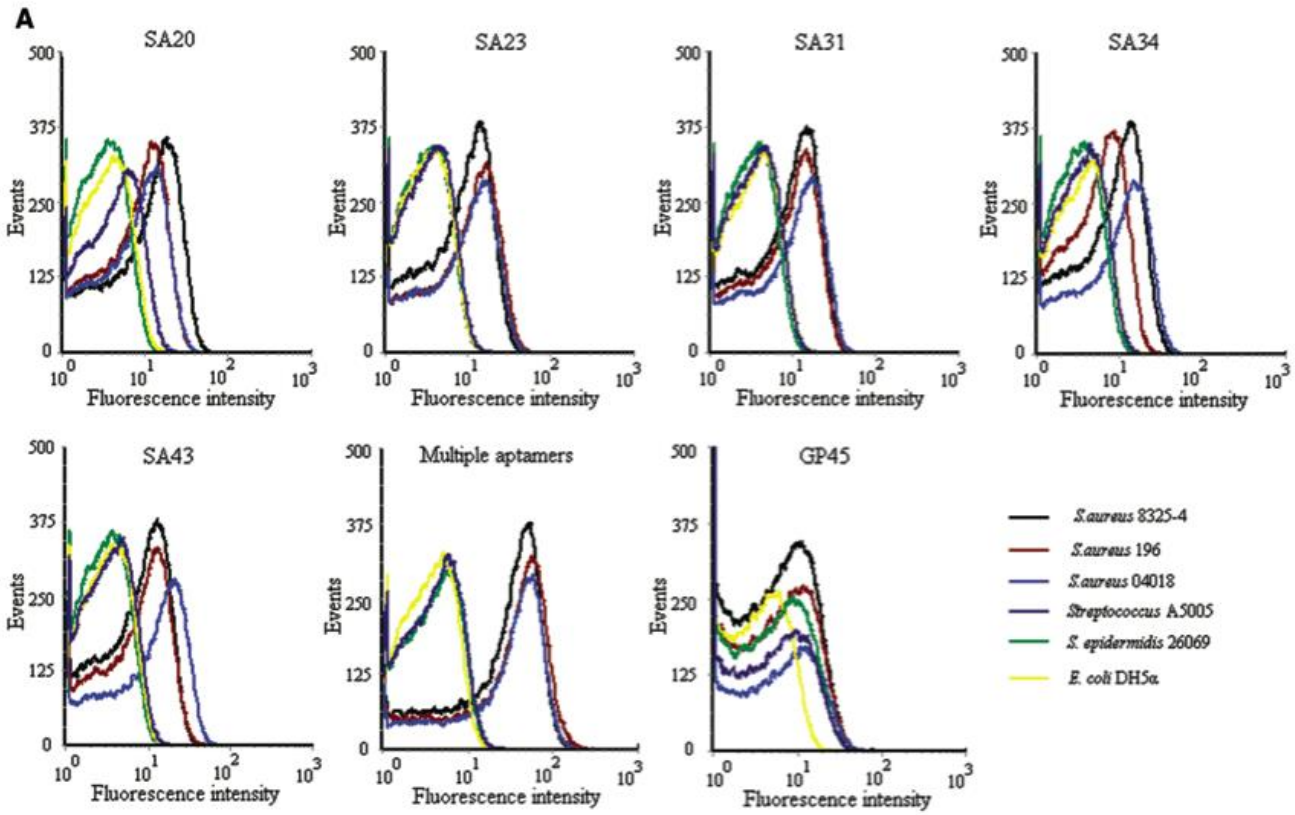


Figure 3-5. Flow cytometry assay for the binding of aptamers with bacteria. The different color curves represent different strains of bacteria.

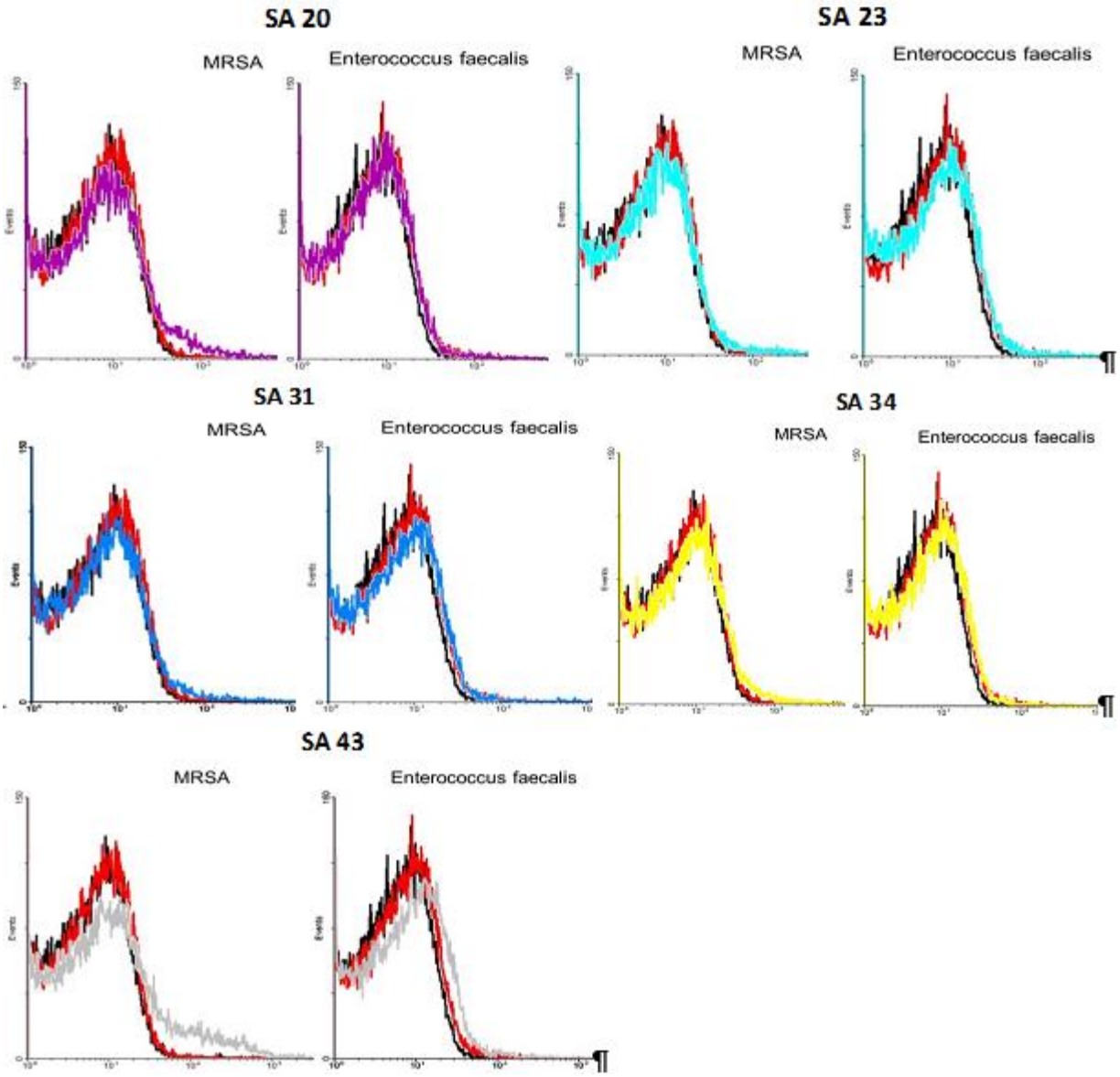


Figure 3-6. Binding assays monitored by flow cytometry of the aptamers developed by Cao's Research Group on *MRSA* bacteria ATCC 43300. In each graph, cells only are in black, random library is in red and the aptamer in the left over color.

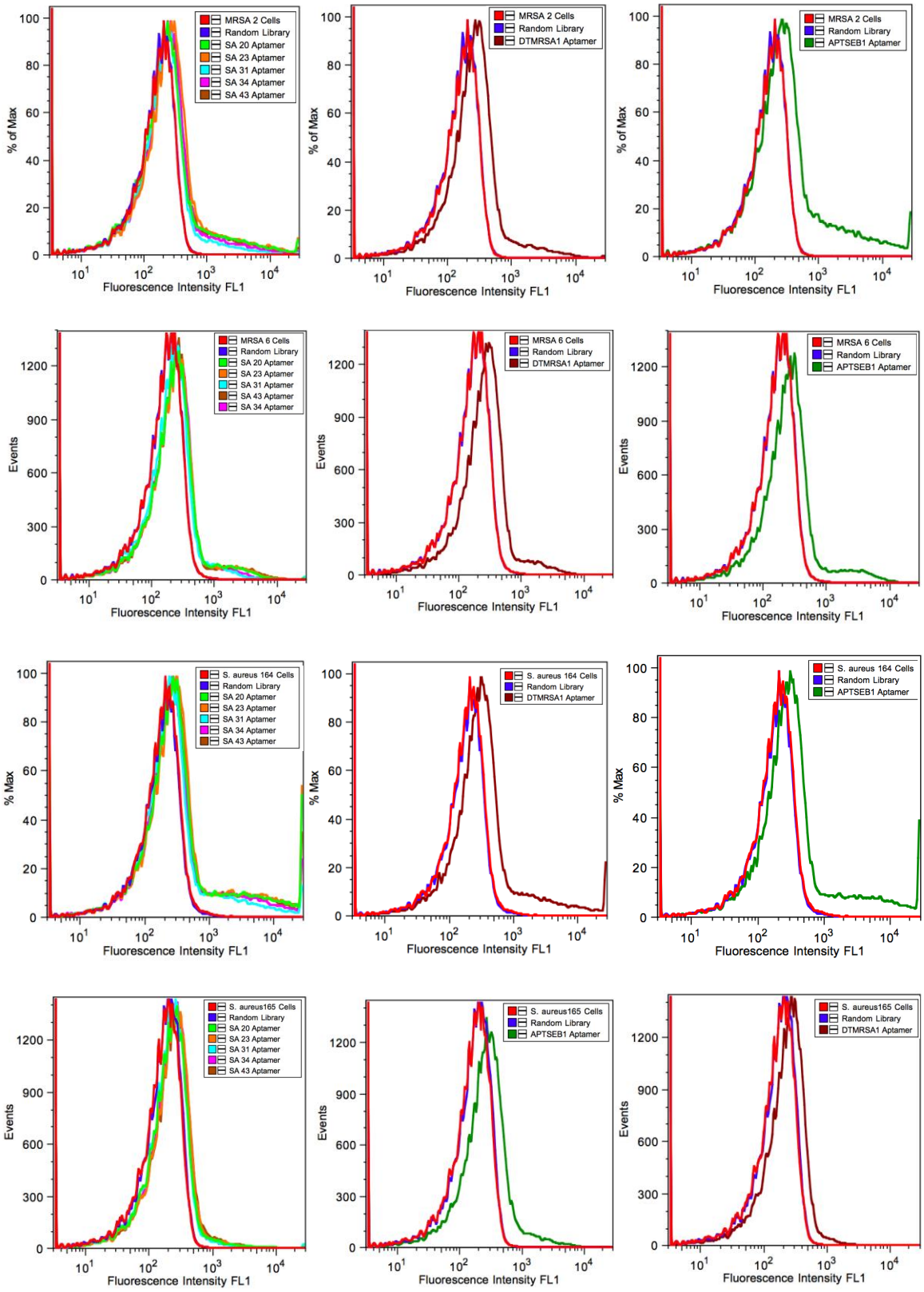


Figure 3-7. Binding assays of Cao's aptamers, DTMRSA1 aptamer and $APT^{SEB1}$ aptamers on clinical *MRSA* and *S. aureus* strains.

Table 3-1. Relative binding of the selected aptamers to various clinical cell lines. Results were obtained with the clinical strains of *MRSA*, *Staphylococcus aureus* and *Enterococcus faecalis* bacteria. (-) no binding; (+) 0-25%; (++) 25-50%; (+++) 50-75%; (++++) 75-100%.

Accepted to the World Journal of Translational Medicine, written by Turek D., Van Simaeys D., Johnson J., Ocsoy I., Tan W., for future publication.

| Clinical Strains | DTMRSA1 | DTMRSA2 | DTMRSA3 | DTMRSA4 |
|---|---|---|---|---|
| *MRSA 2* | +++ | ++++ | +++ | ++++ |
| *MRSA 4* | +++ | +++ | +++ | ++++ |
| *MRSA 6* | ++++ | ++++ | +++ | ++++ |
| *MRSA 7* | +++ | ++++ | +++ | ++++ |
| *S. aureus 164* | - | ++++ | + | +++ |
| *S. aureus 165* | - | ++++ | + | +++ |
| *S. aureus 166* | - | ++++ | + | +++ |
| *E. faecalis 43* | - | ++++ | + | +++ |
| *E. faecalis 44* | - | ++++ | + | ++ |
| *E. faecalis 45* | - | ++++ | + | +++ |

Table 3-2. Aptamer sequences developped by Cao *et al.*[99]

| Name of the Aptamer | Detail of the Sequence |
|---|---|
| SA20 | GCGCCCTCTCACGTGGCACTCAGAGTGCCGGAAGTTCTGCGTTAT |
| SA23 | GGGCTGGCCAGATCAGACCCCGGATGATCATCCTTGTGAGAACCA |
| SA31 | TCCCACGATCTCATTAGTCTGTGGATAAGCGTGGGACGTCTATGA |
| SA34 | CACAGTCACTCAGACGGCCGCTATTGTTGCCAGATTGCCTTTGGC |
| SA43 | TCGGCACGTTCTCAGTAGCGCTCGCTGGTCATCCCACAGCTACGT |

# CHAPTER 4
# MOUSE LIVER CELL SELECTION TARGETING GLYPICAN 3

## Introduction

The liver is the largest internal organ and the largest human gland. It is a complex, multipurpose, indispensable organ. Its major role is to deal with nutrient product of food digestion and detoxifying harmful substances absorbed via the intestine[117]. In part because liver cancer is diagnosed at a late age, 62 years old on average, the survival rate is extremely low[118]. One of the reasons is that in most cases, liver cancers are primary cancers, which means that they originate from the liver itself instead of metastasis. Moreover, hepatocellular carcinoma (HCC), which is the most common cancer, very frequently occurs in conjuction with chronic liver diseases, such as hepatitis B or C, and cirrhosis[119]. Primary carcinoma of the liver, including HCC, is the third most common cancer-related death, with more than 500,000 new cases diagnosed per year in the world[120]. Glypican 3 (GPC3) is a protein upregulated in most hepatocellular carcinomae (HCC).

GPC3, a membrane-associated heparan sulfate proteoglycan, shows a great potential in the early detection of HCC since they are absent in healthy liver tissue. In previous studies targeting three types of cancers, hepatocellular carcinoma (HCC), intrahepatic cholangiocarcinoma and combined hepacellular (ICC) and cholangiocarcinoma (CHC), results of GPC3 expression in liver suggested that GPC3 is a biomarker that is sensitive and specific to well differentiated HCC[47,121]. Improved sensitivity and specificity toward malignancy are observed when additional markers are used for detection; alpha-fetoprotein (AFP) is the most commonly used marker for this purpose[122].

In this chapter, we aimed to develop aptamers specific to Glypican 3 using the cell-SELEX technique. Selections on whole cells do not usually permit us to know the target because the entire membrane of the cell is targeted[75]. In this study, we used human-GPC3 transfected cells to have an over-expression of the protein targeted. Results of the selection and investigation on the aptamer candidates are presented in this study.

## Materials and Methods

### Instrumentation, Reagents and Buffers

Dulbecco's Phosphate Buffered Saline (PBS) was used to prepare the washing buffer (4.5 g/L glucose and 5 mL MgCl2 at 1M) and binding buffer (4.5 g/L glucose, 5 mL MgCl2, 1.0 g/L bovine serum albumin and 100 mg/L tRNA). Gel electrophoresis was prepared and run using TBE buffer: 1X Tris/Borate/EDTA (TBE) buffer (Fisher Scientific Inc., Pittsburg, PA).

The trypsin EDTA 1X used for cell digestion during cell culture came from Cellgro and the non-enzymatic cell dissociation solution (1X) Bioreagent from Sigma was used for cell digestion before any flow cytometry experiments.

All oligonucleotides were synthesized by standard phosphoroamidite chemistry using a 3400 DNA synthesizer (Applied Biosystems) and were purified by reversed-phase HPLC (Varian Prostar). All PCR mixtures were prepared using 50 mM KCl, 10 mM Tris-HCl at pH 8.3, 2.0 mM $MgCl_2$, 2.5 mM dNTPs, 0.5 mM of each primers (Biotin and FITC) and 5 units/mL of Hot Start Taq DNA polymerase (TaKaRa). PCR was run on a Biorad Thermocycler. Electrophoresis gels were cast and run on a Biorad minisub cell GT and read on a GE Image Quant 400.

Monitoring of the selection and of the aptamers candidates binding on the targeted cells was performed by flow cytometry using a FACScan cytometer (BD Immunocytometry Systems). Experiments using the flow sorting technique were carried out using the FACSAria™ IIU Special Order System Cell Sorter (BD Biosciences).

**Cell Lines and Cell Culture Conditions**

The wild mouse liver cancer cell line IMEA was obtained from the Department of Pathology at the University of Florida. Since the protein Glypican 3 was targeted, the positive cell line was obtained by modification of the IMEA wild cell line; this way the only difference between the positive and the negative cell line was the presence of the glypican 3 protein. The same research group from the Department of Pathology transfected the IMEA wild cancer cell line with the human glypican 3 (hGPC3) using a plasmid pcDNA™ 3.1 (Invitrogen). DMEM media was used with the addition of 10% FBS and 5% penicillin-streptavidin antibiotic for the wild IMEA cell line. For the modified cell line hGPC3-IMEA, and in order to maintain the transfected modification throughout the cell culture, the DMEM media was supplemented by 250 mg/mL G418 antibiotic, which blocks polypeptide synthesis by inhibiting the elongation step if the cell does not contain the resistant gene. All cells were cultured in 5 % $CO_2$ atmosphere humidified incubator.

**Cell SELEX Library and Conditions**

For this selection, a shorter library was designed in comparison to the one used in the *MRSA* selection (Chapter 2). The main advantage of using a short library is that it is cheaper to synthesize. The design for such library has to be such that the length is important enough to generate different conformations throughout the random part for cell recognition purposes but short enough to make it significantly cheaper to

synthesize. The library used was the following 57mer: 5'- CGA CAC CTC CAG ACG C $(N)_{25}$ T CGT CCA CTG TGC CTC -3'. The forward primer was labeled with FITC and the reverse primer with biotin in order to monitor the selection through flow cytometry and obtain separation of dsDNA from the PCR into ssDNA using streptavidin columns.

The selection was run using a typical SELEX technique up to 19 rounds[75]. Each dish of cells was washed with both 1000 mL PBS and WB before use and incubations with each pool were done at 4°C for 30 min with the positive cell line and 1 h with the negative cell line while the washing stringency was increase throughout the selection. Both incubations of each DNA pool were done in plate directly to avoid disturbing or modifying the morphology of the cell by digesting them using non-enzymatic buffer. After the temperature optimization of the random library, PCR amplifications were carried out with cycles of 95°C for 30 s, 56.7°C for 30 s, and 72°C for 30 s, and finalized by an extension step of 3 min at 72°C. The selection progression was monitored by flow cytometry to observe the enrichment. Once the selection was over, final pools were submitted for Ion Torrent sequencing and aligned for analysis using MAFFT software.

**Potential Aptamers Binding Assays**

The analyses of the Ion Torrent data led to a few sequence candidates. Those sequences were synthesized using the 3400 DNA Synthesizer (BD) and labeled with Biotin on their 3'-end. Binding assays were performed by incubating 250 nM of the sequence with BB and 300,000 cells at 4°C for 30 min, followed by 2 washes with WB, and another incubation at 4°C for 10 min with binding buffer containing the dye streptavidin-PE-Cy5.5 for the labeling of the cells. After washing the cells twice with WB, the binding of the sequences was monitored through flow cytometry at the appropriate

reading channel, using cells only and random library-biotin labeled as negative controls. The fluorescence was determined by counting 30,000 events.

**Fluorescence-Activated Cell Sorting (FACS)**

The last rounds of the selection (20 to 22 rounds) were done using the cell sorting technique FACS. This technique allows obtaining cell subsets separated from the entire pool of cells. In our case, we were interested in collecting cells from the incubated positive cell line that showed a higher shift than the cells only used as a control. 1 million cells were used for incubation at 4°C with 250 nM library and 60,000 positive cells were isolated on each round.

The cell sorting technique is performed in a system where cells are ejected into air in a stream of sheath fluid. While the stream breaks into droplets, the distance between the orifice that the stream begins and the break off into droplet depends on the orifice size, the pressure of the sheath fluid, the temperature and the viscosity of the fluid. The break up of the stream is stabilized by stationary wave of vibration of known frequency and amplitude applied to the stream. As soon as the cells are ejected, they pass through one or more laser beams and information about the cell is gathered. That critical step is when the cells can be independently charged and will carry a positive charge, a negative charge or remain uncharged. The sorting can then be done using charged plates where charged drops are attracted to the plate of opposite polarity and deflected into collection tubes[123] [Figure 4-1].

## Results and Discussion

**Cell-SELEX on IMEA Cells**

As mentioned in the previous section, the selection was run on mouse liver cancer cells with the aim of getting aptamers specific to the glypican 3 protein. Indeed, plasmid

modified IMEA cells were used to have expression of GPC3, which is not present on the wild IMEA cell line. Human glypican 3 were over-expressed on the positive cell line (hGPC3-IMEA) and the wild IMEA cell line was used for negative selection. Transfected cells contained both the GPC3 gene and the neomycin resistance gene (neo) to be resistant to G418 antibiotic. By culturing positive cells with addition of G418 antibiotic in the media, we ensured that hGPC3-IMEA cells only were surviving.

At the beginning of the selection, 20 pmol of library was used. The random library was a 57mer ssDNA, labeled with FITC on its 3'-end. The selection showed a quick enrichment, starting from round 5, but at that stage, the pools also showed binding to the negative cells. Without any change of conditions, the negative binding seemed to reduce round after round [Figure 4-2]. Nevertheless, reduction of the negative binding seemed to reach a plateau after 10 rounds with no full disappearance. In order to get better results, it was decided to perform a "sandwich" selection, at Round 11, which lies in the pool to be incubated twice with the negative cell line, once before and once after the incubation with the positive cell line. This change of strategy showed successful results and specific enrichment was clearly observed after 19 rounds of selection [Figure 4-3]. The detailed data of the selection up to round 19 is presented in Table 4.1. Negative rounds "x 2" correspond to the rounds where sandwich selection was carried out. At the end of 19 rounds, an enrichment plateau was reached and any negative binding had disappeared.

**Sequencing and Binding Assays**

The cancer cell line HuH7 is a human cell line that naturally carries the protein glypican 3[124]; on the contrary, $HCO_2$ is a cancer human cell line that does not carry the

protein glypican 3 (cell line developed by Dr Chen Liu at the University of Florida). Since the selection was performed on a mouse cell line transfected with the human glypican 3 gene, it was important to check the binding of the last pool on a human cell line, in this case HuH7, that expresses the GPC3 gene and on a human cell line, in this case $HCO_2$, that does not. The last pool of the selection showed a shift on HuH7 and no shift on $HCO_2$ [Figure 4-4]. Those results confirmed the specificity of pool 19 on binding to a cell line with high expression of GPC3 and by extrapolation, a binding to the glypican 3 protein. Based on those results, the last two pools generated, pools 18 and 19, which are the pools with the most enrichment, were sent for sequencing analysis with the Ion Torrent technology provided at CGRC, University of Florida.

In order to ensure sample identification following the sequencing, Multiplex Identifier (MID) adaptors were used, MID1 for library 18 and MID2 for library 19 [Table 4-2][125]. After the sequencing, the primer regions and MIDs of each sequence were removed and the random region of the library was aligned to group the sequences into homologous families [Figure 4-5]. As a point of reference for later results, MID2 row data gave us 1.2 million sequences.

After analyzing the alignments obtained, 6 sequences retained our attention and were synthesized for further screening [Table 4-3 and Figure 4-6].

As it can be observed in Figure 4-6, binding assays of those sequences showed inconsistencies in the results obtained either with the positive or the negative cell lines. Besides inconsistencies in the results, it can be noted that even when binding was observed on the positive cell line, that binding showed no shift increase compared to the binding of the last pool of the selection; an increase in the shift is usually expected when

sequences are isolated and tested. Out of those results, we concluded that those sequences were not good aptamer candidates and carried further analysis of the sequencing row data. The new sequences representing homologous families are presented in Table 4-4.

Those results were compared to the ones from the former analysis, Table 4-3, and it was determined that the number of sequences obtained were in the same range or lower than in the 1$^{st}$ analysis. The enrichment observed at the end of the selection was concluded to be too low to generate aptamer candidates for the glypican 3 protein.

We decided to continue the selection further with a flow sorter in order to get more enrichment of the pool and be able to generate and identify bigger families. The main advantage of using a flow sorter is that it allowed us to isolate cells that showed a different binding in comparison to the random library [Figure 4-7]. By this means, only a reduced amount of cells is isolated, but the pool of sequences obtained at the end of each round is more specific to the target cell membrane. As it can be seen in Figure 4-7A, the threshold was set at the end of the shift of the random library. The cells isolated from the pool were the ones over the threshold and the only ones extracted, amplified and used in order to get the DNA pool for the next round.

Table 4-5 shows the details of the three rounds of selection done using the flow sorter. Since the flow sorter allowed us to control the threshold, no incubation of the pool with the negative cells was necessary. Indeed, only sequences showing a stronger binding than the random library were isolated. After three more rounds performed with the flow cell sorter, binding assays were carried out to check on the enrichment of the pools [Figure 4-8]. The binding results of the pools obtained using the flow sorter were

compared to the last pool of the selection, Library 19, and no binding was observed. During the performance of a selection, it is not surprising to observe a shift back of the pools when conditions are modified, but the shift is usually recovered within two rounds. This return did not occur in our case.

The quality of the cells was questioned at that point and a mycoplasma testing was run. Both IMEA-hGPC3 and IMEA cultural media showed a positive result to mycoplasma. Mycoplasma, from the Greek *mykes* (fungus) and *plasma* (formed) are a genus of bacteria that lack cell wall. They are common contaminants in cell culture and are not detected with a conventional microscope. Mycoplasmal cell culture contamination may induce cellular changes, including chromosome aberrations, modifications in metabolism and cell growth. Any of those changes could impact the success of a cell selection and could explain difficulties in both generating aptamers against GPC3 and getting consistent results.

## Conclusion

The cell-SELEX technique had been used for a couple of decades to generate aptamers against cancer cells. While this technique is able to generate aptamers specific to a particular cell line, the main disadvantage of the cell selection lies on the fact that the target recognized by the aptamer remains unknown by the end of the selection. In this particular selection, we countered that disadvantage by using an original mouse cell line, the IMEA wild cell line, as the counter cell line, and that same cell line modified by transfection of the human glypican 3 gene, the hGPC3-IMEA cell line, in order to have expression of the targeted protein, Glypican 3. In this chapter, the cell-selection against liver cancer were performed in the conditions optimized in the SELEX protocol developed by our research laboratory[75]. After 19 rounds of selection,

too many families of sequences were obtained, with none large enough to be able to generate aptamers. Results were sometimes inconsistent and changes of the protocol by the use of a flow sorter did not solve the problem. The cells used were found to be positive to mycoplasma testing. Contamination of the cells by mycoplasma might have had an impact on the growth and membrane structure of the cells, which could explain the results observed. Challenges in selecting aptamers against liver cancer cells were not isolated; attempts to do so with other liver cell lines by our research laboratory failed in the past year. Since glypican 3 shows great potential as a hepatocarcinoma marker; performing a protein selection, using magnetic beads for instance, could be another option to develop aptamer against this protein.

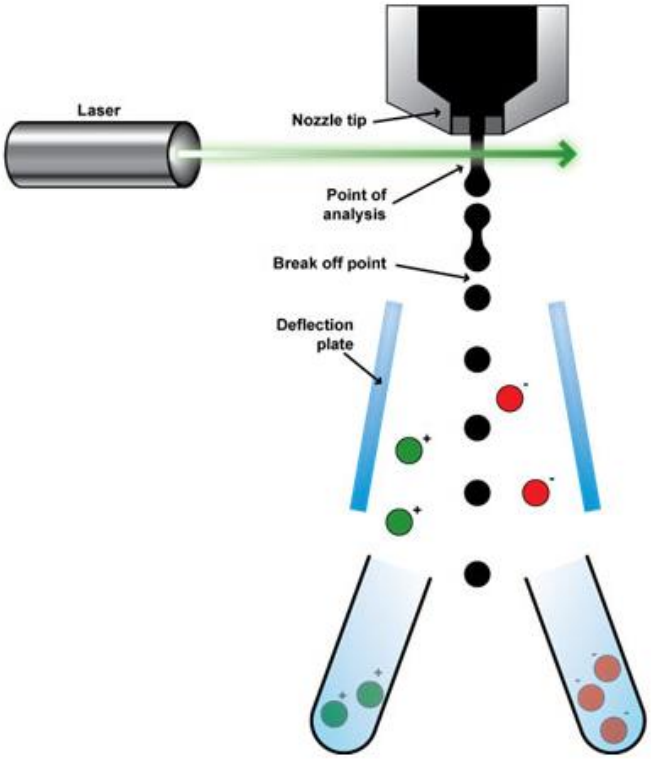


Figure 4.1. Scheme of a generalized cell sorting flow cytometer. Particles are introduced into a column of pressurized sheath fluid, emerge from the nozzle and pass through one or more laser beams. At this point, the cytometer gathers information about the fluorescence characteristic of the cell. The stream is charged when the cell breaks into a drop and drops are separated based on their charge.

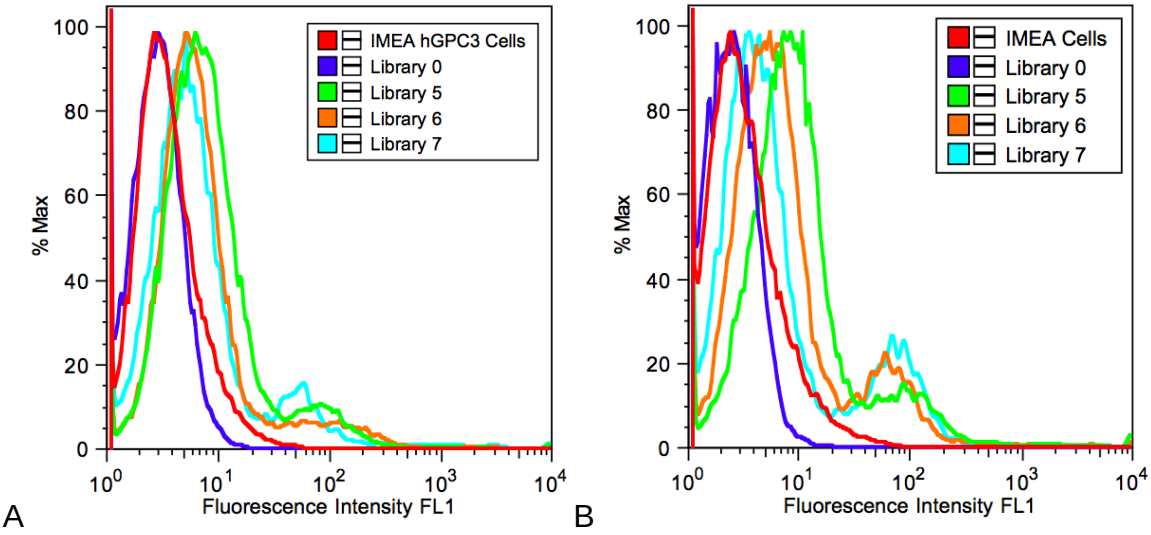


Figure 4-2. Enrichment observed for pools 5 to 7 on both positive and negative cell lines. A) hGPC3-IMEA and B) Wild IMEA respectively. A decrease of negative binding is observed.

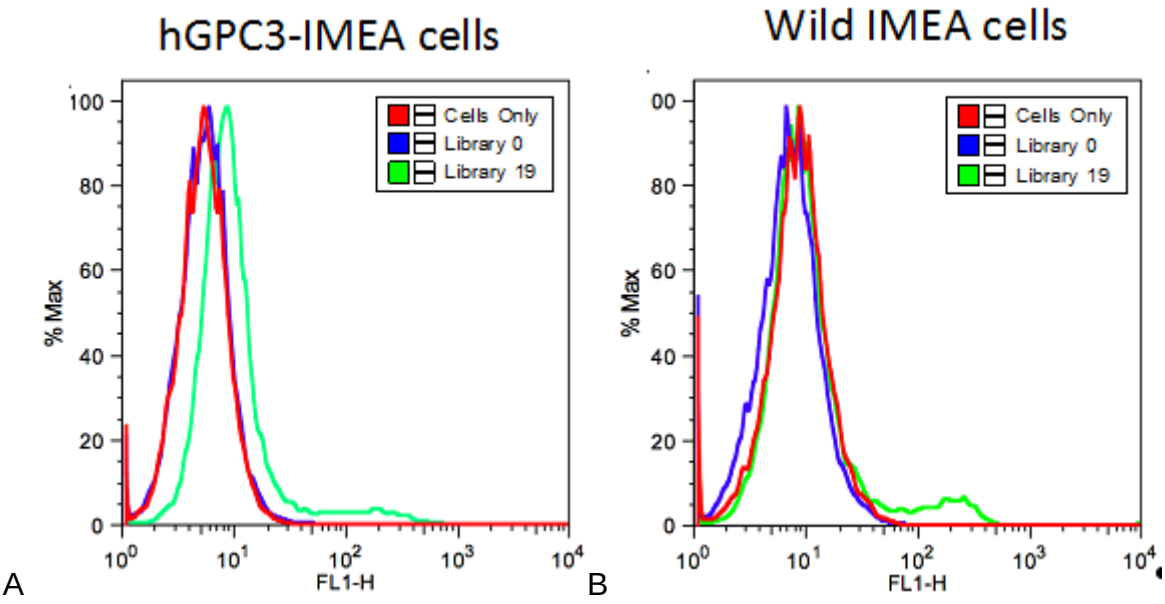


Figure 4-3. Specific enrichment observed through flow cytometry at the end of the selection. A) Using the hGPC3-IMEA cell line and B) Using the wild IMEA cell line.

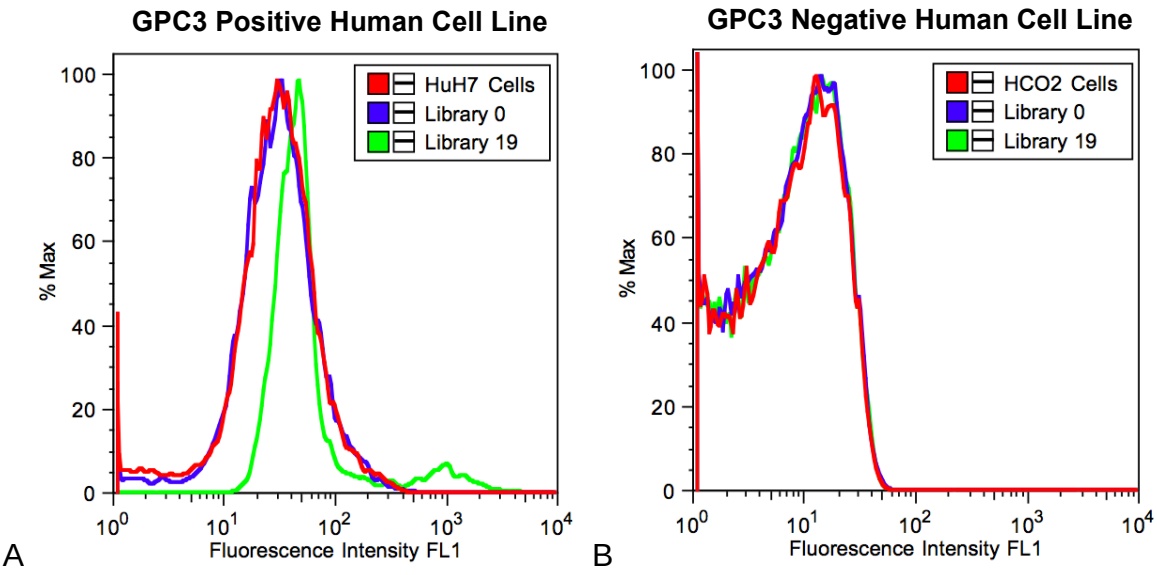


Figure 4-4. Binding observed from the selection pool 19; cells only and random library (Library 0) are used as controls. A) On the HuH7 cell line and B) On the $HCO_2$ cell line.

```
MID2PH:2498:151 ----------------cacctcagc-cgtgtac-------tcct-gccgt----------
MID2PH:2494:192 ----------------cacctcagc-cgtgtac-------tcct-gccgt----------
MID2PH:2496:190 ----------------cacctcagc-cgtgtac-------tcct-gccgt----------
MID2PH:2495:202 ----------------cacctcagc-cgtgtac-------tcct-gccgt----------
MID2PH:2477:227 ----------------cacctcagc-cgtgtac-------tcct-gccgt----------
MID2PH:2467:254 ----------------cacctcagc-cgtgtac-------tcct-gccgt----------
MID2PH:2489:263 ----------------cacctcagc-cgtgtac-------tcct-gccgt----------
MID2PH:2498:270 ----------------cacctcagc-cgtgtac-------tcct-gccgt----------
MID2PH:2522:123 ----------------cacctcagc-cgtgtac-------tcct-gccgt----------
MID2PH:2525:130 ----------------cacctcagc-cgtgtac-------tcct-gccgt----------
MID2PH:2522:137 ----------------cacctcagc-cgtgtac-------tcct-gccgt----------
MID2PH:2516:146 ----------------cacctcagc-cgtgtac-------tcct-gccgt----------
MID2PH:2519:161 ----------------cacctcagc-cgtgtac-------tcct-gccgt----------
MID2PH:2528:178 ----------------cacctcagc-cgtgtac-------tcct-gccgt----------
MID2PH:2523:189 ----------------cacctcagc-cgtgtac-------tcct-gccgt----------
MID2PH:2519:221 ----------------cacctcagc-cgtgtac-------tcct-gccgt----------
MID2PH:2531:232 ----------------cacctcagc-cgtgtac-------tcct-gccgt----------
MID2PH:2518:249 ----------------cacctcagc-cgtgtac-------tcct-gccgt----------
MID2PH:2510:259 ----------------cacctcagc-cgtgtac-------tcct-gccgt----------
MID2PH:2528:257 ----------------cacctcagc-cgtgtac-------tcct-gccgt----------
MID2PH:2510:263 ----------------cacctcagc-cgtgtac-------tcct-gccgt----------
MID2PH:2557:180 ----------------cacctcagc-cgtgtac-------tcct-gccgt----------
MID2PH:2550:210 ----------------cacctcagc-cgtgtac-------tcct-gccgt----------
MID2PH:2569:215 ----------------cacctcagc-cgtgtac-------tcct-gccgt----------
MID2PH:2596:223 ----------------cacctcagc-cgtgtac-------tcct-gccgt----------
MID2PH:2563:229 ----------------cacctcagc-cgtgtac-------tcct-gccgt----------
MID2PH:2571:255 ----------------cacctcagc-cgtgtac-------tcct-gccgt----------
MID2PH:2634:180 ----------------cacctcagc-cgtgtac-------tcct-gccgt----------
MID2PH:2604:220 ----------------cacctcagc-cgtgtac-------tcct-gccgt----------
MID2PH:2629:227 ----------------cacctcagc-cgtgtac-------tcct-gccgt----------
MID2PH:2621:249 ----------------cacctcagc-cgtgtac-------tcct-gccgt----------
MID2PH:2635:250 ----------------cacctcagc-cgtgtac-------tcct-gccgt----------
```

Figure 4-5. Example of sequence alignment using library 19 (MID2).

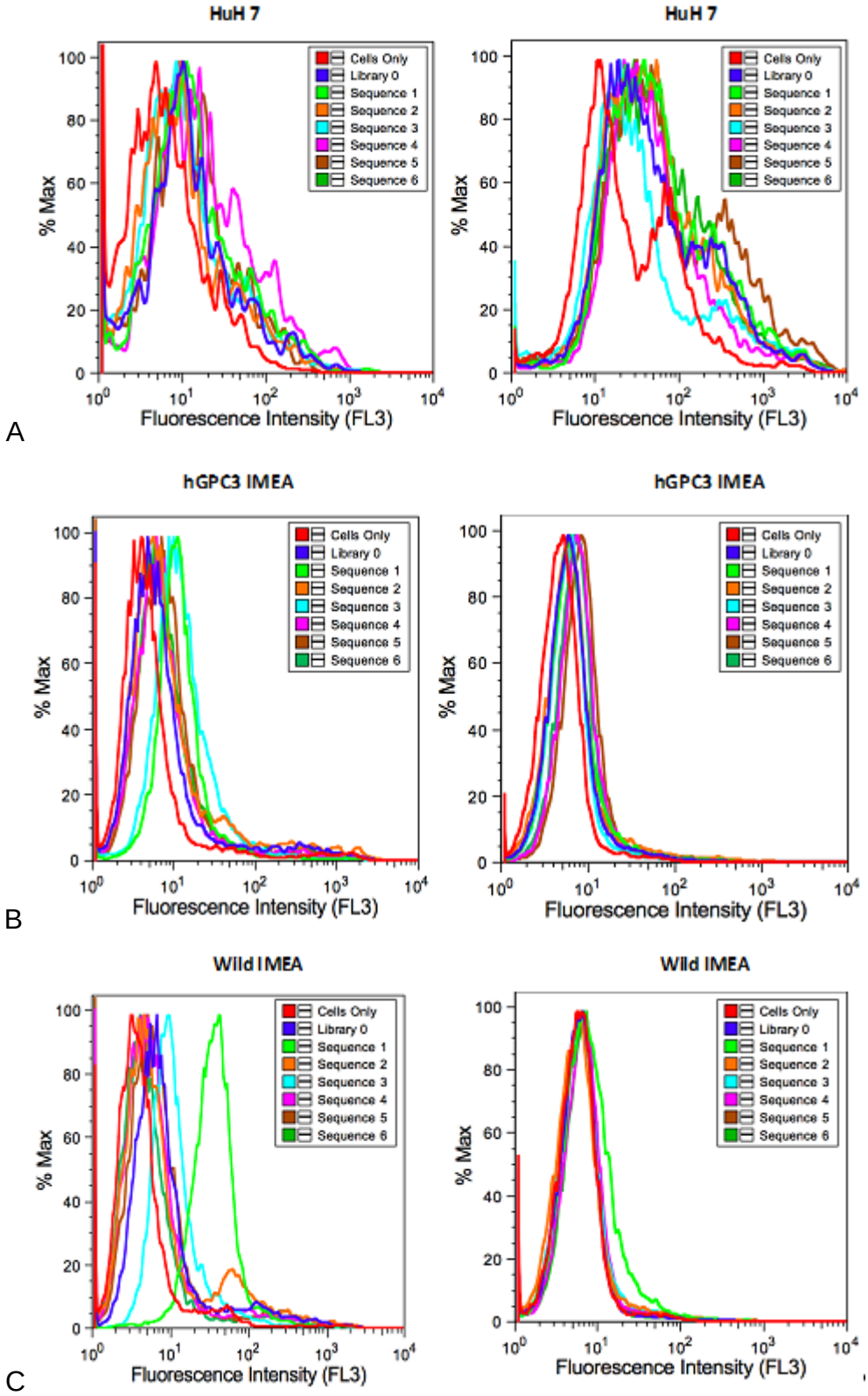


Figure 4-6. Binding assay in duplicate of 6 potential aptamer candidates with flow cytometry using 3 cell lines. A) HuH7; B) hGPC3 IMEA and C) Wild IMEA.

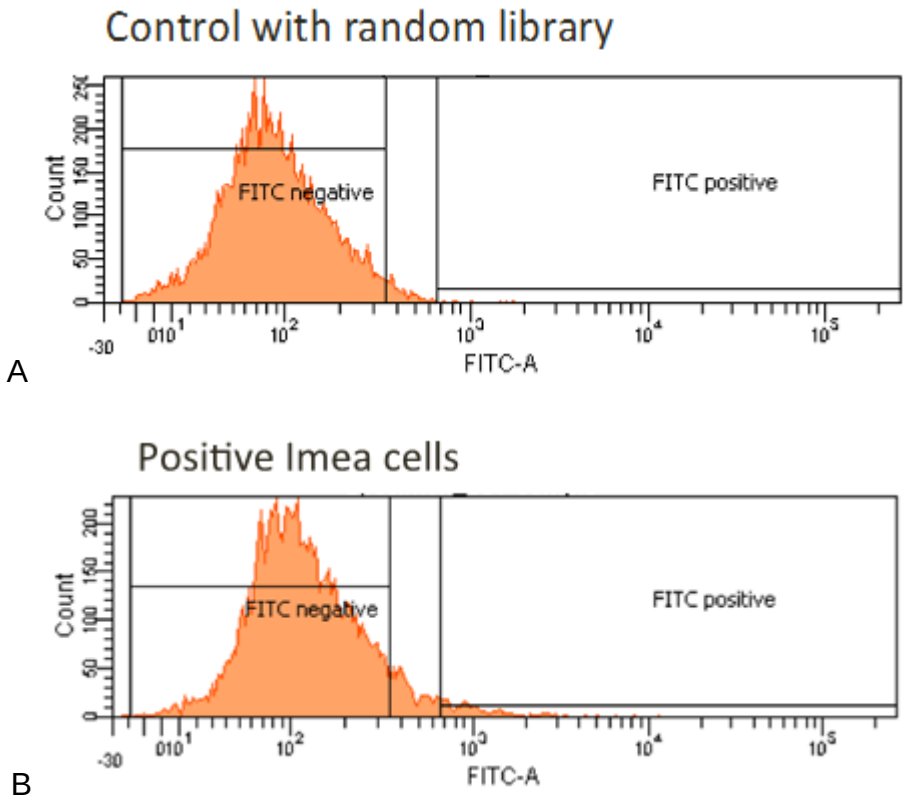


Figure 4-7. Example of theshold setting on the flow cell sorter for IMEA cells. A) Binding of random library and B) Binding of the selection pool.

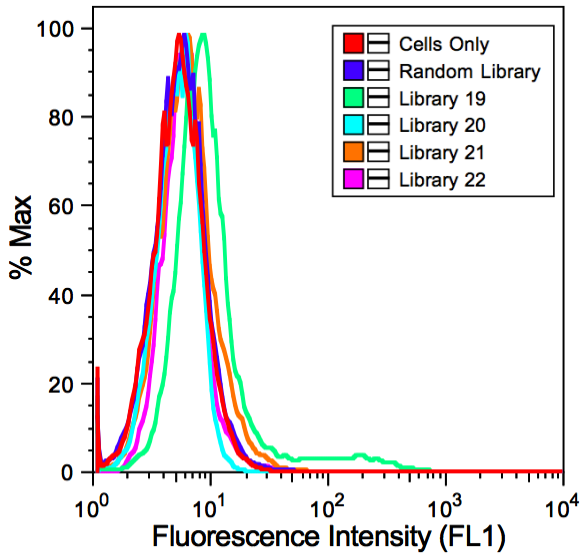


Figure 4-8. Binding assay of the pools obtained with the flow sorter in comparison with the last selection pool “Library 19”.

Table 4-1. Summary of progression of the IMEA cell selection.

| Rounds | Negative round | Number of washes, time, volume of WB | PCR amplification cycles | Volume of eluted DNA at 250 nM |
|---|---|---|---|---|
| 1 | No | 1, 2 min, 3000 µL | 22 | 709.6 µL |
| 2 | Yes | 2, 2 min, 1000 µL | 22 | 652.8 µL |
| 3 | Yes | 2, 3 min, 1000 µL | 19 | 207.2 µL |
| 4 | Yes | 2, 3 min, 1000 µL | 22 | 368.4 µL |
| 5 | Yes | 2, 3 min, 1300 µL | 24 | 197.2 µL |
| 6 | Yes | 3, 3 min, 1000 µL | 18 | 161.6 µL |
| 7 | Yes | 3, 3 min, 1000 µL | 24 | 606.4 µL |
| 8 | Yes | 3, 4 min, 1000 µL | 21 | 651.8 µL |
| 9 | Yes | 3, 4 min, 1000 µL | 19 | 300.0 µL |
| 10 | Yes | 3, 4 min, 1000 µL | 19 | 198.4 µL |
| 11 | Yes x 2 | 3, 4 min, 1000 µL | 21 | 385.2 µL |
| 12 | Yes x 2 | 3, 4 min, 1000 µL | 17 | 198.4 µL |
| 13 | Yes x 2 | 3, 4 min, 1000 µL | 22 | 385.2 µL |
| 14 | Yes | 3, 4 min, 1000 µL | 13 | 128.0 µL |
| 15 | Yes x 2 | 3, 4 min, 1000 µL | 19 | 482.8 µL |
| 16 | Yes x 2 | 2, 4 min, 1000 µL | 22 | 617.6 µL |
| 17 | Yes x 2 | 2, 4 min, 1000 µL | 15 | 418.0 µL |
| 18 | Yes x 2 | 2, 4 min, 1000 µL | 19 | 541.0 µL |
| 19 | Yes x 2 | 2, 4 min, 1000 µL | 18 | 717.6 µL |

Table 4-2. Ten common 10-base extended Multiplex Identifier (MID) used for sequencing.

| Mutiplex Identifier Name | Sequence |
|---|---|
| MID-1 | ACGAGTGCGT |
| MID-2 | ACGCTCGACA |
| MID-3 | AGACGCACTC |
| MID-4 | AGCACTGTAG |
| MID-5 | ATCAGACACG |
| MID-6 | ATATCGCGAG |
| MID-7 | CGTGTCTCTA |
| MID-8 | TCTCTATGCG |
| MID-10 | TCTCTATGCG |
| MID-11 | TGATACGTCT |

Table 4-3. Potential aptamer sequences selected from Analysis 1 of the Ion Torrent data.

| Potential Aptamer Sequences | Sequence Counting |
|---|---|
| CACCTCAGCCGTGTACTCCTGCCGT | 705 |
| CAGACCTCACACACTGCT | 828 |
| GCATGGGCCCAGCACTCCCTTCGGT | 500 |
| CAACCCGGCCCAGTTCCC | 2,526 |
| AACACCGACACCTCCAGACGC | 3,406 |
| CAAGGAGTGGCAGCATCTATTCA | 292 |

Table 4-4. Potential aptamer sequences selected from Analysis 2 of the Ion Torrent data.

| Potential Aptamer Sequences | Sequence Counting |
|---|---|
| ACCACTGCTCGTTCCCGCCTGTCGT | 616 |
| ACCCCAGCTTCGGGACTCCTGCCGT | 486 |
| CACCTCAGCCGTGTACTCCTGCCGT | 756 |
| CCCGGAAACACTCATTCTCC | 560 |
| CAAGAGGAGGTGGCGCAAGCATTAT | 753 |
| CAGAGGTGGCGCCGAAAGCATTTAT | 436 |
| GAGCTCCGACACCTCCA | 596 |
| CAGACCTCACACACTGCTCCGTCGT | 914 |
| CGAGGTGGCGCCCAGCATATATTAT | 426 |

Table 4-5. Summary of progression of the selection using the cell sorter.

| Rounds | Negative round | Number of washes, time, volume of WB | PCR amplification cycles | Volume of eluted DNA at 250 nM |
|---|---|---|---|---|
| 20 | No, cell sorting | 2, 1 min, 1000 µL | 26 | 395.2 µL |
| 21 | No, cell sorting | 2, 1 min, 1000 µL | 23 | 250 µL |
| 22 | No, cell sorting | 2, 1 min, 1000 µL | 24 | 378 µL |

# CHAPTER 5
# THERMOACTIVATION OF GOLD-NANOROD ON OVARIAN CANCER

## Introduction

Ovarian cancer is the ninth most common cancer among women, accounting for 14,000 lethal cases annually in the United States[32]. The ovarian clear cell adenocarcinoma (OCCA) subtype, among others, shows very few early symptoms and poor response to standard treatments[49,126-128]. In the medical field, the most common serum biomarker used for ovarian cancer diagnosis and prognosis is the cancer antigen 125 (CA-125). However, not all ovarian cancers express that protein and the sensitivity of this test is only of 48 %[129]. This high proportion of false positive results is due to the fact that some conditions like pregnancy or cirrhosis elevate the level of CA125. During cancer treatment, chemotherapy and radiotherapy are known for showing a lot of side effects. For that reason, the development of therapy with the use of aptamers that are able to selectively bind to targeted cells may offer the possibility of better treatment. In addition, the use of nanoparticles bound to aptamers presents two main advantages: they are easily synthesized and show low toxicity[94]. Gold-nanorods present absorption at the near-infrared (NIR) range, which make them good candidates for photothermal therapy. In this chapter, we used gold-nanorods (AuNR) coated with aptamers that specifically recognize and internalize into ovarian cancer cells. Their cytotoxicity was studied after thermoactivation with a NIR-laser beam.

## Materials and Methods

### Instrumentation, Buffers and Reagents

Dulbecco's Phosphate Buffered Saline (PBS) was used to wash the cells during experiments and to make binding buffer (addition of 4.5 g/L glucose, 5 mL $MgCl_2$, 1.0

g/L bovine serum albumin and 100 mg/L tRNA). Cetyltrimetylammonium bromide (CTAB) ≥ 96.0% was obtained from Fluka, and tris (2-carboxyethyl) phosphine (TCEP) were obtained from Sigma-Aldrich. Thiol-terminated methoxypoly (ethylene glycol) (mPEG-SH, $M_W$=5000) was purchased from Nanocs.

Counting of cells was performed using a microscope Olympus IX70 (x10) and a hemacytometer Reichert, 0.1 mm Deep, Bright Line® used in couple with a cell counter from Fisher Scientific. For confocal studies, readings were performed on Leica CTR 6500, objective x63 and for MTS assays; readings were done on the Microplate reader VERSAmax. For UV measurements, we used the Cary Bio-300 UV spectrometer (Varian, Walnut Creek, CA). In the cytotoxicity section, NIR laser beaming was performed at the Human Toxicity Department at the University of Florida on a NIR COHERENT Quattro.

**Cell Lines and Cell Culture Conditions**

The ovarian clear cell adenocarcinoma TOV21G and the hepatocarcinoma cell line HuH7 were used for the experiments. For all those cells, DMEM media supplemented with 5% Penicillin-streptavidin and 10% FBS was used during the culture and DMEM media with no supplemental reagent was used during experiment to avoid any cleavage of DNA. All cells were cultured in 5% $CO_2$ atmosphere humidified incubator.

**Aptamer Synthesis and Purification**

The aptamer TOV6 was previously selected by our research group against the ovarian cancer cell line TOV21G[54]. The original aptamer TOV6: 5’-ATC CAG AGT GAC GCA GCA CGG CAC TCA CTC TTT GTT AAG TGG TCT GCT TCT TAA CCT TCA TCG ACA CGG TGG CTT AN-3’ was synthesized with both N=FITC and N=TAMRA dyes; the modified TOV6: 5'-SS-$(OCH_2CH_2)_{12}$-ATC CAG AGT GAC GCA GCA CGG

CAC TCA CTC TTT GTT AAG TGG TCT GCT TCT TAA CCT TCA TCG ACA CGG TGG CTT AN-3' was also synthesized with both N=FITC and N=TAMRA; and two libraries were used depending on the dye for negative control: 5'- ATC CAG AGT GAC GCA GCA $(N)_{40}$ TGG ACA CGG TGG CTT AGT (FITC)-3' and 5'- ATC CAG AGT GAC GCA GCA $(N)_{40}$ TGG ACA CGG TGG CTT AGT (TMR)-3', where N represents A, T, C or G.

All single strain DNA oligomers were synthesized using the ABI 3400 DNA/RNA synthesizer (Applied Biosystem). Controlled pore glasses (CPG) were used on either the 5' or 3'-end for modifications. Upon completion, all ssDNA oligomers were transferred to glass vials for deprotection using AMA at 65°C for 30 min. After cool down, the supernatant was transferred to plastic tubes and a mixture of 250 µL 3M NaCl and 6 mL ethanol was added. DNA precipitated at -20°C for 20 min and tubes were centrifugated at 4000 rpm for 30 min at 4°C. Purification of the DNA samples was completed by HPLC and further purification with a desalting column.

**Gold-Nanorod-Aptamer Conjugate**

Gold-nanorods were synthesized with the procedure described in Yasun *et al.*[130]. TOV6 aptamers were then immobilized on the surface of the nanorods. In order to tether on the surface of the gold nanorods, TOV6 aptamers were first modified with a disulfide functional group on the 5'-terminal (5'-SS-TOV6) and these disulfide groups were cleaved to thiol groups. In the cleavage process, 0.1 mM disulfide modified TOV6 aptamer was incubated with 5 mM TCEP in 50 mM Tris/HCl buffer at pH 7.5 for 1 h at room temperature. Further purification was performed by eluting small portions of TCEP/Aptamer mixture through a NAP-5 desalting column. The final concentration of those portions was calculated from absorbance measurements using a UV-

spectrometer. 100 µL of 1 nM of AuNR solution was centrifuged at 14,000 rpm at 25 °C for 3 min and the supernatant was discarded. The precipitate was re-suspended in 100 µL of 2 mM CTAB. Once those preparations were ready, 0.1 nM of AuNR was incubated with 25 nM of 5'-SH-TOV6 aptamers anf 0.1 mM thiol-PEG ($M_w$=5000) in DNA grade water at room temperature for 12 h followed by centrifugation at 14,000 rpm at 25 °C for 5 min to remove the supernatant that contained the unbound aptamers and SH-PEG. The precipitate was re-suspended in 100 µL of DNA grade water. Both of the TOV6-FITC and TOV6-TMR conjugated AuNRs were prepared the same way.

**Binding Assays**

All binding assays performed in this study were monitored through flow cytometry on the BD Acuri™ C6 Flow Cytometer. For each sample, 300,000 cells were incubated with the solution to test for 30 min. Aptamers were tested at a concentration of 250 nM at 4°C for 30 min, incubated cells were washed twice with 10% PBS and 20,000 cells were monitored with the flow cytometer on channel FL1 since the dye used was FITC.

The software FlowJo© was used to analyze data obtained from the flow cytometry.

**Confocal Assays**

For confocal experiments, good adhesion of cells was ensured by incubating 40,000 cells overnight at 37°C with the corresponding media in glass-bottom petri dishes. Different concentrations of the aptamer TOV6 coupled with the Tamra chromophore (TOV6-TMR) were prepared to observe internalization of the aptamer and the optimum concentration was used to prepare the gold-nanorod-aptamer conjugate (AuNR-TOV6-TMR). All preparations were diluted in media for a final volume of 300 µL and incubated for 8 h at 37°C. Then, cells were washed with 1mL PBS twice and

binding buffer was added for the confocal reading to keep cells alive. Reading of results was performed on the Leica CTR 6500 with the x63 objective.

### Cytotoxicity Assays and Cell Viability Determination

Cytotoxicity assays were performed in three steps: (1) the incubation of the cells with different concentration of TOV6-AuNR-FITC; (2) the NIR laser beaming at 808 nm for 10 min of those solutions; and (3) the MTS reading of those solutions.

After laser beaming, cells were transferred in a 96-well plate and incubated for 48 h at 37°C. Then cells were prepared for the MTS reading. After centrigugation at 1300 rpm for 3 min, 75% of the supernatant was removed and a premixed solution of medium without FBS or PS (100 µL) with MTS solution (20 µL) was added and incubated for 40 min at 37°C before reading. MTS assays are used to determine the percentage of cell viability with a colorimetric method. MTS Promega kit solutions are made of a mixture of MTS (3-(4,5-dimethylthiazol-2-yl)-5-(3-carboxymethoxyphenyl)-2-(4-sulfophenyl)-2H-tetrazolium) and an electron-coupling reagent, PMS (phenazine methosulfate). If cells are metabolically active, their dehydrogenase enzymes will convert the MTS into soluble formazan [Figure 5-1]. Formazan, that shows an absorbance at 490 nm, can then be measured and is directly proportional to the number of living cells in culture[131].

## Results and Discussion

### Conjugated Aptamer-AuNR Binding Study

The ovarian cancer had been previously studied in our group and several aptamers had been generated against the cancer ovarian cell line TOV21G [54]. The aptamer TOV6 was chosen for further application in this chapter. We were interested in binding the aptamer to a gold-nanorod that could further be thermoactivated by a NIR laser beam and determine its cytotoxicity.

In this project design, the aptamer TOV6 was modified upon synthesis on both terminals of the single strand DNA. The 5'-terminal was synthesized with a disulfide bond and the 3'-terminal was synthesized with either FITC or TAMRA dye. The disulfide bond was used to coat the gold-nanorods with TOV6 aptamers and the FITC and TAMRA dyes were used for binding assays and confocal studies, respectively. One of the advantages that aptamers are known for is to be able to be chemically modified without losing binding with their target. In order to check on that particular feature in our design, we performed a binding assay with the flow cytometer of the aptamer alone incubated with TOV21G cells and of the aptamer mounted onto the nanorod. As it can be seen on Figure 5-2, both aptamers and AuNR-aptamers showed binding compared to the random library. Those same aptamers were incubated and tested on HuH7 cells, which are liver cancer cells, and showed no binding, which confirmed the specificity of the aptamers toward the cell line targeted TOV21G [Figure 5-3].

**Internalization Study**

Depending on the target of the aptamer, some of them get to be internalized into the cell. Indeed, if the aptamer binds to a target that is able to go under an endocytosis pathway, then the aptamer can become intracellular. Since the cell-SELEX process does not allow us to know the target, and know their properties, we investigated the internalization through confocal studies. TOV6 aptamers with TAMRA dye were used for that study as well as TOV6-AuNR [Figure 5-4]. The confocal reading was performed after an 8h-incubation of the aptamer or aptamer-AuNR with the cells to ensure that the nanorod had the time to be internalized. Results showed that whether TOV6 or TOV6-AuNR is conjugated to the TOV21G cell line, both do internalize. That property opens a

very interesting feature for the thermoactivation of the nanorod, since the heating will come from the inside of the cells.

**Thermoactivation of the Gold-Nanorods and Cytotoxicity Assays**

Photothermal therapy through the use of Gold-Nanorods is an approach that has been pursued for the past few years and has the potential of being less aggressive than current chemotherapies [132-134]. In our study, we were interested in determining the cytotoxicity of thermoactivation of internalized Gold-nanorods. For that purpose, we prepared samples in quadruplet of TOV21G cells with the following solutions, for a final volume of 400 µL:

- Binding Buffer (Control)
- 0.1 M, 0.2 M, 0.3 M, 0.4 M and 0.5 M AuNR-TOV6 in binding buffer

Half of those samples were subjected to an NIR laser beam (808 nm) for 10 min. The setup of this experiment is shown in Figure 5-5. Then, all solutions were transferred into a 96-well plate and incubated for 48 h at 37°C. The cytotoxicity was finally analyzed through an MTS assay, as described in the material and methods section, and the cell viability was determined with the results obtained with and without NIR laser beaming [Figure 5-6]. Results showed that the thermoactivation of the 0.1 M TOV6-AuNR solution triggered the apoptosis of half of the cells, and those results reached up to 65% of the cells with the 0.4 M (or higher) TOV6-AuNR solution. Cell-only controls with and without laser applied and all AuNR-TOV6 control samples without laser applied provided us useful data. First, the incubation of gold-nanorods-aptamer conjugate did not trigger apoptosis, and second, applying a NIR laser beam for 10 min on live cells did not trigger apoptosis. With those two observations, we concluded that the internalization

of AuNR-TOV6 and its thermal-activation with a NIR-laser showed an important cytotoxicity on ovarian cancer cells.

## Conclusion

The use of nanoparticles and nanorods in the medical field has been investigated for the past 10 years: the 1-100 nm scale is of interest for the biological applications. Nanotoxicity of some nanomaterials has been studied and reviewed[135,136] and in this chapter, we were particularly interested in gold-nanorods. Indeed, bulk gold is well known to be “accepted” by our metabolism and chemically inert, and gold-based compounds have been used clinically as anti-inflammatory agents[137]. As it was described in the sections above, gold-nanorods were synthesized and coated with TOV6 aptamers to allow specific recognition of the complex AuNR-TOV6 towards the ovarian cancer cell line TOV21G. Those conjugates were internalized into the cells after 8 h of incubation and photothermal properties of gold-nanorods were used to provoke the apoptosis of the cells. Results of the cytotoxicity assays demonstrated that 10 min of near-infrared laser beaming was sufficient to trigger the apoptosis of half of the cells with low concentration of nanorods incubated (0.1 M) and up to 65% of the cells when higher concentration of nanorods were incubated (0.4 M and more). The coupling of both aptamer and gold-nanorod technologies created a tool able to target a specific cell line and impact its viability through thermal activation.

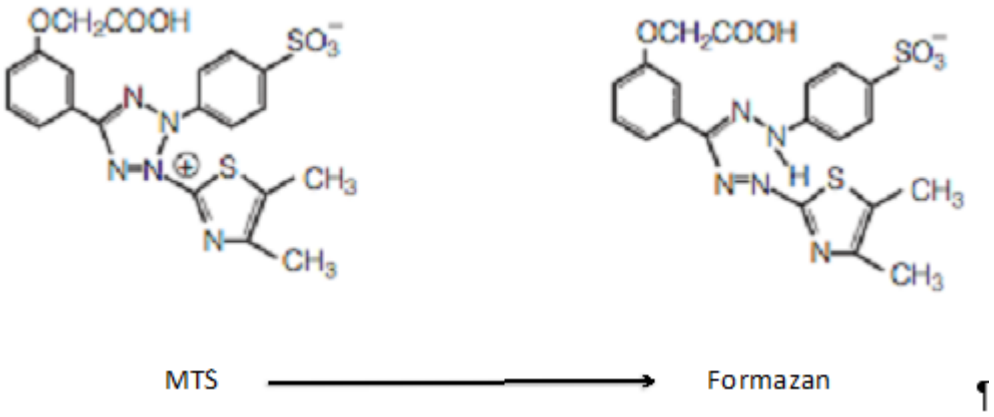


Figure 5-1. Structure of the MTS and its Formazan product.

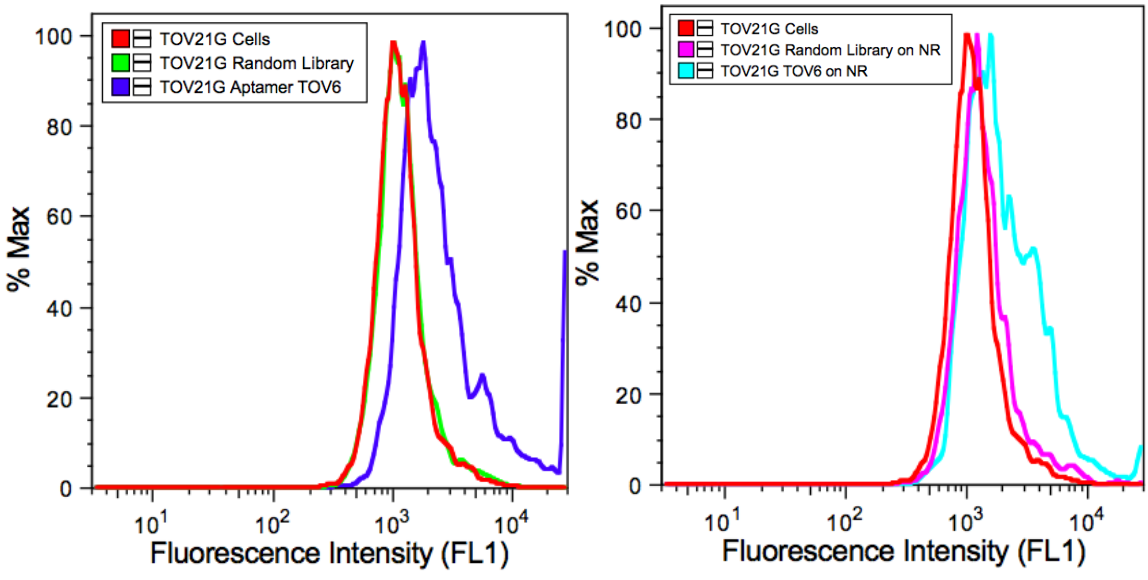


A B

Figure 5-2. Binding assays on TOV21G cells. A) TOV6 Aptamer only; and B) TOV6 Aptamer conjugated to Gold-Nanorods.

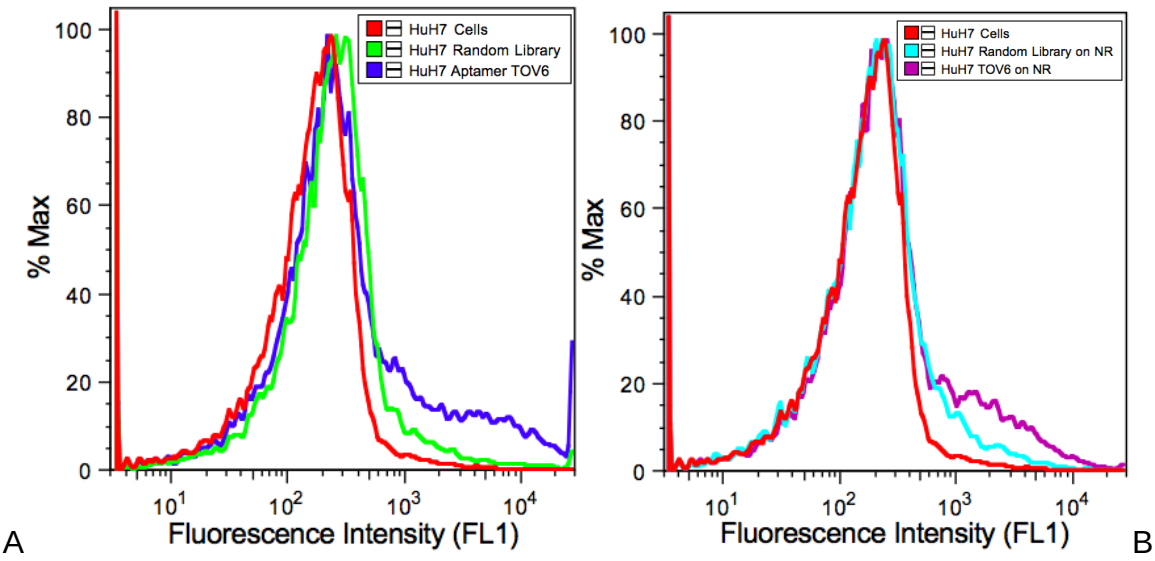


A B

Figure 5-3. Binding assay on HuH7 cells. A) TOV6 Aptamer only; and B) TOV6 Aptamer conjugated to Gold-Nanorods.

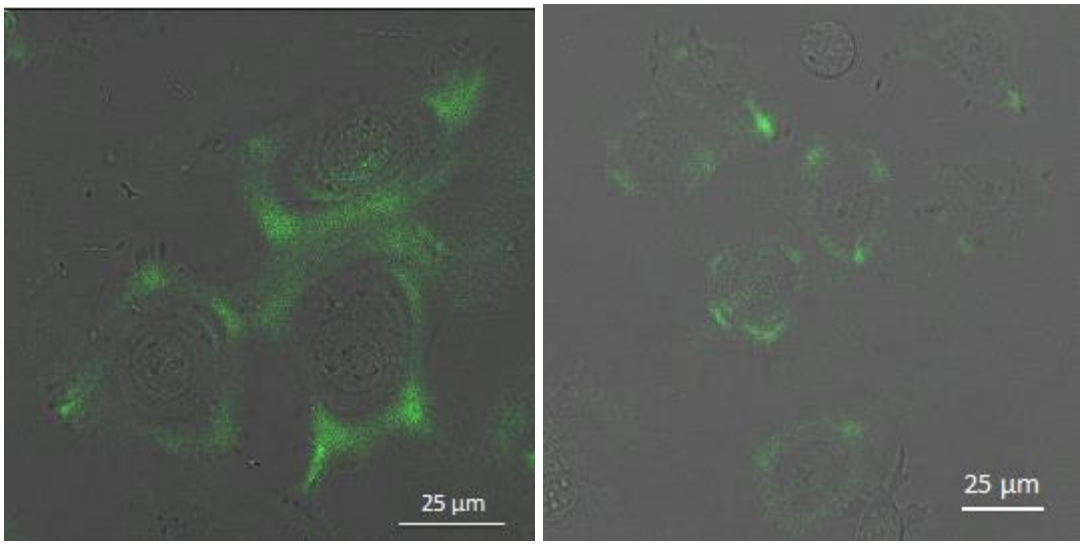


A B

Figure 5-4. Internalization study on TOV21G cells. A) Aptamer TOV6-TMR and B) Conjugate TOV6-TMR-AuNR.

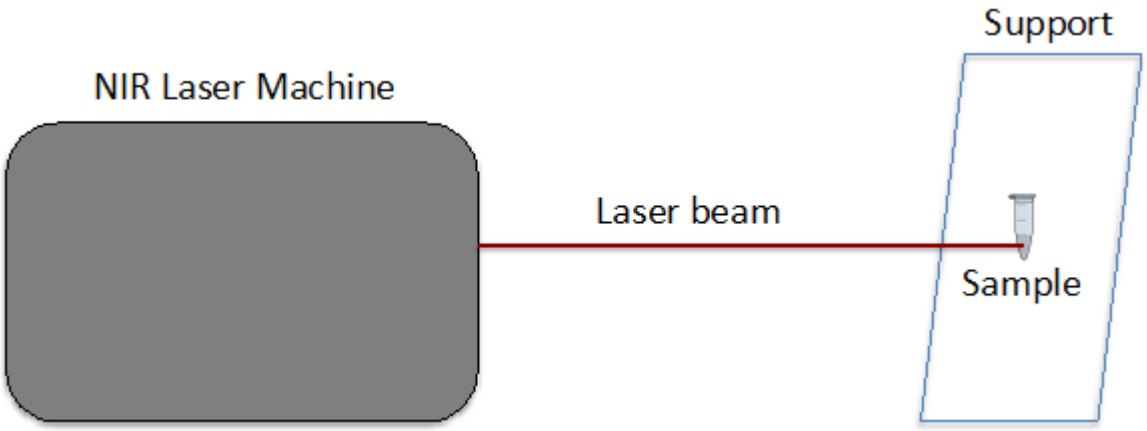


Figure 5-5. Scheme of the NIR laser experiment.

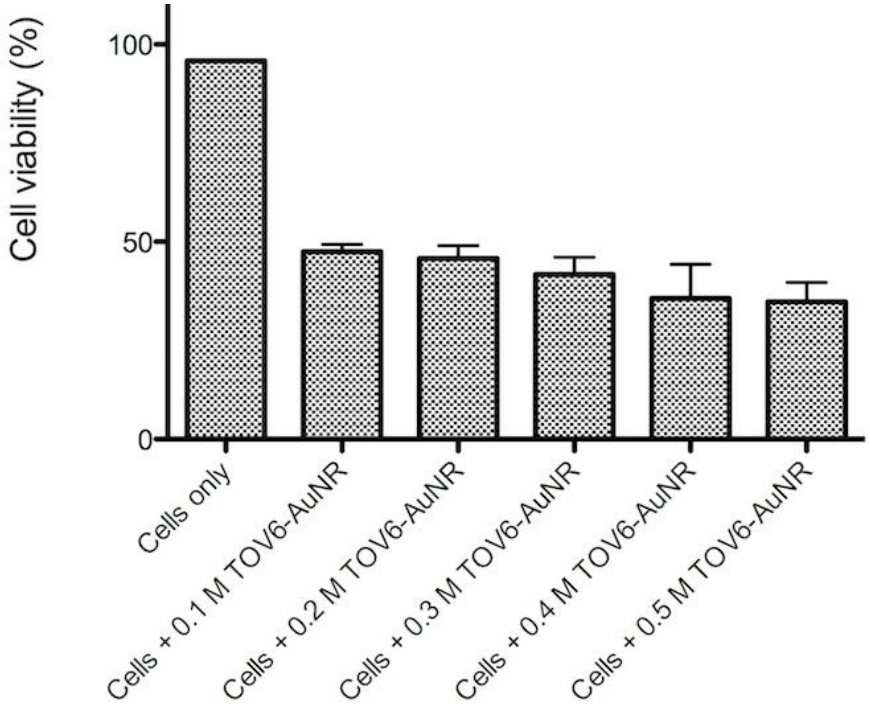


Figure 5-6. Viability of the TOV21G ovarian cancer cells after thermal activation of the gold-nanorods.

# CHAPTER 6
# CONCLUSIONS AND FUTURE WORK

This material could be divided into two main topics: the bacterial project focusing on *Methicillin-resistant Staphylococcus aureus* and the cancer projects with the cell-selection of liver cancer and the cytotoxicity study of Gold-nanorods-aptamer complexes on ovarian cancer cell by thermal activation.

The project on *MRSA* aptamer generation proved the possibility of using the SELEX technique on fixed bacteria cells to develop aptamers binding to *MRSA* that will show the same binding results on live bacteria cells. Four aptamers were generated to recognize the bacteria membrane with Kd constants varying between 90 and 200 nM. Since the smallest the Kd, the tighter the binding, DTMRSA4 is the aptamer showing the best binding properties with a Kd of 95 nM. The aptamer's ability to selectively bind around whole cells presents a potential clinical use of the selected aptamers as nanocarriers for the identification of antibiotic-resistant cell lines in patients. The successful development of an assay that can differentiate the resistance of *Staphylococcus aureus* colonies could facilitate the search for a more effective treatment and management of the disease depending on the strain of the bacteria.

The clinical study of the aptamer recognition showed that the selected aptamers bound to all clinical *MRSA* strains tested, suggesting that the proteins targeted by those aptamers are common for the different *MRSA* strains. DTMRSA1 and DTMRSA3 showed the best specificity, with DTMRSA1 being the better of the two, while DTMRSA2 and DTMRSA4 bound to all three types of bacteria: *MRSA*, *Staphylococcus aureus* and *Enterococcus faecalis.* Further investigation on the aptamers showed that

conjugation to gold-nanoparticles to it did not affect the binding, which was visualized through transmission electron microscopy.

After time, the aptamers generated showed no binding with the bacteria. The observed results and the evolution history of the *Staphylococcus aureus* superbug suggested that the aptamers may have been specific to a common target and that the tested bacteria morphology changed over time. How these highly adaptable bacteria can orchestrate the expression of a variable number of resistance and virulence determinants is a major concern and still a mystery. The *Staphylococcus aureus* bacterium represents a paradigm in its ability to accommodate antibiotic-resistance determinants and to produce an incredible panel of virulence determinants, making these pathogens among the most infectious diseases in humans.

Further studies would expand the present work to an optimized shorter aptamer length and a better understanding of the aptamer target on the membrane of *MRSA* bacteria.

The project on liver cancer cells focused on generating aptamers against the membrane protein Glypican 3. The cell-SELEX technique is able to generate aptamers specific to a particular cell line, but its main disadvantage lies in the fact that the target recognized by the aptamer remains unknown by the end of the selection. In this selection, we countered that disadvantage by using an original mouse cell line, the IMEA wild cell line, as the counter cell line, and that same cell line modified by transfection of the human glypican 3 gene, the hGPC3-IMEA cell line, in order to have expression of the targeted protein, Glypican 3. At the end of the selection, too many families of sequences were obtained, with none large enough to be able to generate

aptamers. Contamination of the cells by mycoplasma might have had an impact on the growth and membrane structure of the cells, which could explain the results observed.

In my opinion, and since selection on liver cells have shown to be challenging in the past year for the group, further investigation on Glypican 3 should be taken with a different approach. A protein selection of Glypican 3 seems more appropriate and could be run using Nickel-NTA (nitrilotriacetic acid) magnetic beads. This technique could also be coupled with regular cell-selection to ensure that sequences binding during the protein selection keep their binding properties once tested on whole cells.

In the final project focusing on thermoactivation of gold-nanorods on ovarian cancer cells, AuNR-TOV6 conjugate were tested on the TOV21G cell line. After internalization of those complexes into the cells and 10 min beaming with a near-infrared laser, up to 65% cell apoptosis was observed. The coupling of both aptamer and gold-nanorod technologies created a tool able to target a specific cell line and impact its viability through thermal activation.

Further cytotoxicity study of Gold-Nanorod-Aptamer complexes should include a temperature study in order to check the temperature observed outside of the cell. Indeed, if the temperature increase spread too much outside the cell, denaturation of neighbor proteins could occur as a side effect.

LIST OF REFERENCES


1. Pasteur, L. A propos de deux malades soignés à l'hôpital Saint-Louis pour pustule maligne. (1877).

2. Ogston, A. Micrococcus Poisoning. *Journal of anatomy and physiology* **17**, 24-58 (1882).

3. Rosenbach, F. Microorganismen bei den Wund-Infections-Krankheiten des; Menschen, Wiesbaden. (1884).

4. Gram, H. Über die isolirte Färbung der Schizomyceten in Schnitt- und Trockenpräparaten. Fortschritte der Medizin 2. (1884).

5. Whitt DD, S.A. *Bacterial Pathogenesis: A Molecular Approach*. (2002).

6. Kluytmans, J., vanBelkum, A. & Verbrugh, H. Nasal carriage of Staphylococcus aureus: Epidemiology, underlying mechanisms, and associated risks. *Clinical Microbiology Reviews* **10**, 505-& (1997).

7. VandenBergh, M.F.Q. & Verbrugh, H.A. Carriage of Staphylococcus aureus: Epidemiology and clinical relevance. *Journal of Laboratory and Clinical Medicine* **133**, 525-534 (1999).

8. VandenBergh, M.F.Q.*, et al.* Follow-up of Staphylococcus aureus nasal carriage after 8 years: Redefining the persistent carrier state. *Journal of Clinical Microbiology* **37**, 3133-3140 (1999).

9. Dancer, S.J. The effect of antibiotics on methicillin-resistant Staphylococcus aureus. *Journal of Antimicrobial Chemotherapy* **61**, 246-253 (2008).

10. Lane, W.R. Methicillin resistance in staphylococci. *Med Jour Australia* **I 49**, 962-965 (1962).

11. *S., L.* The Antibiotic Paradox: How the Misuse of Antibiotics Destroys Their Curative Powers. (*Perseus Cambridge*, 2002).

12. Levy, S.B. & Marshall, B. Antibacterial resistance worldwide: causes, challenges and responses. *Nature Medicine* **10**, S122-S129 (2004).

13. Anomymous. European Antimicrobial Resistance Surveillance System, EARSS Annual Report 2002. (2002).

14. Zapun, A., Macheboeuf, P. & Vernet, T. Penicillin-Binding Proteins and beta-Lactam Resistance. *Antimicrobial Drug Resistance, Vol 1: Mechanisms of Drug Resistance*, 145-170 (2009).

15. Mulligan, M.E.*, et al. Methicillin-resistant Staphylococcus aureus* - A consensus review of the microbiology, pathogenesis, and epidemiology with implications for prevention and management. *American Journal of Medicine* **94**, 313-328 (1993).

16. Hiramatsu, K. Vancomycin-resistant Staphylococcus aureus: a new model of antibiotic resistance. *The Lancet infectious diseases* **1**, 147-155 (2001).

17. Walsh, T.R. & Howe, R.A. The prevalence and mechanisms of vancomycin resistance in Staphylococcus aureus. *Annual Review of Microbiology.* Volume **56**, 657-675 (2002).

18. Walsh, C. Molecular mechanisms that confer antibacterial drug resistance. *Nature* **406**, 775-781 (2000).

19. Millar, B.C., Loughrey, A., Elborn, J.S. & Moore, J.E. Proposed definitions of community-associated meticillin-resistant Staphylococcus aureus (CA-MRSA). *Journal of Hospital Infection* **67**, 109-113 (2007).

20. Gonzalez, C., Rubio, M., Romero-Vivas, J., Gonzalez, M. & Picazo, J.J. Staphylococcus aureus bacteremic pneumonia: Differences between community and nosocomial acquisition. *International Journal of Infectious Diseases* **7**, 102-108 (2003).

21. Lowy, F.D. Medical progress - Staphylococcus aureus infections. *New England Journal of Medicine* **339**, 520-532 (1998).

22. Weems, J.J. The many faces of Staphylococcus aureus infection - Recognizing and managing its life-threatening manifestations. *Postgraduate Medicine* **110**, 24-+ (2001).

23. Brun, Y. & Bes, M. Staphylococcus. In: Précis de bactériologie clinique. 783-830 (ESKA, Paris, 2000).

24. Gomez, M.I.*, et al.* Staphylococcus aureus protein A induces airway epithelial inflammatory responses by activating TNFR1. *Nature Medicine* **10**, 842-848 (2004).

25. Lowy, F.D. Antimicrobial resistance: the example of Staphylococcus aureus. *Journal of Clinical Investigation* **111**, 1265-1273 (2003).

26. Jones, T.F., Kellum, M.E., Porter, S.S., Bell, M. & Schaffner, W. An outbreak of community-acquired foodborne illness due to methicillin-resistant Staphylococcus aureus. *Clinical Infectious Diseases* **33**, 1106-1106 (2001).

27. Bronner, S., Monteil, H. & Prevost, G. Regulation of virulence determinants in Staphylococcus aureus: complexity and applications. *Fems Microbiology Reviews* **28**, 183-200 (2004).

28. Dufour, P.*, et al.* Community-acquired methicillin-resistant Staphylococcus aureus infections in France: Emergence of a single clone that produces Panton-Valentine leukocidin. *Clinical Infectious Diseases* **35**, 819-824 (2002).

29. Yarwood, J.M. & Schlievert, P.M. Quorum sensing in Staphylococcus infections. *Journal of Clinical Investigation* **112**, 1620-1625 (2003).

30. Domart, Y. Therapeutic principles of staphylococcal infections - Role and limitations of standard compounds. *Annales Francaises D Anesthesie Et De Reanimation* **21**, 392-398 (2002).

31. Wolff, M. The management of treatment failures for staphylococcal infections. *Annales Francaises D Anesthesie Et De Reanimation* **21**, 418-423 (2002).

32. American Cancer Society, Cancer Facts and Figures 2005-2013 Report. (http://www.cancer.org).

33. Gonczy, P. Mechanisms of cell division: lessons from a nematode. *M S-Medecine Sciences* **19**, 735-742 (2003).

34. Chartier, N.T., Hyenne, V. & Labbe, J.-C. Mechanisms of asymmetric cell division: from model organisms to tumorigenesis. *M S-Medecine Sciences* **26**, 251-257 (2010).

35. Hayflick, L. & Moorhead, P.S. Serial cultivation of human diploid cell strains. *Experimental Cell Research* **25**, 585-& (1961).

36. Gernez, A. Le Cancer, Dynamique et Eradication. (1969).

37. Bru, A., Albertos, S., Subiza, J.L., Garcia-Asenjo, J.L. & Bru, I. The universal dynamics of tumor growth. *Biophysical Journal* **85**, 2948-2961 (2003).

38. Demicheli, R.*, et al.* An exponential-Gompertzian description of lovo cell tumor-growth from *in-vivo* and *in-vitro* data. *Cancer Research* **49**, 6543-6546 (1989).

39. Beljanski, M. Experimental biology and medicine monographs on interdisciplinar topics Volume **8**. The regulation of DNA replication and transcription: the role of trigger molecules in normal and malignant gene expression*. X+189p. S. Karger: Basel, Switzerland; New York, N.Y., USA. Illus*, X+189P-X+189P (1983).

40. Hanahan, D. & Weinberg, R.A. The hallmarks of cancer. *Cell* **100**, 57-70 (2000).

41. Burzynski, S.R. Antineoplastons - History of the research.1. *Drugs under Experimental and Clinical Research* **12**, 1-9 (1986).

42. Bruix, J. & Sherman, M. Management of Hepatocellular Carcinoma: An Update. *Hepatology* **53**, 1020-1022 (2011).

43. Luo, J.-H.*, et al.* Transcriptomic and genomic analysis of human hepatocellular carcinomas and hepatoblastomas. *Hepatology* **44**, 1012-1024 (2006).

44. Sasisekharan, R. Roles of heparan sulphate glycosaminoglycans in tumor biology. *Glycobiology* **12**, 642-642 (2002).

45. Liu, B.*, et al.* Investigation of the Role of Glypican 3 in Liver Regeneration and Hepatocyte Proliferation. *Faseb Journal* **24** (2010).

46. Komori, H., Nakatsura, T., Beppu, T., Nishimura, Y. & Baba, H. Possibilities of glypican-3-specific immunotherapy for hepatocellular carcinoma. *Gan to kagaku ryoho. Cancer & chemotherapy* **33**, 1742-1744 (2006).

47. Perez Rojas, J.*, et al.* Immunophenotypic classification of 3 cases of hepatocellular adenoma. Differential diagnosis with focal nodular hyperplasia. *Gastroenterologia Y Hepatologia* **36**, 388-395 (2013).

48. Kojiro, M.*, et al.* Pathologic Diagnosis of Early Hepatocellular Carcinoma: A Report of the International Consensus Group for Hepatocellular Neoplasia. *Hepatology* **49**, 658-664 (2009).

49. Williams, T.I.*, et al.* Epithelial ovarian cancer: Disease etiology, treatment, detection, and investigational gene, metabolite, and protein biomarkers. *Journal of Proteome Research* **6**, 2936-2962 (2007).

50. http://www.ovarian.org/types_and_stages.php.

51. Colombo, N.*, et al.* Ovarian cancer. *Critical Reviews in Oncology Hematology* **60**, 159-179 (2006).

52. Hennessy, B.T., Coleman, R.L. & Markman, M. Ovarian cancer. *Lancet* **374**, 1371-1382 (2009).

53. Goff, B. Development of an ovarian cancer symptom index: Possibilities for earlier detection - Reply. *Cancer* **110**, 227-227 (2007).

54. Van Simaeys, D.*, et al.* Study of the Molecular Recognition of Aptamers Selected through Ovarian Cancer Cell-SELEX. *Plos One* **5**(2010).

55. Karst, A.M. & Drapkin, R. Ovarian cancer pathogenesis: a model in evolution. *Journal of oncology* **2010**, 932371 (2010).

56. Patel, D.J. & Suri, A.K. Structure, recognition and discrimination in RNA aptamer complexes with cofactors, amino acids, drugs and aminoglycoside antibiotics. *Journal of biotechnology* **74**, 39-60 (2000).

57. Hermann, T. & Patel, D.J. Biochemistry - Adaptive recognition by nucleic acid aptamers. *Science* **287**, 820-825 (2000).

58. Feigon, J., Dieckmann, T. & Smith, F.W. Aptamer structures from A to zeta. *Chemistry & Biology* **3**, 611-617 (1996).

59. Hoshika, S., Minakawa, N. & Matsuda, A. Synthesis and physical and physiological properties of 4 '-thioRNA: application to post-modification of RNA aptamer toward NF-kappa B. *Nucleic Acids Research* **32**, 3815-3825 (2004).

60. Virno, A.*, et al.* A novel thrombin binding aptamer containing a G-LNA residue. *Bioorganic & Medicinal Chemistry* **15**, 5710-5718 (2007).

61. Di Primo, C.*, et al.* Systematic screening of LNA/2 '-O-methyl chimeric derivatives of a TAR RNA aptamer. *Febs Letters* **581**, 771-774 (2007).

62. Proske, D., Blank, M., Buhmann, R. & Resch, A. Aptamers - basic research, drug development, and clinical applications. *Applied Microbiology and Biotechnology* **69**, 367-374 (2005).

63. Hicke, B.J.*, et al.* Tumor targeting by an aptamer. *Journal of Nuclear Medicine* **47**, 668-678 (2006).

64. Shangguan, D.*, et al.* Aptamers evolved from live cells as effective molecular probes for cancer study. *Proceedings of the National Academy of Sciences of the United States of America* **103**, 11838-11843 (2006).

65. Yang, X.B.*, et al.* Immunofluorescence assay and flow-cytometry selection of bead-bound aptamers. *Nucleic Acids Research* **31**(2003).

66. Kawazoe, N., Ito, Y. & Imanishi, Y. Bioassay using a labeled oligonucleotide obtained by in vitro selection. *Biotechnology Progress* **13**, 873-874 (1997).

67. Drolet, D.W., MoonMcDermott, L. & Romig, T.S. An enzyme-linked oligonucleotide assay. *Nature Biotechnology* **14**, 1021-1025 (1996).

68. Rye, P.D. & Nustad, K. Immunomagnetic DNA aptamer assay. *Biotechniques* **30**, 290-+ (2001).

69. Ramos, E.*, et al.* A DNA aptamer population specifically detects Leishmania infantum H2A antigen. *Laboratory Investigation* **87**, 409-416 (2007).

70. Tombelli, S., Minunni, M., Luzi, E. & Mascini, M. New trends in nucleic acids based biosensors - Florence, Italy, October 25-28, 2003. *Analytical Letters* **37**, 1037-1052 (2004).

71. Jayasena, S.D. Aptamers: An emerging class of molecules that rival antibodies in diagnostics. *Clinical Chemistry* **45**, 1628-1650 (1999).

72. Mairal, T.*, et al.* Aptamers: molecular tools for analytical applications. *Analytical and Bioanalytical Chemistry* **390**, 989-1007 (2008).

73. Ellington, A.D. & Szostak, J.W. *In-vitro* selection of RNA molecules that bind specific ligands. *Nature* **346**, 818-822 (1990).

74. Tuerk, C., Schneider, D. & Gold, L. Successes with Selex. *Biological Chemistry Hoppe-Seyler* **372**, 771-771 (1991).

75. Sefah, K., Shangguan, D., Xiong, X., O'Donoghue, M.B. & Tan, W. Development of DNA aptamers using Cell-SELEX. *Nature Protocols* **5**, 1169-1185 (2010).

76. Stoltenburg, R., Reinemann, C. & Strehlitz, B. SELEX-A (r)evolutionary method to generate high-affinity nucleic acid ligands. *Biomolecular Engineering* **24**, 381-403 (2007).

77. Famulok, M. Oligonucleotide aptamers that recognize small molecules. *Current Opinion in Structural Biology* **9**, 324-329 (1999).

78. Wilson, D.S. & Szostak, J.W. In vitro selection of functional nucleic acids. *Annual Review of Biochemistry* **68**, 611-647 (1999).

79. Koekpinar, O., Walter, J.-G., Shoham, Y., Stahl, F. & Scheper, T. Aptamer-Based Downstream Processing of His-Tagged Proteins Utilizing Magnetic Beads. *Biotechnology and Bioengineering* **108**, 2371-2379 (2011).

80. Murphy, M.B., Fuller, S.T., Richardson, P.M. & Doyle, S.A. An improved method for the in vitro evolution of aptamers and applications in protein detection and purification. *Nucleic Acids Research* **31**(2003).

81. Shin, S., Kim, I.-H., Kang, W., Yang, J.K. & Hah, S.S. An alternative to Western blot analysis using RNA aptamer-functionalized quantum dots. *Bioorganic & Medicinal Chemistry Letters* **20**, 3322-3325 (2010).

82. Terazono, H., Yu, A., Soloviev, M. & Yasuda, K. Labelling of live cells using fluorescent aptamers: binding reversal with DNA nucleases. *Journal of Nanobiotechnology* **8**, 8-Article No.: 8 (2010).

83. Fang, X.H., Sen, A., Vicens, M. & Tan, W.H. Synthetic DNA aptamers to detect protein molecular variants in a high-throughput fluorescence quenching assay. *Chembiochem* **4**, 829-834 (2003).

84. Swensen, J.S.*, et al.* Continuous, Real-Time Monitoring of Cocaine in Undiluted Blood Serum via a Microfluidic, Electrochemical Aptamer-Based Sensor. *Journal of the American Chemical Society* **131**, 4262-4266 (2009).

85. Kang, H.S., Huh, Y.M., Kim, S. & Lee, D.-k. Isolation of RNA Aptamers Targeting HER-2-overexpressing Breast Cancer Cells Using Cell-SELEX. *Bulletin of the Korean Chemical Society* **30**, 1827-1831 (2009).

86. Da Rocha Gomes, S.*, et al.* (99m)Tc-MAG3-aptamer for imaging human tumors associated with high level of matrix metalloprotease-9. *Bioconjugate chemistry* **23**, 2192-2200 (2012).

87. Rockey, W.M.*, et al.* Synthesis and radiolabeling of chelator-RNA aptamer bioconjugates with copper-64 for targeted molecular imaging. *Bioorganic & Medicinal Chemistry* **19**, 4080-4090 (2011).

88. Esposito, C.L., Catuogno, S., de Franciscis, V. & Cerchia, L. New insight into clinical development of nucleic acid aptamers. *Discovery medicine* **11**, 487-496 (2011).

89. Cheng, J.*, et al.* Formulation of functionalized PLGA-PEG nanoparticles for in vivo targeted drug delivery. *Biomaterials* **28**, 869-876 (2007).

90. Wang, A.Z.*, et al.* Superparamagnetic iron oxide nanoparticle-aptamer bioconjugates for combined prostate cancer imaging and therapy. *Chemmedchem* **3**, 1311-1315 (2008).

91. Guo, Y.-P., Guo, L.-H., Yao, Y.-b., Ning, C.-Q. & Guo, Y.-J. Magnetic mesoporous carbonated hydroxyapatite microspheres with hierarchical nanostructure for drug delivery systems. *Chemical Communications* **47**, 12215-12217 (2011).

92. Wu, Y., Sefah, K., Liu, H., Wang, R. & Tan, W. DNA aptamer-micelle as an efficient detection/delivery vehicle toward cancer cells. *Proceedings of the National Academy of Sciences of the United States of America* **107**, 5-10 (2010).

93. Kang, H., O'Donoghue, M.B., Liu, H. & Tan, W. A liposome-based nanostructure for aptamer directed delivery. *Chemical Communications* **46**, 249-251 (2010).

94. Rosi, N.L.*, et al.* Oligonucleotide-modified gold nanoparticles for intracellular gene regulation. *Science* **312**, 1027-1030 (2006).

95. Alkilany, A.M.*, et al.* Cellular uptake and cytotoxicity of gold nanorods: Molecular origin of cytotoxicity and surface effects. *Abstracts of Papers of the American Chemical Society* **237**(2009).

96. Sefah, K.*, et al.* Molecular recognition of acute myeloid leukemia using aptamers. *Leukemia* **23**, 235-244 (2009).

97. Chambers, H.F. & DeLeo, F.R. Waves of resistance: Staphylococcus aureus in the antibiotic era. *Nature Reviews Microbiology* **7**, 629-641 (2009).

98. http://atcc.org.

99. Cao, X.*, et al.* Combining use of a panel of ssDNA aptamers in the detection of Staphylococcus aureus. *Nucleic Acids Research* **37**, 4621-4628 (2009).

100. Chen F, Z.X., Zhou J, Liu S, Liu J. Aptamer inhibits Mycobacterium tuberculosis (H37Rv) invasion of macrophage. Vol. **39** 2157-2162 (*Mol. Bio. Rep*., 2012).

101. Tiemersma, E.W.*, et al.* Geographical and time trends in proportion of methicillin resistant Staphylococcus aureus (MRSA) in Europe (1999-2001) reported through the European antimicrobial resistance surveillance system (EARSS). *Abstracts of the Interscience Conference on Antimicrobial Agents and Chemotherapy* **42**, 88-88 (2002).

102. Love, J.C., Estroff, L.A., Kriebel, J.K., Nuzzo, R.G. & Whitesides, G.M. Self-assembled monolayers of thiolates on metals as a form of nanotechnology. *Chemical Reviews* **105**, 1103-1169 (2005).

103. Longobardi Givan, A. *Flow Cytometry First Principles*, (2001).

104. Hayden, S.C.*, et al.* Aggregation and Interaction of Cationic Nanoparticles on Bacterial Surfaces. *Journal of the American Chemical Society* **134**, 6920-6923 (2012).

105. Carrillo-Carrion, C., Simonet, B.M. & Valcarcel, M. Colistin-functionalised CdSe/ZnS quantum dots as fluorescent probe for the rapid detection of Escherichia coli. *Biosensors & Bioelectronics* **26**, 4368-4374 (2011).

106. Joo, J.*, et al.* A facile and sensitive detection of pathogenic bacteria using magnetic nanoparticles and optical nanocrystal probes. *Analyst* **137**, 3609-3612 (2012).

107. Xiu, Z.-m., Zhang, Q.-b., Puppala, H.L., Colvin, V.L. & Alvarez, P.J.J. Negligible Particle-Specific Antibacterial Activity of Silver Nanoparticles. *Nano Letters* **12**, 4271-4275 (2012).

108. Lara, H.H., Ayala-Nunez, N.V., Ixtepan Turrent, L.d.C. & Rodriguez Padilla, C. Bactericidal effect of silver nanoparticles against multidrug-resistant bacteria. *World Journal of Microbiology & Biotechnology* **26**, 615-621 (2010).

109. DeGrasse, J.A. A Single-Stranded DNA Aptamer That Selectively Binds to Staphylococcus aureus Enterotoxin B. *Plos One* **7**(2012).

110. Klumpp, S., Zhang, Z. & Hwa, T. Growth Rate-Dependent Global Effects on Gene Expression in Bacteria. *Cell* **139**, 1366-1375 (2009).

111. Robinson, D.A.*, et al.* Re-emergence of early pandemic Staphylococcus aureus as a community-acquired meticillin-resistant clone. *Lancet* **365**, 1256-1258 (2005).

112. Jevons, M.P., Rolinson, G.N. & Knox, R. Celbenin-resistant *Staphylococci. British Medical Journal* **1**, 124-+ (1961).

113. Kreiswirth, B.*, et al.* Evidence for a clonal origin of Methicillin resistance in *Staphylococcus aureus*. *Science* **259**, 227-230 (1993).

114. Musser, J.M. & Kapur, V. Clonal analysis of Methicillin-resistant Staphylococcus aureus strains from intercontinental sources - association of the Mec gene with divergent phylogenetic lineages implies dissemination by horizontal transfer and recombination. *Journal of Clinical Microbiology* **30**, 2058-2063 (1992).

115. Fitzgerald, J.R., Sturdevant, D.E., Mackie, S.M., Gill, S.R. & Musser, J.M. Evolutionary genomics of Staphylococcus aureus: Insights into the origin of methicillin-resistant strains and the toxic shock syndrome epidemic. *Proceedings of the National Academy of Sciences of the United States of America* **98**, 8821-8826 (2001).

116. http://www.mirror.co.uk/news/technology-science/science/new-deadly-mrsa-strain-way-663012. http://www.mirror.co.uk/news/technology-science/science/new-deadly-mrsa-strain-way-663012.

117. Kanel, G.a.K., J. *Atlas of liver pathology*, (2010).

118. http://cancer.org.

119. http://www.liverfoundation.org.

120. Raoul, J.-L. Natural history of hepatocellular carcinoma and current treatment options. *Seminars in Nuclear Medicine* **38**, S13-S18 (2008).

121. Shirakawa, H.*, et al.* Glypican-3 is a useful diagnostic marker for a component of hepatocellular carcinoma in human liver cancer. *International Journal of Oncology* **34**, 649-656 (2009).

122. Sawada, Y., Sakai, M., Yoshikawa, T., Ofuji, K. & Nakatsura, T. A glypican-3-derived peptide vaccine against hepatocellular carcinoma. *Oncoimmunology* **1**, 1448-1450 (2012).

123. Davies, D. *Flow Cytometry: Principles and Applications*.

124. Miao, H.-L.*, et al.* Knockdown of GPC3 inhibits the proliferation of Huh7 hepatocellular carcinoma cells through down-regulation of YAP. *Journal of Cellular Biochemistry* **114**, 625-631 (2013).

125. Roche. http://www.liv.ac.uk/media/livacuk/centreforgenomicresearch/The_GS_FLX_Titanium_Chemistry_Extended_MID_Set.pdf.

126. Crotzer, D.R.*, et al.* Lack of effective systemic therapy for recurrent clear cell carcinoma of the ovary. *Gynecologic Oncology* **105**, 404-408 (2007).

127. Munkarah, A., Chatterjee, M. & Tainsky, M.A. Update on ovarian cancer screening. *Current Opinion in Obstetrics & Gynecology* **19**, 22-26 (2007).

128. Reynolds, E.A. & Moller, K.A. A review and an update on the screening of epithelial ovarian cancer. *Current Problems in Cancer* **30**, 203-232 (2006).

129. Haga, Y., Sakamoto, K., Egami, H., Yoshimura, R. & Akagi, M. Evaluayion of serum CA125 values in healthy-individuals and pregnant-women. *American Journal of the Medical Sciences* **292**, 25-29 (1986).

130. Yasun, E.*, et al.* Enrichment and Detection of Rare Proteins with Aptamer-Conjugated Gold Nanorods. *Analytical Chemistry* **84**, 6008-6015 (2012).

131. http://www.promega.com/products/cell-health-and-metabolism/cell-viability-assays/celltiter-96-aqueous-non_radioactive-cell-proliferation-assay-_mts_/.

132. Esposito, G.*, et al.* Nanotechnology and vascular neurosurgery: an in-vivo experimental study on microvessels repair using laser photoactivation of a nanostructured hyaluronan solder. *Journal of Biological Regulators and Homeostatic Agents* **26**, 447-456 (2012).

133. de Freitas, L.F.*, et al.* In vivo photothermal tumour ablation using gold nanorods. *Laser Physics* **23**(2013).

134. Ratto, F.*, et al.* Photothermal effects in connective tissues mediated by laser-activated gold nanorods. *Nanomedicine-Nanotechnology Biology and Medicine* **5**, 143-151 (2009).

135. Colvin, V.L. The potential environmental impact of engineered nanomaterials (vol 21, pg 1166, 2003). *Nature Biotechnology* **22**, 760-760 (2004).

136. Lewinski, N., Colvin, V. & Drezek, R. Cytotoxicity of nanoparticles. *Small* **4**, 26-49 (2008).

137. Finkelstein, A.E.*, et al.* Auranofin - New oral gold compound for treatment of Rheumatoid-Arthritis. *Annals of the Rheumatic Diseases* **35**, 251-257 (1976).

# BIOGRAPHICAL SKETCH

Diane Turek was born in Pau, France. She studied chemical and physical engineering in Bordeaux, France, at the graduate school ENSCPB and obtained her Engineering Master degree in 2009. One year before, in 2008, while completing her engineering Master, she joined Dr Wagener's research group where she performed research on drug delivery using polymers, and sunscreen chromophore modifications. She obtained her Chemistry Master degree in 2011 and continued into a PhD in the biochemistry division. She received her PhD in Chemistry in 2013 under the tutorage of Dr Weihong Tan.